The ALS-Associated Protein, TDP-43, Functions to Regulate Drosophila Larval Motor Behavior and Physiology in a *Cacophony*-Dependent Manner

by

Kayly Mary Lembke

A DISSERTATION

Presented to the Department of Physiology & Pharmacology

and the Oregon Health & Science University

School of Medicine

in partial fulfillment of

the requirements for the degree of

Doctor of Philosophy

July 2017

Oregon Health & Science University

_____

CERTIFICATE OF APPROVAL

_____

This is to certify that the Ph.D. dissertation of

Kayly Mary Lembke

has been approved on July 24th, 2017

_____

Advisor, David B. Morton, Ph.D.

_____

Member and Chair, Sue Aicher, Ph.D.

_____

Member, Steve Matsumoto, Ph.D.

_____

Member, Doris Kretzschmar, Ph.D.

"Let me not die while I am still alive."

-Jewish Prayer

"Nothing in life is to be feared, it is only to be understood."

-Marie Curie

TABLE OF COTENTS

INDEX OF FIGURES

CHAPTER 5

APPENDIX FIGURES

LIST OF ABBREVIATIONS

A2: Abdominal Segment 2

A7: Abdominal Segment 7

ALS: Amyotrophic Lateral Sclerosis

BRP: Bruchpilot

CAC: Cacophony

$cac^{exon7\Delta(6)}$: *Cacophony* Exon 7 Deletion Line

$cac^{exon7\Delta(8)}$: *Cacophony* Exon 7 Deletion Line

$Ca_V2.2$: type 2, N-type voltage gated calcium channel

cDNA: complementary DNA

CNS: Central nervous system

CPG: Central Pattern Generator

CRISPR-CAS: Clustered Regularly Interspaced Short Palindromic Repeats – CRISPR

associated protein

EJPs: Excitatory Junctional Potentials

GAL4: Yeast Transcription Activation Protein

GluR: Glutamate Receptor

ISN: Intersegmental Nerve

mCD8::GFP: Membrane Tethered GFP Fusion Protein

mEPPs: Miniature End Plate Potentials

mEPCs: Miniature End Plate Currents

NMJ: Neuromuscular Junction

PKA-C3: Protein Kinase A C3 catalytic subunit

PLTX-II: synthetic peptide plectreurys toxin

RNAi: RNA Interference

RPR: *Reaper*

TBPH: TAR DNA Binding Protein Homolog (Drosophila)

tbphΔ: TBPH mutant

TDP-43: Transactive Response DNA Binding Protein 43

TrpA1: Transient Receptor Potential A1

UAS: Upstream Activation Sequence

-UTR: Untranslated Region

VNC: Ventral Nerve Cord

ACKNOWLEDGEMENTS

Graduate school has been one of the longest, hardest experiences of my life. It has also been one of the most rewarding and joyful. I have many, many people to thank and acknowledge for their expertise and support over the course of my training.

First, I must thank my mentor Dr. David Morton. He had the patience of Job throughout this entire process. He challenged me to always critically exam and thoughtfully interpret the data I generated. He let me pursue my interests in lab ad supported my attending the Drosophila Neurobiology course at Cold Spring Harbor. And from him, I will always remember that Punk ended with The Clash. I will forever be grateful for having trained in his lab.

Second, in the preparation of this work, I must thank the members of my Dissertation Advisory Committee: Dr. Sue Aicher, Dr. Steve Matsumoto, Dr. Sean Speese, and Dr. Doris Kretzschmar. Thank you for your helpful feedback and insights to the data I presented. Thank you also for being accessible outside of DAC meetings. Also, thanks to Steve for letting me use his dissection microscope for the entirety of my training.

Third, I must thank Dr. Jer Cherng Chang, Dr. Charles Scudder, and Alex Law. Jer Cherng was a true ally and collaborator in lab. I learned an immeasurable amount from his constant questions, some of which were useful (inside joke), his molecular expertise, and his "golden eye" for detail. I must also thank him for daily morning coffee and eventually forgiving my Hello Kitty prank. I must thank Charlie for teaching me the electronics of the rig. He was my electrophysiology sensei and was instrumental in

writing the programs used to analyze the extracellular recordings. Finally, Alex Law has been a terrific lab manager and collaborator. He has a great pair of hands and I am happy I have witnesses him begin to think like a scientist.

Graduate school at OHSU, for me, has been a constant test in resilience, and it is right that I acknowledge those cheerleaders in my life who helped get me to the point of writing this document. Judy Stewart, our former lab manager, is a wonderful human being and provided immeasurable support, guidance, and encouragement both when I first joined the lab, and throughout this entire process. Thank you! Humongous thanks to national treasure Jackie Wirz. She once told me "You are not the person you were," changing my life. When I needed someone to tell me I was capable, or someone to make me laugh or buy me coffee, she always did. That might not seem like a lot, but there are very few true student advocates on campus and she is one. Thanks also for the diamond-studded pipette! Gigantic thanks also to universal treasure Rick Goranflo. Not enough students appreciate everything he does for us, but they should. I could always count on him for a smile and a laugh, perspective and solutions.

My friends in PMCB and Graduate Student Organization (GSO) – especially Lizzy Sunderhaus, without whom I would not know what an internal hernia is; Shannon Liudahl, for always having great ideas and making me laugh; Marilynn Chow and Edmar Castro, my restaurant and Frasier buddies; and Sarah Wicher, my Physiology and Pharmacology coffee buddy (even though she didn't thank me in her acknowledgements).

Finally, but never lastly, I must thank my family for their constant love and support. As an Army kid, family has always been everything to me. I am blessed to have

parents who always prioritized my education. No matter the directions I took, they supported and encouraged me to be the very best I could be; to be all I could be. Thanks to my mom, Wendy, my dad, Keith, my sister, Jessy, and my brothers, Scott and Josh. I love all of you so much. I would also like to acknowledge Jessy's help with adapting Figure 1. To mom, Jessy, and Josh: it has been a wild ride, guys, but I am so thankful I have been able to ride it with you.

He gives power to the weak, and those who have no might, he increaseth strength. Even the youths shall faint and be weary, and the young men shall utterly fall: But they that wait upon the Lord shall renew their strength; they shall mount up with wings as eagles; they shall run, and not be weary; and they shall walk, and not faint. Isaiah 40: 29-31

ABSTRACT

Amyotrophic Lateral Sclerosis is the most common adult onset motor neurodegenerative disease. The etiology of the disease remains obscure, and as such there is no effective treatment or cure. TDP-43 is a nuclear RNA and DNA binding protein associated with 96% of ALS patient pathology. Tissue samples taken post-mortem from patients show a loss of nuclear localization and the presence of TDP-43 in cytoplasmic inclusions in the cell body. Whether the pathogenesis of the disease is driven by loss of nuclear function, gain of cytotoxicity with the formation of the cytoplasmic inclusions, or some other yet unidentified cause is not known. The goal of the research presented here was to understand the downstream effects of loss of nuclear TDP-43 function on motor behavior and physiology, using *Drosophila melanogaster* as a model. The results I present here show that behavioral motor defects associated with loss of Drosophila TDP-43 are driven by the loss of the voltage gated calcium channel *cacophony*, not at the neuromuscular junction, but rather in cells located centrally in the protocerebrum of the brain.

CHAPTER 1

Introduction

Amyotrophic Lateral Sclerosis (ALS) is the most common adult onset motor neurodegenerative disease. In the United States and Europe, it affects 2-16 individuals per 100,000 individuals per year. Its pathogenesis is marked by progressive muscle wasting and atrophy, which ultimately lead to patients' paralysis and death due to respiratory failure. Though it has been over 150 years since ALS was first described as a disease, the causes remain unknown and there are currently no known cures. Median patient survival is 3 years from diagnosis.

A BRIEF HISTORY OF AMYOTROPHIC LATERAL SCLEROSIS

Jean Martin Charcot: The Napoleon of Neuroses

ALS was first described in 1865 by the French neurologist Jean Martin Charcot (Guillain and Bailey, 1959). Charcot was one of the most prolific and influential neurologists of the nineteenth century. He not only refined the clinical descriptions of Parkinson's disease from those first reported in 1817 by James Parkinson, he was the first to identify and characterize Multiple Sclerosis, Charcot-Marie-Tooth Disease, and Charcot's Disease (now called ALS), among others (Guillain and Bailey, 1959; Goetz, 2011).

In 1862, Charcot entered La Salpetriere, then a fairly young teaching hospital, and began studying hysteria (Bogousslavsky and Moulin, 2010). At that time, two schools of thought were dominant in the teaching hospital: psychiatry and alienist, the original term for psychology (Bogousslavsky and Moulin, 2010). Neither of these schools considered hysteria to be more than a sickness of the mind without a physical cause, and patients

with hysteria were largely ignored. Charcot was one of the first to consider it a natural disease and believed that the hysteria these patients showed was a symptom of organic focal brain diseases. In 1872, Charcot became Professor of Pathological Anatomy and in 1882 the Faculty of Medicine in Paris created and appointed him the first chair of Clinique des maladies du systeme nerveux (Bogousslavsky and Moulin, 2010).

When observing a case, Charcot's approach relied upon detailed observations of neuropathology and neuroanatomy (Guillain and Bailey, 1959; Bogousslavsky and Moulin, 2010). The very identification of ALS as a distinct disease owes itself to his devotion to detail. In 1865, three years after starting at La Salpetriere, Charcot examined a woman with spastic paralysis and contractures of both arms and legs that was caused by sclerosis of the lateral columns (Guillain and Bailey, 1959). Upon examining other patients displaying muscular atrophy in concurrence with spasticity, he proposed this was a new, distinct disease (Guillain and Bailey, 1959). Importantly, it should be noted that even in the beginnings of reporting his observations on patient anatomy, he asserted this was a *systems* disease (Guillain and Bailey, 1959).

In his summary of the disease, Charcot reported the disease "begins with a paresis that progressively affects all four extremities…in which the lower extremities are more involved than the upper ones" and "progressive muscular atrophy, which involved principally the muscles of the upper extremities" (Guillain and Bailey, 1959). He made notes that the "thenar [group of muscles on the palm of the human hand at the base of the thumb] and hypothenar [three muscles that innervate the little finger] eminences are sometimes remarkably flattened" which he correlated, post mortem, with a "more or less marked degeneration of the anterior horn cells, particularly at the levels of the cervical

enlargement of the spinal cord" (Guillain and Bailey, 1959). From its first clinical descriptions, ALS was described as a complicated, heterogeneous disease.

It should also be noted that these observations pre-dated many important milestones in neuroscience (Robinson, 2001). The first papers from Camillo Golgi reporting data using his stain did not appear until 1873. Ramon y Cajal did not touch Golgi's stain until 1887. Wilhelm von Waldeyer did not use the word neuron to describe the cell body and its processes until 1891. And the word synapsis, the word that would eventually be synapse, was not used until 1897, when it appeared in *A Textbook on Physiology* (compiled by Michael Foster), in a section written by Charles Scott Sherrington. In it, Sherrington described the synapse as "the tip of [an axon] is not continuous with but merely in contact with the substance of the dendrite or cell body in which it impinges" (Robinson, 2001).

The identification and first description of ALS thus predates the adoption of essential theories and practices that would drive the evolution of what we currently call Neuroscience. ALS research in the twentieth century reflects the rapid advances in basic science that marked the last century.

The Twentieth Century Conundrum

The challenge of ALS research in the twentieth century was to take patient symptoms from the clinic and extrapolate pathology, etiology, and treatment or cure. In the first half of the century, data on ALS were derived solely from clinical descriptions and patient physicals and autopsies. There was argument over its distinctness as a disease. There was debate upon whether ALS was solely a neurological disorder or

whether it had a psychological component. There was strong disagreement on its prevalence and etiology. As more sophisticated methodology allowed for single cell analysis, biochemical studies, and finally molecular and genetic analysis, more and more data was gathered. Yet, the full cause of the disease remained elusive.

ALS literature in the first half of the 20th century, until approximately 1955, dealt primarily with reporting and correlating patient symptoms with anatomical changes, as well as identifying possible causes of symptom onset, be it genetic or sporadic. By 1947, there were documented case reports on over 400 patients (Ziegler, 1930; Swank and Putnam, 1943; Wechsler et al., 1944; Veit, 1947) in the United States, as well as those from Europe, Asia, and the Pacific Islands. These patients were all of varying ethnicities and ages, backgrounds and socioeconomic classes. From these cases, a generalized description of disease manifestation description was set that still holds true today. First, the disease generally includes early weakness, muscle atrophy, fibrillations and/or fasciculations, and frequent troubles with speech and swallowing. There is no one precipitating factor or group of factors for the disease, though a small percentage of cases are from an inherited form. The disease occurs in males to females in a 2:1 ratio and the average age of presentation is 50. Racial and ethnic background does not correlate with disease occurrence or predisposition, with the notable exception of the documented Guam cases. And, though it is still classified as a rare disease, arguments appeared as early as 1947 that argued it was more common than reported (Veit, 1947).

Patients with ALS would be monitored through disease progression and autopsied at death, in order to correlate their symptoms to changes in pathology and anatomy. By 1950, there was a comprehensive understanding of symptom-pathology. Both the lower

motor neurons of the spinal cord and brain were classified as affected. The characteristic

muscular atrophy, weakness and paralysis, fasciculations, and loss of reflexes (Jackson

and Bryan, 1998) were consistent with degeneration of anterior horn cells and a decrease

in the number of large motor cells (Jackson and Bryan, 1998). Early cellular descriptions

noted chromatolysis, a term for the dissolution of the Nissl substance, or rough

endoplasmic reticulum, in the cell body of remaining large neurons (Jackson and Bryan,

1998). Loss of myelin at nerve fibers and peripheral nerves was reported, as well as a

general reduction in the number of fibers. Diseased ventral horn cells and motor nuclei in

the medulla were likewise associated with muscular atrophy, and muscles innervated by

these cells showed atrophic changes, that is an increase in sarcolemma nuclei, fibrillar

splitting, and fatty acid infiltration (Jackson and Bryan, 1998). In the brain stem,

degeneration due to cortical cell changes was observed in the various fasciculi of the

corticospinal system, leading to the death of upper motor neurons (Jackson and Bryan,

1998). Also, degenerative changes in the upper motor neurons and Betz cells, giant

pyramidal cells in the 5th layer of the grey matter in the primary cortex, was observed

(Jackson and Bryan, 1998).

These patient pathologies lead to a generalized symptom-pathology disease

progression outline that is still used today, which retains many of the symptoms

originally described by Charcot. Muscular atrophy, weakness, fasciculations, and loss of

reflexes are a result of loss of function of the anterior horn cells (Lawyer Jr and Netsky,

1953; Jackson and Bryan, 1998). Early signs of the disease include wasting of the small

hand muscles, such as the interossei and lumbricales (Lawyer Jr and Netsky, 1953;

Jackson and Bryan, 1998). As the disease progresses, the wasting becomes more

pronounced and bilaterally symmetrical, and spreads to the muscles of the shoulder girdle and upper arm (Lawyer Jr and Netsky, 1953; Jackson and Bryan, 1998). In the head, muscles of the tongue, palate, and pharynx will atrophy (Lawyer Jr and Netsky, 1953; Jackson and Bryan, 1998). As the disease continues to progress, the leg muscles will likewise atrophy and is concurrent with fibrillations, fasciculations, and a loss of some reflexes (the loss of reflexes is dependent upon the number of atrophying fibers) (Lawyer Jr and Netsky, 1953; Jackson and Bryan, 1998). Loss of abdominal reflexes, tendon jerks, and extensor plantar responses were attributed to involvement of the corticospinal tracts (Jackson and Bryan, 1998).

In 1902, W.R. Gowers made the earliest hypothesis on cellular causes of the disease. Gowers wrote on the topic of abiotrophy, the phenomenon of defective vitality, and the dependence of muscular atrophy seen in degenerative diseases, like ALS, on nerve nutritional deficiency (Gowers, 1902). He argued that the degeneration of the nerves in these disease is not a consequence of muscular atrophy, but rather some deficiency at the nerve (Gowers, 1902). His lecture on abiotrophy in diseases of muscular atrophy is the first printed proposal asserting motor degeneration in ALS is initiated by a cellular deficiency in neurons themselves.

In the 1930's and early 1940's, clinicians tested whether vitamin supplementation, for example Vitamin E, could stop or reverse ALS progression (Davison, 1943). Unfortunately it did not. In 1955, the idea was re-asserted that a "deficiency factor in the pathogenesis of [ALS]" was possible because there is a "prolonged strain on the structures involved" (Ask-Upmark and Meurling, 1955). Indeed, most post-war work

sought to describe the distinct cellular morphology and pathology of ALS (Hirano and Iwata, 1978).

The heterogeneity of hypotheses about the causes and cellular determinant of ALS that appear from the 1960's onward, reflect the rapid evolution of systems, biochemical, and cellular biology concurrent at this time. Different groups investigated a variety of causes, including genetically inherited abnormalities of anterior horn cell function, slow viruses, Polio, lead and heavy metal poisoning, nuclear, geographical predispositions, and diet (Bradley, 1977). Most of these studies produced confounding and contradictory results.

The first study looking at biochemical changes to motor neurons from ALS patients appeared in 1973 from Savolainen and Palo (Savolainen and Palo, 1973). Using ultracentrifugation and fractionation of organelles, they biochemically analyzed neuronal cell membranes, axons, and myelin from the brains of two Finnish ALS patients immediately following death (Savolainen and Palo, 1973). Their results indicated that the cell membranes and myelin from the ALS patients had reduced protein levels, compared to those from non-ALS individuals (Savolainen and Palo, 1973). Though crude in their approach, this was the fist paper to show biochemical evidence of protein composition changes with ALS pathogenesis.

Four years later, in 1977, working upon advances in understanding axonal transport, W.G. Bradley asserted a model in which ALS etiology was dependent upon deficiencies at either the nucleus, what was then called "protein synthetic machinery",

mitochondria, the lysosomal system, plasmalemma, neurotubules, neurofilaments, and/or Schwann cells (Bradley, 1977).

Identification of SOD1 and TDP-43

Currently, there are four main clinical presentations of ALS (Tan et al., 2017). The most common is limb-onset ALS with a combination of upper motor neuron and lower motor signs (Tan et al., 2017). This presentation represents approximately 70% of patient cases (Tan et al., 2017). The second most common ALS presentation is bulbar onset which subsequently spreads to the limbs and accounts for approximately 25% of patient cases (Tan et al., 2017). The final two clinical presentations of ALS represent approximately 5% of cases (Tan et al., 2017). The third involves the less common primary lateral sclerosis with pure upper motor neuron involvement (Tan et al., 2017). The fourth and final clinical presentation involves progressive muscular atrophy with pure lower motor neuron involvement (Tan et al., 2017). ALS patients do not show loss of brain tissue and atrophy of the motor cortex is observed in less than 25% of patient cases (Tan et al., 2017).

There are two classifications of ALS: sporadic and familial, both of which are clinically indistinguishable (Tan et al., 2017). Approximately 96% of patient cases are classified as sporadic, rather than familial (Tan et al., 2017). The first gene identified as having a function in ALS pathogenesis was Super Oxide Dismutase 1 (SOD1). In 1993, mutations in SOD1 were identified to be associated with familial ALS (Rosen, 1993) and researchers worked to develop a mouse model of SOD1 mutation. However, these patients accounted for only 2% of total ALS cases and do not show the same pathology that the majority of ALS cases present, namely cytoplasmic inclusions in neurons

(Jackson and Bryan, 1998; Casci and Pandey, 2015a; Guerrero et al., 2016; Tan et al., 2017).

In 2006, the primary protein component of the cytoplasmic inclusions in motor neurons, found in approximately 96% of ALS cases, was identified to be TDP-43 (Neumann et al., 2006). TDP-43 was present in cytoplasmic inclusions in the both the upper and lower motor neurons, as well as frontal and temporal cortex, in tissue samples collected post-mortem from patients (Guerrero et al., 2016). In mammals, TDP-43 is expressed broadly in the heart, lung, liver, spleen, kidney, muscle, and brain (Neumann et al., 2006).

INTRODUCTION TO TDP-43

TDP-43 proteinopathy accounts for approximately 96% of ALS cases in the United States (Cozzolino et al., 2012). An RNA and DNA binding protein, cells are especially sensitive to changes in TDP-43 expression levels and localization. The Drosophila ortholog of TDP-43 is called TBPH, Tar Binding Protein Homolog. The two genes are orthologous.

Description of the TDP-43 gene and protein

Transactive Response DNA Binding Protein 43, abbreviated as TDP-43, is a member of the heterogeneous nuclear ribonucleoprotein (hnRNPP) family, and is highly conserved among human, mouse, *D. melanogaster,* and *C. elegans* (Guerrero et al., 2016). An RNA and DNA binding protein encoded by the *TARDBP* gene. TDP-43 was

first identified by its interactions with the HIV transactive response DNA; it binds to the polypyrimidine-rich motif of the HIV transactive response DNA (Ou et al., 1995; Neumann et al., 2006). It was later identified independently as part of a protein complex involved in the splicing of the cystic fibrosis transmembrane conductance regulator gene (Neumann et al., 2006).

TARDBP is located on chromosome 1 of humans and contains 6 transcribed exons. Of these 6 exons, the main protein is translated from exons 2-6, producing a 414 amino acid protein (Pesiridis et al., 2009). The gene contains two RNA recognition motif domains, one nuclear localization signal, and a glycine-rich C-terminus (Ou et al., 1995; Ayala et al., 2005; Neumann et al., 2006). Most sporadic mutations occur in the C-terminus of TDP-43, in the domain encoded by exon 6 (Pesiridis et al., 2009). There are multiple phosphorylation, acetylation, ubiquitination, and sumolation cites on TDP-43 (Neumann et al., 2006; Pesiridis et al., 2009). There is also an enrichment of multiple phosphorylation sites at the C-terminus (Hasegawa et al., 2008).

Functions of TDP-43

In healthy cells, TDP-43 localizes predominately at the nucleus (Neumann et al., 2006) where it binds most forms of RNA from a variety of genes, including its own *TARDP* (Wang et al., 2004; Ayala et al., 2005; Arai et al., 2006; Buratti and Baralle, 2011; Avendaño-Vázquez et al., 2012; Hazelett et al., 2012). Thus, a major function of TDP-43 is regulation of gene expression (Wang et al., 2004; Ayala et al., 2005; Arai et al., 2006; Buratti and Baralle, 2011; Avendaño-Vázquez et al., 2012; Hazelett et al., 2012). Specific functions of TDP-43 include transcriptional repression, regulation of pre-RNA maturation and alternative splicing, mRNA transportation, microRNA biogenesis,

interaction with noncoding RNA, autoregulation, and translational regulation (Guerrero et al., 2016). TDP-43 has also been observed to co-localize in cytoplasmic inclusions with Poly-A binding protein-1 (PABP-1), a cytoplasmic stress granule marker (Dewey et al., 2012; McGurk et al., 2014).

TDP-43 is essential for development; homozygous endogenous TDP-43 knock out mice are embryonic lethal, dying between day 3.5 and 8.5 (Kraemer et al., 2010; Sephton et al., 2010; Shan et al., 2010; Wu et al., 2010; Guerrero et al., 2016). Furthermore, post-natal induced homozygous knock-out causes rapid lethality (Kraemer et al., 2010; Sephton et al., 2010; Shan et al., 2010; Wu et al., 2010; Guerrero et al., 2016). Heterozygous knock-out mice are viable, and eventually develop mild motor defects with age (Kraemer et al., 2010; Guerrero et al., 2016). Post-natal deletions of endogenous TDP-43 in only motor neurons and spinal cords of mice also produce muscle atrophy and motor neuron loss (Iguchi et al., 2013). Suppression of TDP-43 in motor neurons results in increased mitochondrial density in neurites, as well as increased numbers of abnormal neurites and decreased cell viability (Wang et al., 2013; Guerrero et al., 2016).

TDP-43 expression levels are tightly regulated in healthy cells and therefore thought to hold a function in maintaining cellular homeostasis (Lejeune and Maquat, 2005). Discreet pools of motor neurons have been observed to be differentially sensitive to changes in TDP-43 expression (Spiller et al., 2016). In a transgenic inducible rNLS8 mouse model that forms both cytoplasmic TDP-43 proteinopathy and loss of TDP-43 nuclear localization, 7 motor neuron pools were found to respond differently to TDP-43 proteinopathy. Motor neurons in the oculomotor, trigeminal, and facial nuclei were

unaffected (Spiller et al., 2016). Motor neurons in the hypoglossal nucleus and the spinal cord were lost after 8 weeks of transgenic expression (Spiller et al., 2016). Within the spinal cord, slow motor neurons survived to end stage and remained innervated, whereas the fast fatigable motor neurons were lost after 8 weeks and were the first to present axonal dieback (Spiller et al., 2016). It should be noted that, despite there being a variety of loss- and gain-of function TDP-43 mouse models, this was the first model to report both a loss of nuclear localization concomitant with cytoplasmic TDP-43 inclusions.

Outstanding Questions

There are several outstanding questions regarding the functional role of TDP-43 in driving ALS. Patient tissue samples taken post-mortem have shown that, at end life, TDP-43 has depleted from the nucleus of cells and formed insoluble protein aggregates in the cytoplasm. Whether it is the loss of TDP-43 nuclear function or the formation of protein aggregates that is necessary or sufficient to drive ALS pathogenesis remains an outstanding paradox.

TDP-43 protein pathology is characterized primarily by cytoplasmic accumulation of TDP-43 protein into round inclusions, skeins, or threads that are coincident with nuclear clearing of TDP-43 (Neumann et al., 2006; Pesiridis et al., 2009). These inclusions can occur in the presence of C-terminal breakdown and/or cleavage, but this C-terminal breakdown and/or cleavage does not drive the formation of these aggregates (Ayala et al., 2008; Pesiridis et al., 2009). TDP-43 phosphorylation state, however, can drive formation of cytoplasmic aggregates, as mutations in the C-terminus that either prevent phosphorylation or lead to hyperphosphorylation have both been observed to

drive TDP-43 protein aggregation (Pesiridis et al., 2009). The initial cause of these

sporadic mutations in TDP-43 is not known.

DROSOPHILA AS A MODEL SYSTEM TO UNDERSTAND TDP-43 FUNCTION

Though it is unclear whether ALS results from loss of nuclear TDP-43 or a gain

in cytoplasmic toxicity associated with formation of insoluble protein aggregates, the

progression of ALS clearly depends upon a change in TDP-43 function. The Drosophila

ortholog of TDP-43 is TBPH. The protein forms of the gene are functionally

homologous. The power of Drosophila genetic tools enabled us to model the loss of

nuclear function by generating a TBPH loss of function mutant fly. This fly was then

behaviorally characterized and RNA-seq analysis performed to understand the molecular

basis of the changes in behavior.

Drosophila as a Model System for Neurodegenerative Disease

Drosophila is one of the oldest model systems in use today. Thomas Hunt

Morgan, upon the rediscovery of Mendelian inheritance in 1900, first used the fruit fly as

a system to investigate genetics in his lab at Columbia. Since then, Drosophila has been

used to make paramount discoveries that have shaped modern understanding of genes,

chromosomes, inheritance, complex behaviors, and immunology (St Johnston, 2002;

Bellen et al., 2010; McGurk et al., 2015).

The fruit fly life cycle is one of holomeabolism, i.e. complete metamorphosis. It

comprises of 4 life stages: embryo, larva, pupa, and adult. Adult female flies can lay up

to 400 eggs, each one containing an embryo (Greenspan, 1997). Those eggs will hatch

12-15 hours later into first instar larvae (Greenspan, 1997). The larval stages last

approximately 4 days and include two molts (Greenspan, 1997). The first instar larva

molts into the second instar and then the third instar larva (Greenspan, 1997). With each

molt the size of the larva increases exponentially. At the end of the third instar, the larva

enters the puparium, or pupal case, much like a caterpillar enters the cocoon. The adult

fly will eclose following 4 days of metamorphosis (Greenspan, 1997). In total,

metamorphosis from embryo to adult is usually 7 days, though this can be manipulated

by changes in temperature (Greenspan, 1997). As an ectothermic species, fruit fly

development and behavior depends upon ambient temperatures.

The power of Drosophila as a model system lies in its complex simplicity.

Drosophila have a short-lifespan, high fecundity, small number of chromosomes (4

chromosomes compared to 23 in humans), and fewer neurons (250,000 compared to

100,000,000,000 in humans). Yet, these simplicities belie the complexity of connectivity

and structure of its central nervous system (CNS) and the complex behaviors adult fruit

flies present. Though "less complicated" than the mammalian brain, the Drosophila CNS

shares organizational similarities with the vertebrate brain; both are composed of neurons

and glia that form structurally distinct sub-regions that are protected by a blood brain

barrier (McGurk et al., 2015). Also, of the known disease-causing human genes,

approximately 70% of them have homologs in Drosophila (Rubin et al., 2000; McGurk et

al., 2015).

Easily yielded genetic manipulations, such as the binary GAL4-UAS system, also

place Drosophila as an attractive model system for neurodegeneration (Brand and

Perrimon, 1993; Jenett et al., 2012). The GAL4-UAS system enables specific, targeted gene expression in discreet subsets of cells (Brand and Perrimon, 1993). GAL4 is a yeast modular protein that acts as a transcription activator in a variety of organisms, in addition to Drosophila (Brand and Perrimon, 1993). For cell-specific expression, GAL4 can be placed under the control of a native gene promoter (Brand and Perrimon, 1993). The GAL4 construct is colloquially referred to as the "driver" and there are hundreds of drivers for subsets of neuron families, structures, and tissue (Jenett et al., 2012; Vogelstein et al., 2014; McGurk et al., 2015). When expressed, GAL4 binds to UAS, which is the upstream activation sequence $CGG-N_{11}-CCG$, where N can be any base (Brand and Perrimon, 1993). The UAS is fused to the target gene, and, once GAL4 binds the UAS, the target gene will be expressed. Thus, this system allows for specific expression of targeted genes, for example a voltage gated calcium channel, in a driver specific set of cells, for example motor neurons, in a disease genetic background.

TBPH Loss of Function Mutants

The Drosophila ortholog of TDP-43 is TBPH. Like TDP-43 loss- and gain- of function models in mice, both exogenous and endogenous TBPH studies have shown maintaining normal TBPH protein levels in various cell types is critical for normal physiological functions (Casci and Pandey, 2015b). In flies, overexpression of either the human form of TDP-43 or the endogenous TBPH gene causes a significant reduction in lifespan (Hanson et al., 2010; Vanden Broeck et al., 2013; Casci and Pandey, 2015b). Likewise, reduced expression or complete knock-outs of TBPH cause reduced lifespan and motor defects (Feiguin et al., 2009; Hazelett et al., 2012; Diaper et al., 2013a, 2013b) Knock-down of TBPH in adult muscle cells, using the temperature inducible Gal80-

driver and UAS-RNAi, causes reduction in motor function (Diaper et al., 2013a).

Inducible knock-out of TBPH in glial cells also causes motor dysfunction, but only in

aged flies (Diaper et al., 2013b). Homozygous deletion of the endogenous TBPH gene

causes adult lethality; the animals will develop through the larval stages but will fail to

eclose from the pupal case (Hazelett et al., 2012; Diaper et al., 2013b). Therefore, TBPH

appears to be necessary for development and maintenance of normal physiological

functions.

Like TDP-43, TBPH is an RNA and DNA binding protein that functions to

regulate the expression of a variety of genes. In order to model the downstream effects of

loss of nuclear TDP-43, our lab created a TBPH deletion line. This deletion line, denoted

TBPHΔ, was created by removing the TBPH 5'-UTR via p-element excision (Hazelett et

al., 2012). These animals show two phenotypes: adult lethality, where the pupae fail to

eclose from the pupal case, and severe locomotion defects in the third instar larval stage

(Hazelett et al., 2012; Chang et al., 2014).

In order to identify classes and subclasses of genes whose expression was

changed with loss of TBPH, RNA-seq analysis was performed on the TBPH mutant

animals (Hazelett et al., 2012). In total, the expression of 910 gene transcripts was

differentially changed with loss of TBPH; transcripts of 681 genes were up-regulated,

while the transcripts of 229 genes were down-regulated (Hazelett et al., 2012). A majority

of differentially expressed transcripts encoded genes with conserved functions as DNA

binding proteins, histone binding and modification proteins, and RNA metabolism

proteins (Hazelett et al., 2012). Selecting for genes with predicted TBPH binding sites

and known functions in neurotransmission, the gene *cacophony* was one of several genes

identified as having a significantly changed splicing index in the TBPH mutant (Hazelett et al., 2012). *Cacophony* encodes the type-II voltage gated calcium channel that is necessary for full evoked neurotransmission at the neuromuscular junction (Kawasaki et al., 2002; Lee et al., 2014b). As vertebrate orthologs of *cacophony* have been identified as targets of TDP-43 binding in RIP-seq (RNA Immunoprecipitation sequencing) data collected from cortical neurons (Sephton et al., 2011), the interaction between TBPH and *cacophony* was of particular interest.

Though the index of *cacophony* splice forms was significantly changed in TBPH mutants, the overall transcript levels of *cacophony* were unchanged (Hazelett et al., 2012; Chang et al., 2014). However, using an antibody engineered against *cacophony*, Western analysis showed that TBPH mutant whole larvae have a 50% reduction in *cacophony* protein expression (Chang et al., 2014). This reduction was maintained at the boutons of the neuromuscular junction (Chang et al., 2014). Finally, the locomotion defects presented by TBPH mutant larvae were rescued by genetically restoring *cacophony* in all motor neurons, suggesting it is the TBPH dependent loss of *cacophony* driving the locomotion defects. Further analysis of the *cacophony* transcripts expressed in TBPH mutants revealed an enrichment of transcripts lacking exon 7. This observation was of particular note because of the fourteen described *cacophony* protein isoforms, only one lacks exon 7 (http://flybase.org/).

From these observations, it appeared that locomotion defects associated with loss of TBPH were due to the TBPH –dependent reduction in *cacophony* protein expression. What changes in physiology at the neuromuscular junction and within the motor circuit that drove the locomotion defect, however, are not known. We therefore asked the

following questions that guide the work presented here in chapters 2, 3, 4, & 5. First,

what physiology of the larval neuromuscular junction is changed in at TBPH dependent-

and *cacophony* dependent- manner? Second, is the larval locomotion defect driven by the

loss of *cacophony* in all motor neurons or in a subset of neurons in the motor circuit?

Third, does the enrichment of *cacophony* exon 7 deleted transcripts recapitulate defects in

larval locomotion observed in TBPH mutants?

NEUROANATOMY OF THE DROSOPHILA LARVA

Larval Connectivity & Crawling Behavior

The larval CNS is comprised of a brain and ventral nerve cord. The brain consists

of two lobular hemispheres that, during pupation, will become the brain and optic lobes

of the adult fly. The ventral nerve cord is comprised of the subesophigeal ganglion and

neuromeres that house motor neurons which project out of the CNS to innervate body

wall muscles (Figure 1B) (Landgraf et al., 1997; Kim et al., 2009).

Motor neurons of third instar larva are derived from 30 distinct neuroblasts and,

once differentiated, are maintained throughout metamorphosis (Landgraf et al., 1997;

Schmid et al., 1999; Hoang and Chiba, 2001). These motor neurons leave the ventral

nerve cord and project onto their target muscles via the intersegmental, segmental, or

transverse nerve (Landgraf et al., 1997; Schmid et al., 1999; Hoang and Chiba, 2001).

Because the experiments in this dissertation are done on the neuromuscular junction of

muscle 6/7, I will only describe the intersegmental nerve (Figure 1B). The intersegmental

nerve is further comprised of 3 nerve branches: ISN, ISNb, and ISNd, all of which target

internal muscles (Kim et al., 2009). Precise patterns of motor neuron connectivity depend

on the selective connection between the axon and muscle target and the establishment of a unique dendritic arborization pattern that determines the specificity and degree of synaptic input (Kim et al., 2009).

There are two broad classifications of motor neurons in Drosophila: low threshold and high threshold (Schaefer et al., 2010). Low threshold motor neurons are classified as Type 1b, or "big" neurons. These motor neurons have bigger synaptic terminals and project onto a single muscle (Schaefer et al., 2010). Conversely, high threshold motor neurons are classified as Type 1s, or "small" neurons (Schaefer et al., 2010). These motor neurons form smaller synaptic terminals and project onto groups of muscles (Schaefer et al., 2010). There are reported differences in membrane potential, voltage threshold, and delay-to-spike between these two motor neuron types.

It should be noted that the classifications of "low" and "high" threshold for mammalian and crayfish motor neurons are not conserved with Drosophila motor neurons (Schaefer et al., 2010). Unlike mammalian and crayfish motor neurons, there is not evidence for dividing Drosophila 1b and 1s motor neurons into tonic and phasic types (Schaefer et al., 2010). Also, whereas ordered motor neuron recruitment in mammals is explained by the size principle, in that motor units are recruited from low-force, slow-twitch to high-force, fast-twitch based on the size of the load (Henneman et al., 2011), recruitment of Drosophila motor neurons does not follow this principle (Schaefer et al., 2010). Drosophila motor neurons of the same identity have been observed to use different strategies to generate recruitment and firing (Schaefer et al., 2010).

The motor neuron that innervates muscle 6 and muscle 7 projects out of the ventral nerve cord by the ISNb (Kim et al., 2009). MN6/7-1b is unipolar and its highly branched dendritic arbor projects into the contralateral neuropil (Kim et al., 2009). Motor neurons project their dendritic projections in a stereotyped fashion and the selective connection between the motor neuron axon and muscle target is coordinated by the positioning of motor dendrites within the neuropil (Landgraf et al., 2003; Kim et al., 2009). The dendritic morphologies of individual motor neurons are stereotyped in position and orientation from segment to segment and animal to animal (Kim et al., 2009). They are maintained through embryogenesis to the formation of the pupal case, though they are increased and significantly expanded by the end of the late third instar (Kim et al., 2009).

Larval crawling is generated by peristaltic locomotion. It comprises alternating shortening phases and lengthening phases in which oblique and longitudinal muscle contract in turn (Peron et al., 2009). For forward displacement, muscle contractions begin in the lower abdominal segments of the larva and traverse up the body wall (Figure 1A)(Fox et al., 2006). In otherwise normal larvae, peristaltic waves are rhythmic and are ultimately the result of stimulation by the central pattern generators (CPGs) (Fox et al., 2006; Peron et al., 2009). These are neural oscillatory circuits within the central nervous that receive information from both motor neurons and sensory nerves (Inada et al., 2011; Gjorgjieva et al., 2013; Fushiki et al., 2016). The frequency of body wall contractions can be taken as an index of contractile responses (Peron et al., 2009).
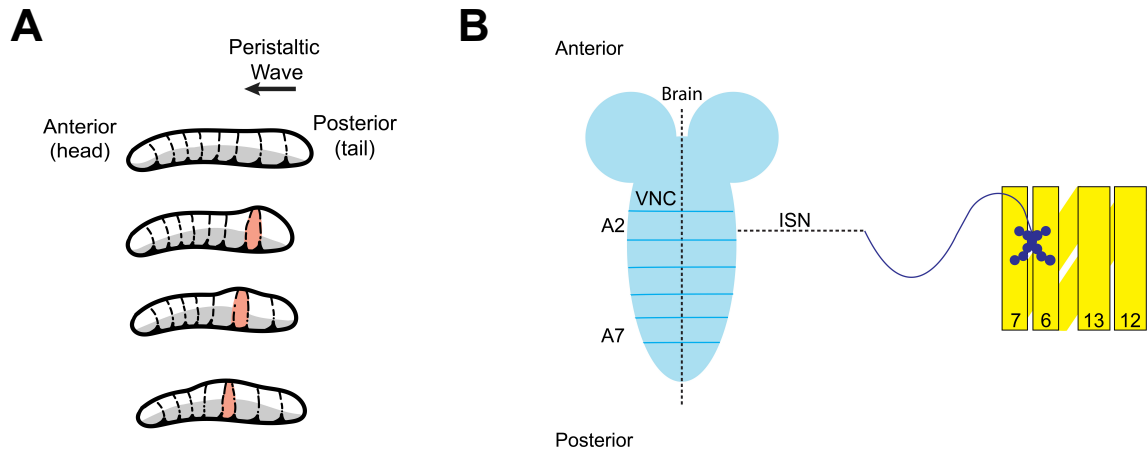
Figure 1. Larval locomotion and central nervous system. **A.** Forward larval locomotion is generated by the progression of peristaltic waves along the body wall in a posterior to anterior direction. **B.** Moto neurons are housed in the ventral nerve cord (VNC). The motor neuron innervating muscle 6 and muscly 7 in each abdominal segment leaves the VNC by the intersegmental nerve (ISN). It forms boutons on muscle 6 and 7. Figures adapted from Kohsaka et al 2012, and Hoang and Chiba 2001, respectively, with Jessica Lembke.

The Larval Neuromuscular Junction

A single Drosophila larva is comprised of 3 thoracic and 8 abdominal segments body wall segments. Each abdominal hemisegment is comprised of 30 body wall muscles, all highly stereotyped and innervated by one or more motor neurons. The larval body wall muscles lie in the internal surface of the body, just below the epidermis of the cuticle, and form an internal layer surrounding the viscera (Peron et al., 2009). It should

be noted that muscles in abdominal segments 2-7 are identically ordered and no muscle

crosses the dorsal midline (Peron et al., 2009). In total, there are 32 motor neurons in

each abdominal segment (Menon et al., 2013). While the neuromuscular junction displays

stereotyped connectivity, it also displays developmental and functional plasticity (Menon

et al., 2013).

In very general terms, the larval neuromuscular junction is comprised of the

presynaptic motor neuron and the postsynaptic muscle (Menon et al., 2013). During

development, differentiated motor neurons project their axons out of the ventral nerve

cord toward their target muscles (Broadie and Bate, 1993; Chen and Featherstone, 2005).

Once the axonal growth cones make contact with the target muscle, glutamate receptors

and discs large, the Drosophila homolog of membrane associated guanylate kinase

(MAGUK), will cluster at the contact site (Broadie and Bate, 1993; Chen and

Featherstone, 2005; Gorczyca et al., 2007). It should be emphasized that, unlike the

vertebrate neuromuscular junction that releases the neurotransmitter acetylcholine, the

Drosophila neuromuscular junction uses ionotropic glutamate receptors that are

homologous to the AMPA-type glutamate receptors in the mammalian brain (Menon et

al., 2013). The growth cone differentiates into the presynaptic terminal and forms a

bouton that contains multiple active zones, or sites of neurotransmitter release.

Postsynaptic scaffolds that resemble mammalian postsynaptic densities will form around

the bouton, forming the subsynaptic reticulum. Bouton formation occurs by the end of

embryogenesis (Broadie and Bate, 1993; Chen and Featherstone, 2005; Menon et al.,

2013) and from embryo hatching to late third instar, as the surface area of each muscle

increases 100 fold, boutons are continuously added to maintain the necessary synaptic drive through larval growth (Schuster et al., 1996; Liu et al., 2010; Menon et al., 2013).

There are broadly three types of boutons: I, II, and III that differ in size, shape, neurotransmitter released, size of the subsynaptic reticulum, and glutamate receptor composition (Gorczyca et al., 1993, 2007; Jia et al., 1993; Monastirioti et al., 1995; Landgraf et al., 2003; Menon et al., 2013; Gan et al., 2014). Type I boutons are found at muscle 6/7 and can be further differentiated into two distinct types: 1b, designated such for their "big" size and are formed by low threshold motor neurons (described previously), and 1s, designated such for their "small" size and are formed by high threshold motor neurons (also described previously) (Jia et al., 1993; Hoang and Chiba, 2001; Menon et al., 2013). Each neuromuscular junction has approximately 20-50 type I boutons, each with approximately 10 active zones (Menon et al., 2013). At muscle 6/7 however, the boutons are innervating both muscles and each bouton has approximately 20 active zones (Menon et al., 2013). Type II boutons are smaller than 2 μm in diameter and contain both dense core vesicles, which carry glutamate, and small clear vesicles, which contain octopamine (Jia et al., 1993; Monastirioti et al., 1995; Gan et al., 2014). Type III boutons are intermediate in size between type I and type II; they contain dense-core vesicles of different sizes and densities that carry glutamate, insulin-like peptide, and leucokinin-1 (Gorczyca et al., 1993; Jia et al., 1993; Landgraf et al., 2003; Gan et al., 2014). Type II boutons are found on muscles 12 and 13 and type III boutons are found on muscle 12. Neither type of bouton shows subsynaptic reticulum or stain for discs large, which function to regulate the size, shape, and function of synaptic structures (Gorczyca et al., 2007; Menon et al., 2013). It is interesting to note that muscle 12 is innervated by

all three bouton types, suggesting the presence of a selective membrane trafficking system at each bouton (Gorczyca et al., 1993, 2007; Jia et al., 1993).

Each active zone is formed by a T-bar structure comprised of the scaffold protein bruchpilot (Kawasaki et al., 2004; Harris and Littleton, 2015). Bruchpilot is the Drosophila homolog of the vertebrate ELKS/CAS (Wagh et al., 2006). This structure acts as a docking station for glutamate containing synaptic vesicles. T-bar structures colocalize with the type II voltage gated calcium channel *cacophony,* which is the primary source of extracellular calcium entry into the presynaptic space (Kawasaki et al., 2002, 2004). In fact, bruchpilot loss of function mutants show loss of T-bar structures and loss of *cacophony* localization at active zones (Wagh et al., 2006). Calcium regulation affects bouton growth and calcium entry through *cacophony* creates calcium microdomains and triggers synaptic vesicle fusion and bouton formation (Rieckhof et al., 2003a; Xing et al., 2005; Menon et al., 2013). *Cacophony* is essential to development; genetically knocking-out *cacophony* is embryonic lethal (Kawasaki et al., 2002).

When an action potential stimulates the opening of *cacophony* channels and the subsequent release of glutamate into the synaptic space, it will bind the postsynaptic glutamate receptors (GluRs). Drosophila express five glutamate receptors, designated GluRIIA, GluRIIB, GluRIIC/III, GluRIID, and GluRIIE (Harris and Littleton, 2015). These assemble into two possible 4-subunit configurations (Harris and Littleton, 2015). Each subunit configuration must contain either GluRIIA or GluRIIB, as they are redundant yet essential for development, as knocking-out both subunits is embryonic lethal (Harris and Littleton, 2015).

Larval body wall muscles are super-contractile in that they are able to contract to a length well below 50% of their resting length (Peron et al., 2009). Each muscle is composed of a single multinucleated fiber attached to the cuticle through its internal projections (apodemes) (Gramates and Budnik, 1999; Peron et al., 2009). Innervation of the larval body wall muscles in larvae is highly complex and is dependent upon multiple innervations. Contraction of the body wall muscles is not triggered by action potentials, but rather by post-synaptic potentials that are graded in amplitude and duration (Peron et al., 2009). The amplitude and duration of the postsynaptic potential from various types of boutons allows fine tuning of the muscle contractile response (Peron et al., 2009).

There are two types of neurotransmitter release that occur at the neuromuscular junction: evoked and spontaneous release (Engel, 2008; Melom et al., 2013; Frank, 2014). Evoked neurotransmitter release occurs in response to an action potential, in which the membrane potential of the cell is rapidly depolarized. Evoked release stimulates the rapid, mass release of glutamate into the terminal, ultimately leading to muscle contraction (Engel, 2008; Melom et al., 2013; Frank, 2014). Spontaneous release is the stochastic release of a single quantum of glutamate into the terminal (Engel, 2008; Melom et al., 2013; Frank, 2014). This type of release is thought to be important for maintaining synapse health, homeostasis, and tonicity of the synapse (Melom et al., 2013; Frank, 2014). While some active zones participate in both evoked and spontaneous release, there is evidence that some active sites will only participate in one or the other (Melom et al., 2013).

Both spontaneous and evoked neurotransmitter release at the neuromuscular junction are physiological mechanisms maintaining synaptic homeostasis. Homeostatic

mechanisms broadly stabilize various cellular properties within a range of physiologically

appropriate values (Harris and Littleton, 2015). At the Drosophila neuromuscular

junction, synaptic homeostasis is maintained by both *cacophony* and GluRs, as well as

other cellular players within signaling networks at the neuromuscular junction (Müller

and Davis, 2012; Frank, 2014; Harris and Littleton, 2015). Homeostatic plasticity can

easily be observed when GluR function is impaired, for example by the mutant

GluRIIA^{sp16} fly line (Müller and Davis, 2012; Frank, 2014). Synaptic homeostasis is

revealed by the subsequent decrease in mEPP amplitude but unchanged EJP amplitude.

The Muscle 6/7 Neuromuscular Junction as a Model System

The neuromuscular junction at muscle 6/7 is the most common larval

neuromuscular junction studied. This is for several reasons: the muscle are easily

identified and accessible, they are innervated by Type 1 boutons, and they are

isopotential, meaning there is little attenuation of the change in membrane potential along

the length of the muscle (Peron et al., 2009; Harris and Littleton, 2015).

Both evoked and spontaneous neurotransmission can be measured as postsynaptic

changes in membrane potential at muscle 6/7. Larvae can be dissected along the dorsal

midline, thus exposing the ventral musculature (Engel, 2008). The CNS can be removed

by cutting the motor nerves where they exit the ventral ganglion (Engel, 2008). Single

sharp electrode recordings can then be made at muscle 6 or muscle 7 (Engel, 2008).

Spontaneous release is measured as miniature end plate potentials (mEPPs). The

amplitude of these events corresponds to the minimum amplitude of a postsynaptic

potential and constitutes the unitary component, or quantum, of more evoked synaptic

potentials (Peron et al., 2009). These amplitudes should be 1mV and occur independent of extracellular calcium (Jan and Jan, 1976). The frequency of spontaneous release can also be quantified. This phenomenon has implications in regulating synapse strength, health, and synaptic homeostasis (Müller and Davis, 2012; Frank, 2014).

Evoked release is measured as excitatory junctional potentials (EJPs). This release is stimulated by the rapid depolarization of the presynaptic membrane potential, which causes the rapid fusion of many neurotransmitter containing synaptic vesicles. EJP amplitudes are typically between 20-25mV (Jan and Jan, 1976; Peron et al., 2009). This amplitude can vary depending upon extracellular calcium concentrations.

VOLTAGE GATED CALCIUM CHANNELS

TBPH mutants show a decrease in the expression of *cacophony*, the type II voltage gated calcium channel. Genetically restoring *cacophony* in motor neurons of TBPH mutants rescues defects in larval locomotion, suggesting locomotion defects in TBPH mutants are due to loss of *cacophony*. It has previously been shown that application of the calcium channel agonists BayK and FPL64176 to zebra fish embryos expressing human TDP-43 with an ALS point mutation G348C, alleviated motor defects (Armstrong et al. 2013). The interaction between forms of TDP-43 and voltage gated calcium channels, therefore, appears to regulate normal locomotive behavior.

Introduction to Voltage Gated Calcium Channels

Voltage gated calcium channels are multimeric proteins containing a pore-forming α- subunit and accessory β- and α2δ-subunits (Rieckhof et al., 2003). The α – subunit determines the main biophysical and pharmacological properties of the channel (Dolphin, 2009). In vertebrates, there are 10 voltage gated calcium channel α- subunits that fall into 3 distinct families: type 1, type 2, and type 3 (Dolphin, 2009; Ryglewski et al., 2012a). These can be further refined by activation, high threshold and low threshold, and pharmacological, L, N, P/Q/R, S, properties (Rieckhof et al., 2003). The high threshold L & N and the low threshold T channels are conserved throughout vertebrates and invertebrates; most vertebrate ion channel families are represented by a single fly gene (Rieckhof et al., 2003).

Voltage gated calcium channels assume several functions within the cell. Among these, they mediate inward calcium currents that depolarize the cellular membrane potentials, mediate excitability, and provide intracellular calcium signals that can activate gene transcription and neurotransmitter release (Rieckhof et al., 2003b; Gray et al., 2007; Dolphin, 2009; Lipscombe et al., 2013b). One mechanism the cell can use to achieve functional specificity is in subtle changes in channel isoform expression caused by differential splicing (Lipscombe et al., 2013a). Alternative splicing occurs at sites important for controlling channel activity, thus creating an array of functionally distinct channels (Gray et al., 2007). For example, analyses on the population of voltage gated calcium channel isoforms in different mouse brain regions, throughout development, has shown that the composition of voltage gated calcium channel mRNA splice isoforms varies by cell-type, development stage, and neuronal activity (Bell et al., 2004; Gray et

al., 2007). Alternative splicing generates subtle structural changes in the channel that can affect channel biophysics, density, targeting, post-transcriptional modifications, and coupling to downstream signaling pathways (Gray et al., 2007). Therefore, alternative splicing can act as a functional modifier within the cell (Lipscombe et al., 2013a).

The type 2, N-type voltage gated calcium channel ($Ca_V2.2$) has been implicated in synaptogenesis and regulation of gene expression (Brosenitsch and Katz, 2001). The C-terminus of the gene coordinates channel inactivation, modulation by G-proteins, modulation by calmodulin (as there is a CAM binding site), and protein-protein interactions that regulate activity and/or target the channel to specific cellular compartments (Gray et al., 2007). Inclusion and exclusion of specific exons of the channel are tissue-specific and confer functional specificity. For example, in mice, exon 37a is expressed preferentially in the dorsal root ganglia, where it functions to increase the sensitivity of the N-type channel to the voltage independent form of G-protein modulation (Gray et al., 2007). Therefore, natural variants of $Ca_v2.2$ can regulate the global activity of the channel within the context of the cellular milieu.

Cacophony, the Drosophila Type II Voltage Gated Calcium Channel

The *cacophony* gene encodes the α- subunit of the Drosophila type II voltage gated calcium channel, which is homologous to the vertebrate $Ca_V2.2$ (Kawasaki et al., 2002). During embryogenesis, *cacophony* contributes the major calcium current (Peng and Wu, 2007). In third instar larvae, *cacophony* is expressed broadly throughout the CNS. At the neuromuscular junction, it is the primary entry point of extracellular calcium to the presynaptic space (Kawasaki et al., 2004). In the somatodendritic region of motor neurons, it carries the major component of the voltage-dependent calcium current; when

cacophony is knocked down with RNAi, there is a significant reduction in somatically recorded voltage-dependent calcium currents (Worrell and Levine, 2008). At excitatory cholinergic synapses in the adult fly brain, it has also been observed to drive action potential-independent release of neurotransmitter (Gu et al., 2009).

Cells within the Drosophila CNS are extremely sensitive to changes in *cacophony* expression levels. C*acophony* is an essential gene and complete knock-outs are embryonic lethal (Kawasaki et al., 2002; Hou et al., 2008). Additionally, changes in *cacophony* expression can modulate animal behavior (von Schilcher, 1977; Smith et al., 1998; Chang et al., 2014). Reduction in *cacophony* expression causes reduced larval crawling (Hazelett et al., 2012; Chang et al., 2014). Expression of *cacophony* hypomorphic mutants is associated with a reduction by 50% in EJP amplitudes of third instar larvae, as well as courtship lovesong defects in adult flies (Smith et al., 1998; Kawasaki et al., 2000; Rieckhof et al., 2003a). Overexpression of *cacophony* can increase adult activity (Wiemerslage and Lee, 2015).

There are 14 defined *cacophony* isoforms (http://flybase.org/). However, the expression of each isoform in different regions of the Drosophila CNS is not defined. We do know, however, that the expression of *cacophony* is regulated by TBPH, and that loss of TBPH via p-element excision causes a 50% reduction in *cacophony* protein expression (Chang et al., 2014). And though the levels of *cacophony* transcript in whole animals are unchanged, the population of *cacophony* isoforms is changed with loss of TBPH (Chang et al., 2014). There is an enrichment of transcripts lacking exon 7 (Chang et al., 2014). Of the 14 defined *cacophony* isoforms, only 1 lacks exon 7, suggesting it is an exon holding functional importance to the channel.

OUTSTANDING QUESTIONS AND HYPOTHESES

There is ample evidence that expression of TDP-43, and its Drosophila ortholog TBPH, is necessary for motor behavior and that changes in expression levels of those proteins causes adverse effects on locomotion. In Drosophila larvae, we have shown that TBPH mutants present defects in larval crawling that is rescued by genetically restoring *cacophony,* the type II voltage gated calcium channel, in motor neurons. We therefore sought to identify TBPH-dependent changes in physiology, both peripherally at the neuromuscular junction and centrally within the motor circuit, that drove this defect in larval crawling and to understand the mechanism of *cacophony* rescue.

As *cacophony* is necessary for evoked neurotransmitter release at the neuromuscular junction, we hypothesized TBPH mutants would show decreased amplitudes of evoked release, but no change in spontaneous release. As motor neurons are sensitive to TBPH expression levels and TBPH mutants show fewer peristaltic waves, we hypothesized the motor nerves of TBPH mutants would show abnormal, non-patterned, non-rhythmic bursting patterns. Finally, as TBPH mutants show enrichment in *cacophony* transcripts lacking exon 7, and expressing *cacophony* isoforms rescues TBPH mutant crawling defects, we hypothesized loss of exon 7 in all *cacophony* transcripts would lead to loss of protein expression and larval locomotion defects.

The goal of this research is to understand the functional importance of nuclear TDP-43. By identifying mechanistic players in the etiology of ALS-associated phenotypes, we hope to understand the early phases of disease pathogenesis and identify potential targets of intervention.

CHAPTER 2

Materials & Methods

ANIMALS

All Drosophila stocks were reared at 25°C using standard procedures (Greenspan, 1997). The D42-GAL4 motor neuron driver (w^*; P{GawB}D42), UAS-*CACOPHONY* (*w**; P{UAS-cac1-EGFP}422A), UAS-TRPA1 (w*; P{UAS-TrpA1(B).K}attP2), and UAS-rpr.c (5824. w^{1118}; P{UAS-rpr.C}14) fly strains were obtain from the Bloomington stock center (http://flytocks.bio.indiana.edu/). The following Janelia GAL4 drivers were also obtain from the Bloomington stock center: R83E12-GAL4 (w^*,P{GMR82E12-GAL4}attP2, R12A09-GAL4 (w^*;P{GMR12A09-GAL4}attP2, R15A04-GAL4 (w^*; P{GMR15A04-GAL4}attP2, R75C05-GAL4 (w^*; P{GMR75C05-GAL4}attP2.

The TBPH null mutant, UAS-TBPH and TBPH-GAL4 driver lines were described previously (Hazelett et al., 2012). In most experiments, the background control line A1 was used. The A1 line was generated at the same time as the TBPH null mutant line by precise excision of a transposon located just upstream of the TBPH gene (Hazelett et al., 2012). The GluRIIA^{sp} line was obtained from the Davis Lab. In experiments with the GluRIIA^{sp} fly line, the background control line w1118 was used (Petersen et al., 1997). The UAS-mCD8::GFP; UAS-LacZ::NLS fly line was a gift of Dr. Sean Speese.

Alex Law, with Jer Cherng Chang, generated the cacexon7Δ lines in the following way. Fly embryos expressing the nuclease Cas9 under the control of the vasa promoter (vas-Cas9; y[1]M{vas-Cas9.RFP-}ZH-2A w[1118]/FM7a, P{w[+mC]=Tb[1]}FM7-A) were injected with one plasmid containing two guide RNAs and injected at a concentration of 200 ng/ul. The RNAs target Cas9 to sites on either side of the *cacophony* exon 7, resulting in two double strand breaks repaired by homologous

recombination. The guide RNA sequences were designed using the *Drosophila* RNAi Screening Center CRISPR2 web tool (http://www.flyrnai.org/crispr2/). The sequences selected were located in the coding regions flanking exon 7. The two crRNAs were cloned into two sibling vectors, and then these two independent crRNA cassettes fused into a single plasmid for increased injection efficiency. Ultimately two homozygous lines, $cac^{exon7\Delta(6)}$ and $cac^{exon7\Delta(8)}$, were isolated and maintained as independent lines.

CRAWLING ASSAYS

Third instar larvae were rinsed in PBS and placed on 2% agarose plates at either room temperature or 30C. The crawling paths of the larvae were recorded for 5 minutes using a moticam 1000 connected to a PC and using the MIPlus07 software (Motic Images). The surface temperature of the agarose plates was monitored with a temperature sensor connected to a LabQuest® Mini (Vernier) connected to a PC. The distance traveled in each video was traced and quantified using ImageJ software (http://imagej.nih.gov/ij/). The number of full poster-anterior peristaltic waveforms and the number of head turns were counted from these videos for each genotype. The distance of displacement for each forward crawl was also measured from these videos, as well as the duration of each wave, using the ImageJ software.

ELECTROPHYSIOLOGICAL METHODS

Intracellular recordings were made from the larval body wall muscle 6 in abdominal segment 3 using glass microelectrodes as previously described (Engel, 2008). Recordings were carried out at room temperature in extracellular HL3 saline which contained (in mM): 70 NaCl, 5 KCl, 20 MgCl$_2$, 10 NaHCO$_3$ 115 sucrose, 5 trehalose, 5 HEPES, and either 0.5, 1.0, or 2.0 CaCl$_2$ (as specified in text). Membrane potentials were recorded using an Axoclamp-2A amplifier (Axon Instruments), digitized at 10 kHz and stored with a Digidata 1440A digitizer (Axon Instruments) connected to a PC (Dell). Excitatory junctional potentials (EJPs) were generated by injecting current into severed axons, at 0.5 Hz, via a suction electrode and an A310 Accupulser (World Precision Instruments) through an isolation transformer. The average single EJP amplitude of each recording was taken from 30-35 EJPs, whose amplitudes were measured using Clampfit 10.2 software (Molecular Devices, Axons Instruments). Spontaneous miniature end plate potentials (mEPPs) were recorded over 3 minutes and analyzed using Mini Analysis 6.0.0.7 (Synaptosoft Inc.). Quantal content was calculated as the ratio of mean EJP amplitude divided by the mean mEPP amplitude, and then averaging recordings across all NMJs for a given genotype. For acute *cacophony* block, larvae were incubated in plectreurys toxin (PLTX-II, from Alomone Labs) for 5 minutes.

To record patterns of motor activity from the ventral nerve cord, third instar larvae were cut open along their dorsal midline, pinned open and extracellular recordings were made from peripheral nerves projecting from the 2nd and 7th neuromeres of the

intact central nervous system. Nerves were suctioned *en passant* with a glass suction electrode and recorded using an A-M Systems Differential AC Amplifier, digitized at 10kHz and stored with the Digidata 1440A digitizer as above. Recordings were made in HL-3.1, which contained (in mM): 70 NaCl, 5 KCl, 4 $MgCl_2$, 10 $NaHCO_3$ 115 sucrose, 5 trehalose, 5 HEPES, and 1.8 mM $CaCl_2$. To activate the motor program and stimulate fictive crawling, preparations were acutely incubated with 30 µM pilocarpine (Johnston and Levine, 1996). Recordings were made over 10 minutes and bandpass filtered (100Hz to 10 kHz) using Clampex software (Molecular Devices).

Sampled data from the nerves in the 2nd and 7th abdominal segments and a time stamp from the Digidata 1400A were passed to a custom program as comma-delimited text files. The program rectified and averaged the data into 1000-1200 50 ms bins. For each epoch of binned data, plots were prepared and auto- and cross-correlations were computed after subtracting the mean value for the epoch, which greatly increased the readability. The autocorrelation can be visualized as sliding a copy of the first half of the epoch across the full epoch and computing a correlation coefficient for each 50-ms increment in delay. Delays at which peaks align in the two data epochs produce high positive correlations, while delays at which peaks align with valleys produce high negative correlations. Generally, given measurements, Y_1, Y_2, …., Y_N at time X_1, X_2, …., X_N, the lag k autocorrelation function r is defined as:

$$r_k = \frac{\sum_{i=1}^{N-k}(Y_i - \bar{Y})(Y_{i+k} - \bar{Y})}{\sum_{i=1}^{N}(Y_i - \bar{Y})^2}$$

Time of the first peak after t=0 yields the period of the bursts in each trace. Cross correlations are computed according to a similar method except that the two half-data epochs are derived from data from both traces (2nd and 7th abdominal segments) in the same animal. The cross correlation r at delay d of two series x(i) and y(i) where I = 0, 1, 2,…,N-1, is defined as:

$$r = \frac{\sum_i[(x(i) - mx)(y(i - d) - my)]}{\sqrt{\sum_i(x(i) - mx)^2}\sqrt{\sum_i(y(i - d) - my)^2}}$$

Where mx and my are the means of the corresponding series.

Again, times at which peaks in two traces align produce high correlations. The first peak of the cross correlation gave the time delay between the A7 and A2 bursts. Averaged, auto-, and cross-correlation data were written as comma delimited text files that were readable by Microsoft Excel for additional manipulation (sometimes trace amplitudes were normalized) and plotting.

IMMUNOHISTOCHEMISTRY

To visualize the expression pattern of the GAL4 lines used, each driver line was crossed with the w*; UAS-mCD8::GFP; UAS-LacZ fly line. Third instar larva from these crosses were filleted, while keeping their CNS's intact, in ice-cold HL3 saline and fixed in 4% paraformaldehyde in PBS with 1% Triton X for 10 minutes at room temperature, followed by 15 minutes at room temperature with agitation. Preparations were then washed with PBS with 1% Triton X three times for 5 minutes with agitation at room

temperature. Samples were blocked in SEA Block (CALBIOCHEM) for 15 minutes at room temperature. The preparations were then incubated 3 times overnight at 4°C in anti-GFP in 50% glycerol (1:200; Thermo Fisher).

Following incubation in primary antibodies, the preparations were washed 4 times for 30 minutes in PBS with 1% Triton X with agitation. The preparations were then incubated 3 times overnight at 4°C in goat anti-rabbit IgG Alexa Fluor 488 (ThermoFisher). Following incubation, samples were washed four times for 30 minutes in PBS with 1% Triton X and incubated for 30 minutes in vectashield (Vectorlabs). The samples were then mounted in vectashield and imaged using an Olympus FV1000 laser scanning confocal.

To visualize *cacophony* at boutons of the NMJ, third instar larvae were filleted in HL-3 saline solution and fixed in Bouin's solution for 15 mins at room temperature. Samples were rinsed in an ethanol series, 10%-50% ethanol for 10 minutes each, and then rinsed in PBS with 1% Triton X for 30 minutes at room temperature. Samples were then blocked overnight in normal goat serum (ThermoFisher) at 4°C overnight.

The samples were then incubated in anti-cacophony at two concentrations (1:2000 or 1:4000) at 4°C overnight (Chang et al., 2014). The next day, samples were washed in PBS with 1% Triton X, 5 times for 10 minutes each, and then incubated overnight in biotin-conjugated goat anti rabbit antibody (1:1000 in 50% glycerol; ThermoFisher) at 4°C. Samples were then washed 5 times in PBS with 1% Triton X and incubated in Alexa Fluor 647 conjugated streptavidin (1:500 in 50% glycerol; ThermoFisher) at room temperature for one hour.

Samples were then again incubated in PBS with 1% Triton X for 30 minutes at room temperature, followed by an overnight incubation in normal goat serum at overnight in normal goat serum at 4°C. The preparations were then incubated overnight in anti-Brp (nc82 at 1:100; DSHB), washed 5 times in PBS with 1% Triton X, incubated for four hours at room temperature in goat anti-mouse Alexa Fluor 488, and washed in PBS with 1% Triton X. Following a 30 minute incubation in vectashield (Vectorlabs), the samples were mounted in vectashield and imaged using an Olympus FV1000 laser scanning confocal.

Cacophony fluorescence was quantified using ImageJ software. Image files were opened, split into bruchpilot and *cacophony* channels, and z-stacks compiled. The bruchpilot channel was used to identify and select the bouton regions of interest. The area and mean fluorescence of *cacophony* were then measured for each region of interest by ImageJ and total *cacophony* fluorescence calculated by multiplying the two measurements.

ELECTRON MICROSCOPY

To visualize the active zone ultrastructure of the NMJ in third instar TBPH mutants and control animals, we used a protocol adapted from Jia et al 1993. TBPH mutants and control animals were first filleted in HL-3 solution, the CNS removed, and fixed for 30 minutes in Modified Trump's Fixative. The preps were rinsed 3 times in 0.1 M cacodylate buffer plus sucrose 3 times for 10 minutes, post-fixed with 1% osmium tetroxide for 30 minutes, rinsed 3 times in 0.1 M sodium cacodylate for 10 minutes, and 3

times in distilled water for 10 minutes. Preparations were stained *en bloc* in 2% aqueous

uranyl acetate for 30 minutes, dehydrated in a graded ethanol series, and infiltrated with

Spurr's embedding resin.

Blocks were trimmed and oriented so that the longitudinal muscles in segments 3

or 4 could be visualized and 70 nm sections cut, either in cross –section or longitudinally,

on a Leica UC7 ultramicrotome. Sections were picked up on mesh grids and counter-

stained with aqueous uranyl acetate and Reynold's lead citrate. Images were collected on

an FEI Tecnai Spirit at 80 kV.

COURTSHIP ASSAYS

Courtship behavior was monitored using a custom acrylic apparatus that consisted

of 14 chambers measuring approximately 1 cm wide, 4 cm long, and 0.6 cm high

(Morton et al., 2010). Each chamber was divided in half with a removable paper barrier.

Five-day-old virgin males and virgin females were placed in each half of the chamber

using an aspirator. The flies were allowed to recover for 20 minutes and the paper barrier

subsequently removed. All 14 chambers were then recorded simultaneously using a

moticam 1000 connected to a PC and using the MIPlus07 software (Motic Images). Two

parameters were measured: the time to copulation and the percentage of males that

copulated within four hours of barrier removal. Virgin males and females were kept

isolated in vials in groups of approximately 10-15 before use.

CHAPTER 3

Cacophony expression in motor neurons rescues larval crawling defects, but not changes in NMJ physiology, in a Drosophila TDP-43 loss of function mutant.

ABSTRACT

Defects in the RNA-binding protein, TDP-43, are known to cause a variety of neurodegenerative diseases including amyotrophic lateral sclerosis (ALS) and frontotemporal lobar dementia (FTLD). A variety of experimental systems have shown neurons are sensitive to TDP-43 expression levels, yet the specific functional defects resulting from TDP-43 dysregulation have not been well described. We have previously shown that removing the Drosophila TDP-43 ortholog, TBPH, caused locomotion defects as third instar larvae. Furthermore, loss of TBPH caused a reduction in the expression of *cacophony*, the type II voltage-gated calcium channel; genetically restoring *cacophony* in motor neurons in TBPH mutant animals was sufficient to rescue the locomotion defects. In the present study, we examined the relative contributions of neuromuscular junction (NMJ) physiology to the locomotion defects. At the NMJ, we showed mEPP amplitudes and frequency require TBPH. Restored *cacophony* expression in motor neurons rescued mEPP frequency but not mEPP amplitude. These results suggest that the behavioral defects associated with loss of TBPH throughout the nervous system are not driven by peripheral defects, but rather central defects.

INTRODUCTION

TBPH null mutants show two important phenotypes: adult lethality and defective crawling in third instar larvae (Hazelett et al., 2012). TBPH mutants also show a reduction in *cacophony* protein expression in whole third instar larvae, which is sustained at NMJ boutons (Chang et al., 2014). Genetically restoring *cacophony* in the TBPH mutant, using the GAL4-UAS system and a set of pan-neuronal GAL4 drivers, rescued the crawling defect associated with the mutant (Chang et al., 2014). Using the classically described motor neuron driver D42-GAL4 to drive UAS-cacophony also rescued the third instar larval crawling defect, suggesting loss of cacophony, specifically in motor neurons, drives the crawling defect.

Though D42-GAL4 is classically described as a motor neuron specific driver, it also shows broad expression in sensory neurons along the body wall (Sanyal, 2009). While these sensory neurons can modulate the motor circuit, they are not themselves motor neurons. Therefore, I tested whether restoring *cacophony* in more discreet subsets of motor neurons could also illicit a rescue of the crawling defect, using driver lines for more discreet sets of motor neurons and neurons whose activation modulates motor behavior (Sanyal, 2009; Vogelstein et al., 2014).

Cacophony is the primary voltage gated calcium channel at the Drosophila NMJ and it is required for full evoked neurotransmission, but has not been reported to modulate spontaneous neurotransmitter release (Kawasaki et al., 2000, 2002; Kuromi et al., 2004; Lee et al., 2014b). As the TBPH mutant shows reduced *cacophony* protein expression at the NMJ, we hypothesized that TBPH mutants would show defective

evoked neurotransmitter release, but unchanged spontaneous release. At active zones, *cacophony* localizes into clusters around the bruchpilot T-bar structures (Kittel et al., 2006). Expression of mutant bruchpilot is associated with a decrease in *cacophony* expression, mis-localization of *cacophony* away from active zones, and changes in active zone ultrastructure. Therefore, we also visualized the active zone structure of TBPH mutants to determine if subsequent changes in ultrastructure were present.

RESULTS

Expressing cacophony in centrally located neurons rescues the TBPH mutant crawling defect

Larval crawling is a highly stereotyped behavior characterized by the synchronous contraction of muscles on the left and right side of the larval body (Fox et al., 2006). Forward crawling is generated by peristaltic waves of muscle contractions which travel from posterior to anterior body wall segments (Fox et al., 2006). These peristaltic waves are generated by central pattern generators and are dependent upon firing of motor neurons in the ventral nerve cord (Inada 2011). We have previously shown that loss of TBPH causes a dramatic reduction in larval crawling distance, which can be rescued by driving *cacophony* expression in motor neurons using the D42-GAL4 driver (Chang et al., 2014). These results suggested that the reduced crawling distances were therefore due to a motor neuron specific defect in the TBPH mutants. However, closer inspection of the D42-GAL4 driver has revealed it shows expression not only in motor neurons of the ventral nerve cord, but also cells in the protocerebrum of the brain and peripheral sensory neurons along the body wall (Sanyal, 2009). Therefore, we examined another motor

neuron driver described as being more specific for motor neurons, OK6-GAL4 (Sanyal, 2009). As previously described, expressing TBPH with the TBPH-GAL4 driver only partially rescued the larval crawling defects (Figure 1A). By contrast, expressing *cacophony* in motor neurons using the OK6-GAL4 driver in the TBPH mutant was more effective at restoring the distance crawled than rescue with TBPH (Figure 1A).

Although OK6-GAL4 showed more restricted expression specific to the motor neurons in the ventral nerve cord, it also showed expression in the brain hemispheres (Sanyal, 2009). To explore in more detail which cells require expression of *cacophony* to restore locomotion in the TBPH mutants, I tested a variety of driver lines that showed restricted expression in discreet sets of cells in the ventral nerve cord and brain. The drivers I selected had been shown to affect larval crawling behaviors (Vogelstein et al., 2014). The drivers tested were R75C05-GAL4, which is expressed in the AVM001b/2b cells in the brain, R82E12-GAL4, which is expressed in the A08n cells in the central nervous system, R12A09-GAL4, which is expressed in the TINa cells in the ventral nerve cord, and R15A09-GAL4, which is expressed in the SeIN161 cells in the central nervous system (Vogelstein et al., 2014). While these driver lines have been mapped, very little is known about them functionally beyond behaviors reported by Vogelstein et al 2014. Larvae show a higher probability of escape behavior when AVM001b/2b cells are activated with channel rhodopsin (Vogelstein et al., 2014). A08n cells overlap with nociception neurons and larvae show strong escape behavior when these cells are activated (Vogelstein et al., 2014). TINa neurons are labeled as interneurons (IN) and, when activated, larvae display strong turn-turn behavior (Vogelstein et al., 2014). SeIN161 cells are also labeled as interneurons (IN) and, when activated, larvae also show

strong turn-turn behavior, similar to TINa activation (Vogelstein et al., 2014). It is important to note that, unlike using the TBPH driver to restore TBPH levels, which partially rescued adult lethality (Hazelett et al., 2012), none of the drivers used to express *cacophony* were able to rescue lethality.

These experiments revealed two additional drivers, R75C05-GAL4 and R12A09-GAL4 that were sufficient to rescue locomotion when used to express *cacophony* in the TBPH mutant background (Figure 3.1A). Of the two, only R75C05-GAL4 was sufficient to rescue the crawling defect to the same extent as the motor neuron driver OK6-GAL4. R75C05-GAL4 drives expression in the AVM001b/2b neurons whose cell bodies are located in the protocerebrum of the Drosophila brain. Activation of these cells had previously been shown to produce a 20% increased probability of larval escape behavior during larval crawling (Vogelstein et al., 2014). Larval escape behavior is a sub-behaviotype of larval crawling. It is presented in response to noxious stimuli from which the larva wishes to escape. In its most mild form, it presents as forward crawling sans turn-turn behavior (Ohyama et al., 2013). In its most intense form, it often includes escape rolling, in which the larva rolls to escape the negative stimuli (Ohyama et al., 2013). In the supplemental videos reported by Vogelstein et al 2014, larvae expressing channel rhodopsin under the R75C05-GAL4 driver show strict forward crawling behavior, but no escape rolling, when the channel rhodopsin is activated. This result suggests activation of the AVM001b/2b cells is sufficient to drive mild escape behavior.

The total distance crawled is a relatively crude measure of the output of the motor program and is insufficient to identify specific defects in the motor program of TBPH mutant animals. To examine the TBPH mutant crawling behavior in more detail, we

quantified the frequency of posterior-anterior peristaltic waves, the time in which it took these waves to traverse the body completely, and the total displacement resulting from each wave. We then examined how driving *cacophony* in all motor neurons and more discreetly in the AV00M1b/2b cells altered these parameters (Figure 3.1B-E).

A Larval Crawling

B Frequency of peristaltic waves
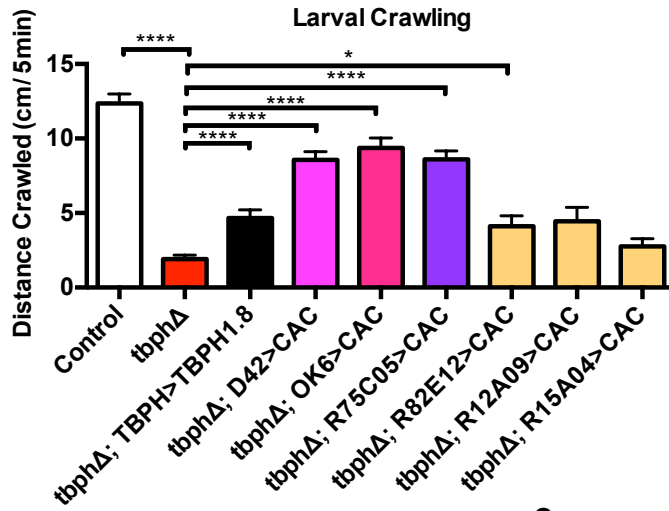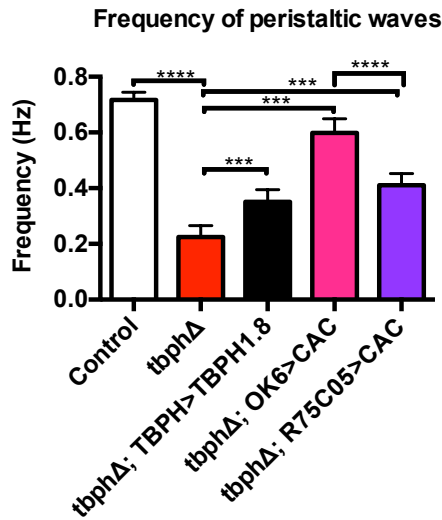
C Duration of peristaltic wave during crawling
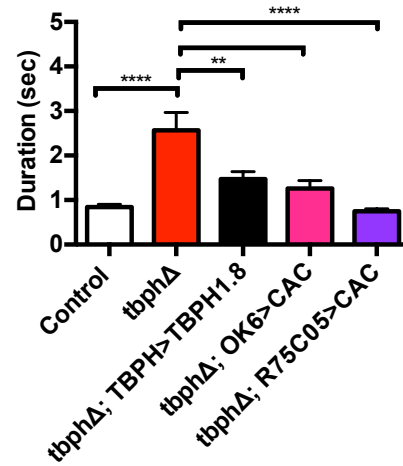
D Peristaltic waves producing displacement
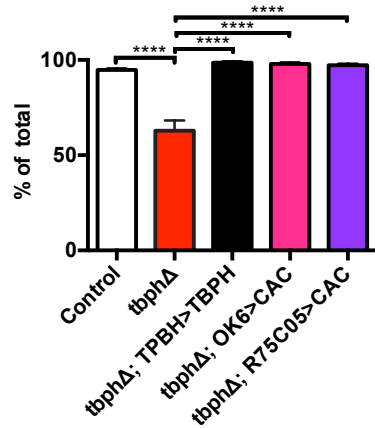
E Displacement per wave
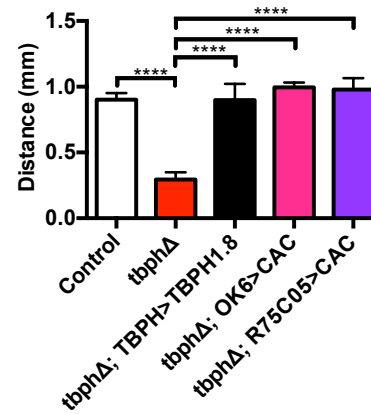
Figure 3.1. TBPH mutant larvae show defective motor behavior, which can be rescued by *cacophony* expression in selected neurons. **A.** TBPH null mutants crawl shorter distances than control larvae, which is partially rescued with the expression of a TBPH cDNA using a TBPH-GAL4 driver in the TBPH mutant background. Expression of *cacophony* in motor neurons using either the D42-GAL4 or the more specific OK6-GAL4 driver also rescues this effect. A variety of addition drivers were also used to express *cacophony,* the most effective of which was the R75C05-GAL4 driver. **B-E**. A more detailed examination of the crawling behavior shows *cacophony* expression in either motor neurons or using the R75C05-GAL4 driver rescues all measured components of crawling behavior. **B.** Frequency of peristaltic waves. Loss of TBPH led to an 80% reduction in the number of complete waves that progressed along the body, which was partially rescued with TBPH or *cacophony* expression. **C.** Duration of peristaltic wave. The time taken for a complete peristaltic wave to traverse the larva was significantly increased in TBPH mutants, which was rescued with either TBPH or *cacophony* expression. **D.** Number of waves producing displacement. The peristaltic waves in TBPH mutants were less likely to cause the larvae to move forward compared to controls, which was also rescued by TBPH and *cacophony* expression. **E.** Distance moved per peristaltic wave. For those waves that fid produce displacement, the distance travelled was reduced in TBPH mutants, which was again rescued by TBPH and *cacophony* expression. Data shown represent the mean and SEM of at least 10 animals and were analyzed using ordinary one-way ANOVA with a Sidak's multiple comparisons test (*** $p < 0.001$, ** $p < 0.01$, *$p < 0.05$).

TBPH mutants show an 80% reduction in the number of complete posterior-anterior peristaltic waves in the 5-minute observation period compared to background controls (Figure 3.1B). This reduction was partially rescued by expressing TBPH with the TBPH driver, and a more complete rescue was achieved by expressing *cacophony* in motor neurons using the OK6-GAL4 driver (Figure 3.1B). Similarly, driving *cacophony* with R75C05-GAL4 also partially rescued this parameter, although not as fully as the motor neuron driver (Figure 3.1B). The time taken for a complete peristaltic wave to travel the length of the larvae took approximately twice as long in TBPH mutant larvae compared to control animals (Figure 3.1C). This parameter was also rescued by TBPH and by driving *cacophony* with both motor neuron and R75C05-GAL4 drivers. Of the 50 complete posterior-anterior peristaltic waves TBPH mutants completed over 5 minutes, approximately 60% of these failed to produce forward displacement (Figure 3.1D), which was measured as averaging 0.25mm (Figure 3.1E). This contrasts with the control and all the rescues in which almost each complete peristaltic wave produced displacement of approximately 1.0 mm (Figure 3.1E).

These results show that the behavioral defects in TBPH mutants can be rescued not only by restoring *cacophony* broadly in all motor neurons, but also, surprisingly, by selectively restoring it in the discreet set of AVM001b/2b neurons located in the brain. There are relatively few qualitative or quantitative differences in the restoration of the behavior by expressing *cacophony* in these two different populations of neurons.

To verify the expression patterns of the OK6-GAL4 and the R75C05-GAL4 driver lines used in these experiments, both driver lines were crossed with flies expressing UAS-mCD8::GFP. Animals expressing OK6>mCD8::GFP show broad expression within lateral motor neurons of the neuropil, as well as expression in cells located in the brain (Figure 3.2B). This expression pattern matches those previously reported (Sanyal, 2009). Animals expressing R75C05>mCD8::GFP show localized, bilateral expression in two cells whose cell bodies appear to be housed in the protocerebrum of the brain (Figure 3.2C). This expression is identical to the expression pattern reported by Vogelstein et al. 2014, in which those cells were identified as AVM001b and AVM002b. It should be noted that axonal projections from those cell bodies were occasionally observed (one in approximately 6 preparations) extending into the ventral nerve cord, but never leaving the CNS.

A D42>mCD8::GFP

B OK6>mCD8::GFP

C R75C05>mCD8::GFP

D TBPHΔ; R75C05>mCD8::RFP
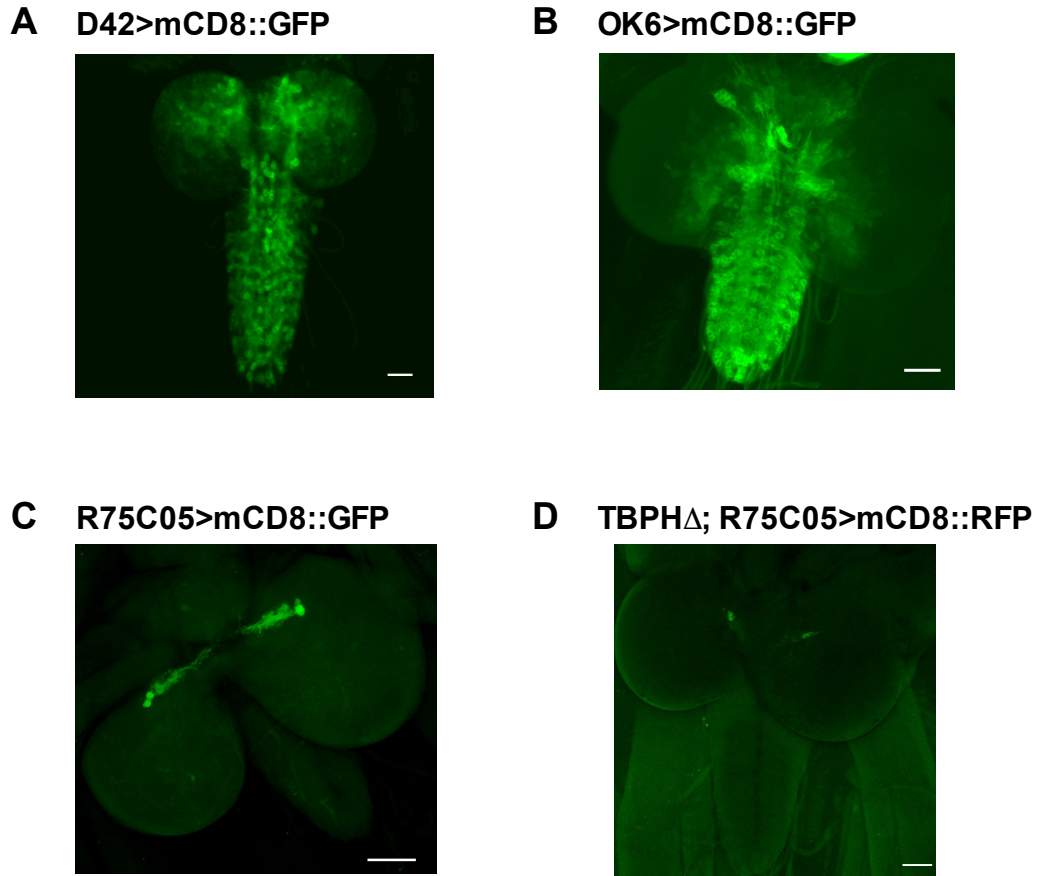
Figure 3.2. Expression patterns of the GAL4 drivers. **A.** Expression pattern of D42-GAL4 driving UAS-mCD8::GFP expression. Signal is enhanced with GFP antibody. **B.** Expression pattern of OK6-GAL4 driving UAS-mCD8::GFP expression; signal is enhanced with GFP antibody. **C.** Expression of R75C05-GAL4 driving UAS-mCD8::GFP; signal is enhanced with GFP antibody. D. Expression of R75C05-GAL4 driving UAS-mCD8::GFP in the TBPH mutant background (TBPHΔ) Scale bars represent 50 μM.

Synaptic transmission at the NMJ

Cacophony is required for evoked neurotransmitter release at the larval NMJ (Kuromi et al 2004, Kawasaki et al 2004). Because there is a significant reduction in

cacophony localization at the NMJ of TBPH mutants (Chang et al, 2014), it seemed

likely that evoked synaptic transmission would be defective in TBPH mutants.

Surprisingly, when I measured the amplitude of the evoked excitatory junctional

potentials (EJPs) in TBPH mutant larvae, I found no significant difference compared to

controls (Figure 3.3A). In addition to measuring evoked neurotransmitter release, we

analyzed spontaneous neurotransmitter release by measuring the amplitude and frequency

of miniature end plate potentials (mEPPs). At 1 mM calcium, TBPH mutants had

significantly smaller mEPPs compared to control animals (Figure 3.3D). These

observations were similar to those reported for another TBPH mutant allele (Vanden

Broeck et al., 2013). To determine whether this reduction was due to the loss of TBPH, I

expressed UAS-TBPH in the TBPH mutants using the TBPH-GAL4 driver. The mEPP

amplitude was significantly increased, confirming the reduced size in TBPH mutants was

due to loss of TBPH. However, expressing *cacophony* either in the motor neurons or in

the AVM001b/2b cells with the R75C05-GAL4 driver, failed to rescue this phenotype

(Figure 3.3D).

The frequency of spontaneous vesicle release in TBPH mutants was also

quantified. The frequency of mEPPs in TBPH mutants was significantly lower than that

of control animals (Figure 3.3E). This reduction was not rescued by expressing TBPH

under the control of the TBPH promoter (Figure 3.3E). It was, however, restored by

expressing *cacophony* in motor neurons using the OK6 driver (Figure 3.3E). Notably,

there was no significant increase in the frequency of mEPPs when *cacophony* was

expressed in the TINa (with the R12A09-GAL4 driver) or AVM001b/2b cells (with the

R75C05-GAL4 driver), suggesting the alterations in mEPP frequency were not associated with the behavioral defects of TBPH mutants (Figure 3.3E).

The finding that the TBPH mutants have unchanged EJP amplitudes despite having reduced mEPP amplitudes suggested that synaptic homeostasis had compensated for the reduced mEPP amplitude. Synaptic homeostasis is the process whereby synaptic strength is maintained within physiological ranges, especially when faced with perturbations of synaptic function, such as the loss of presynaptic voltage gated calcium channels or post-synaptic glutamate receptors (Turrigiano, 2007). At the Drosophila NMJ, there is accumulating evidence for several parallel signaling pathways acting to generate changes in quantal content to compensate for an altered post-synaptic response (Turrigiano, 2007). Based on these findings, quantal content of the EJP in TBPH mutants was calculated and shows that there is a significant increase in quantal content (Figure 3.3F), confirming that the NMJ in TBPH mutants is capable of synaptic homeostasis. Previous studies have shown that the signaling pathways that generate homeostasis converge on *cacophony* to enhance presynaptic calcium influx and thus neurotransmitter release (Frank 2009; Müller & Davis, 2012).

As *cacophony* levels are reduced in TBPH mutants and they nevertheless exhibit synaptic homeostasis, it is possible that no further homeostasis was possible. To test this, I imposed a post synaptic challenge by genetically expressing a loss of function allele of the alpha-2 subunit of the glutamate receptor (GluRIIA[sp16]; Petersen et al., 1997) in the TBPH mutant. As expected, the EJP amplitude in the GluRIIA[SP16] mutants was unchanged while the mEPP amplitude was reduced, thereby indicating higher quantal content compared to controls (Figure 3.3F) as previously described (Petersen et al.,

1997). When this mutation was combined with the TBPH mutant, there was no

additional increase in quantal content (Figure 3.3F).
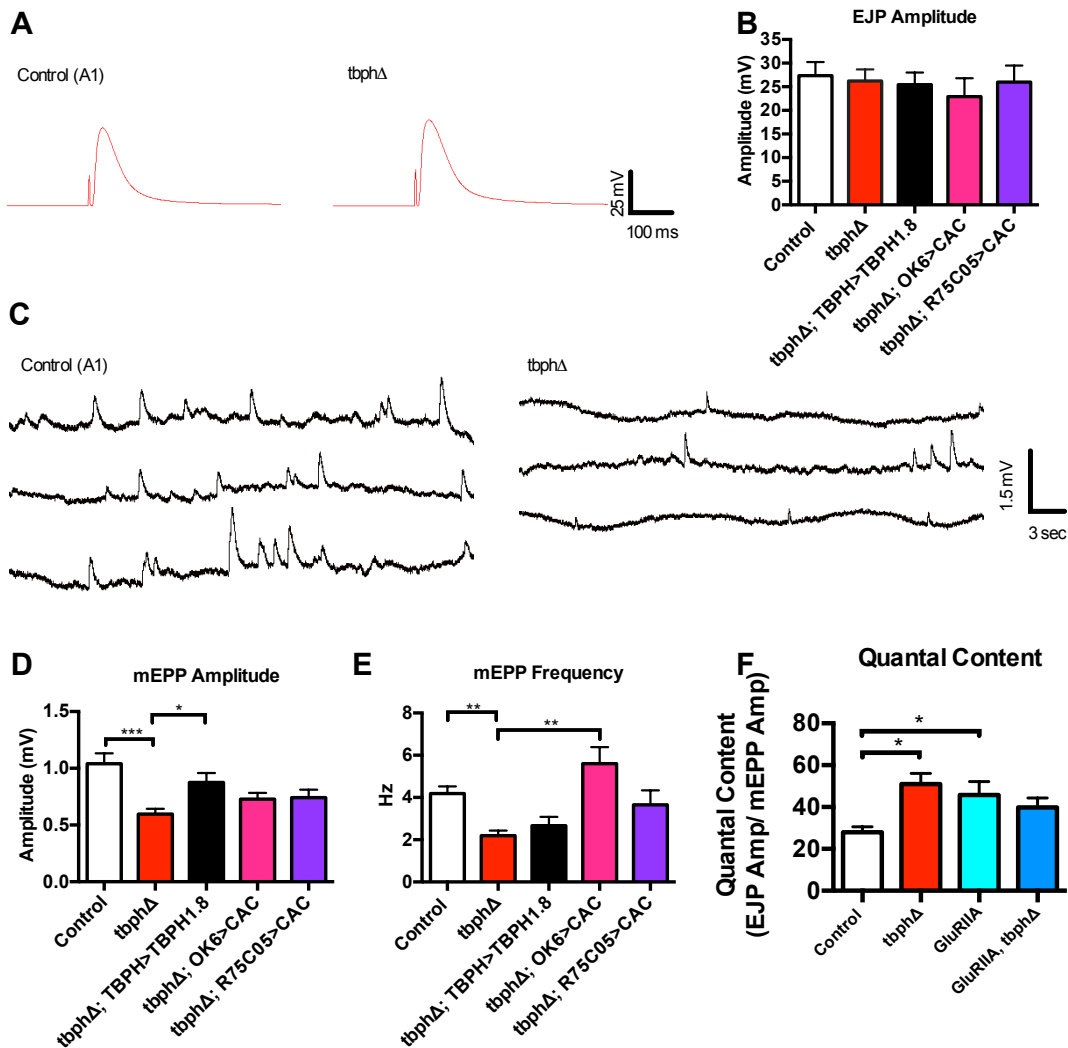
Figure 3.3. Synaptic physiology at the larval NMJ is defective in TBPH mutants. **A.**

Representative examples of excitatory junctional potentials (EJPs) from control and

TBPH mutant larvae. **B.** EJP amplitude is unchanged in all genotypes tested. **C.**

Representative example of miniature end plate potentials (mEPPs) control and TBPH

mutant larvae showing smaller and less frequency mEPPs in TBPH mutants. **D.** The

mEPP amplitude is reduced in TBPH mutants (red), which is rescued by expression of

TBPH (black), but not by expression of *cacophony* (pink). **E.** The mEPP frequency is

reduced in TBPH mutants and is not rescued by TBPH expression, but is rescued by

expression of *cacophony* in motor neurons, but not with the R75C05-GAL4 driver. **F.**

Quantal content. The quantal content of the EJPs was calculated as the ratio of EJP

amplitude to mEPP amplitude as was increased in both TBPH and glutamate receptor

mutants. The double mutant showed no further increase in quantal content. All

experiments were carried out in 1 mM calcium. Data represent the mean and SEM of at

least 10 animals and were analyzed using ordinary one-way ANOVA with a Sidak's

multiple comparisons test (*** $p<0.001$, ** $p< 0.01$, * $p <0.05$).

TBPH mutants do not show defective active zone ultrastructure at the NMJ

　　　Cacophony localizes with bruchpilot and other active zone scaffold proteins of the

bouton (Kittel et al., 2006; Fouquet et al., 2009). Mutations in either bruchpilot, or the

scaffold protein RIM, have been shown to affect *cacophony* localization at active zones

and impact active zone ultrastructure (Kittel et al., 2006; Fouquet et al., 2009). As TBPH

mutants show a reduction in *cacophony* localization at the NMJ, it was possible that their

ultrastructure was changed. Though we had already determined that the number and size

of boutons in TBPH mutants was unchanged using light microscopy (Hazelett et al.,

2012; Chang et al., 2014), such a method could say nothing about active zone

ultrastructure. I therefore looked at TBPH mutant ultrastructure using electron microscopy.

TBPH mutant and control animal third instar larvae were filleted, fixed, embedded in resin, and boutons on muscle 6 and 7 from abdominal segments 3 and 4 observed using an electron microscope (Figure 3.4). T-bar structures and clear, glutamate-containing vesicle clustering observed, as was mitochondrial load. No obvious changes to T-bar structure or vesicles clustering were observed between TBPH mutants and wild type animals (Figure 3.4A'-D'). Mitochondrial load also appeared unchanged (Figure 3.4B' &D').

YW1118

A — m6, m7 (Cross-section)

A' — M, M, M (Cross-section)

B (Longitudinal)

B' — M, M, 500 nm (Longitudinal)

TBPHΔ

C — m7

C' — M

D

D' — M, M, M
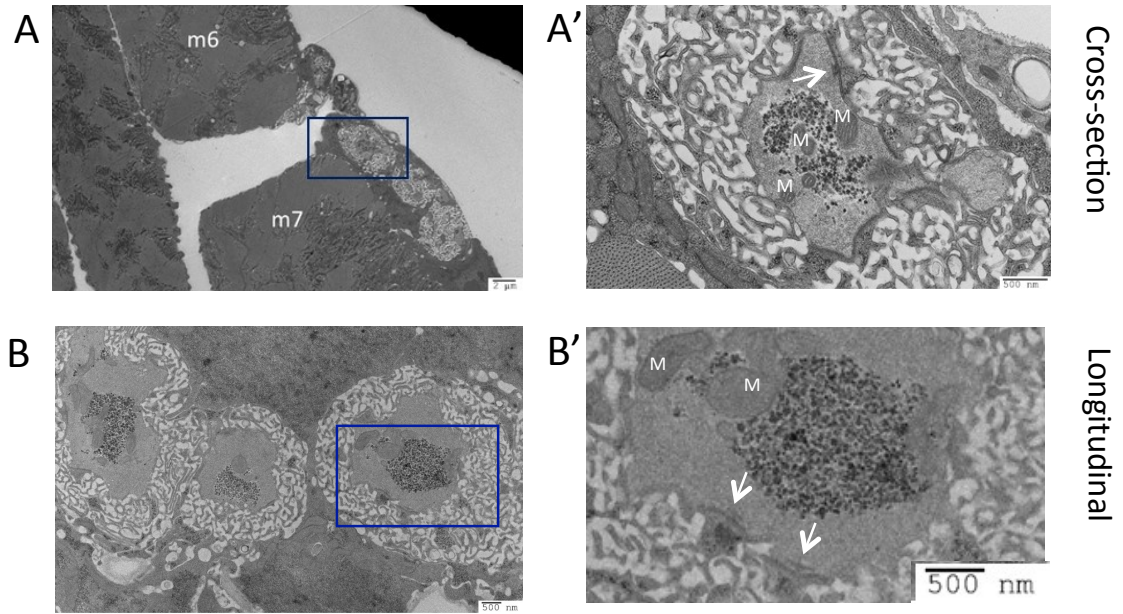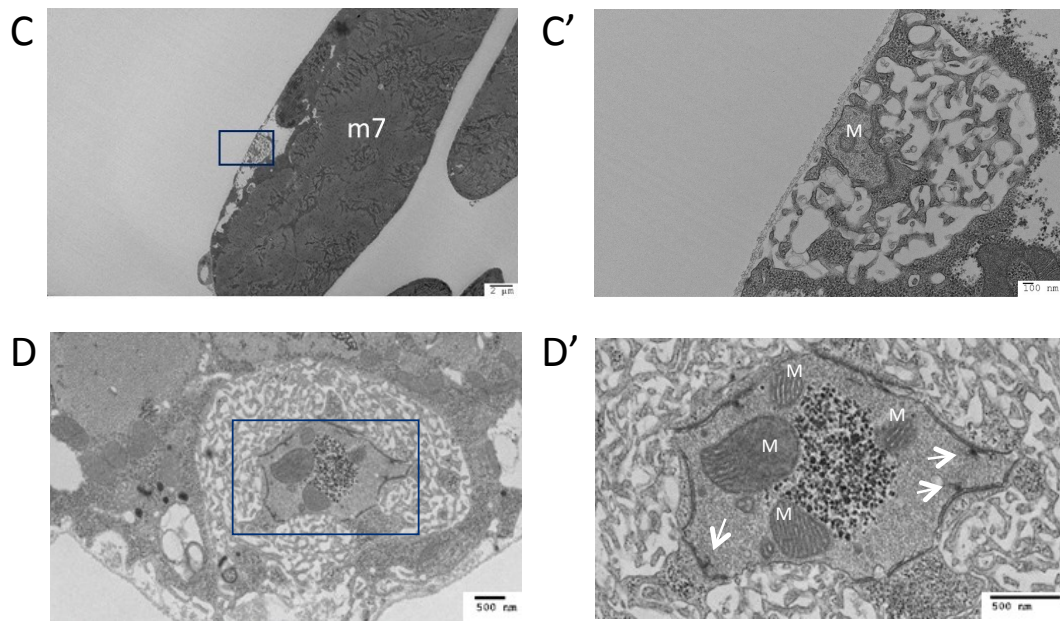
Figure 3.4. Electron micrographs of boutons on muscle 6 and 7 show active zone ultrastructure is unchanged in TBPH mutants. **A-A'**. Cross-section of muscle 6 (m6) and muscle 7 (m7) in YW1118 third instar larvae. The blue box in A indicates the area shown

in A'. White arrows indicate T-bar structures that form the active zones. Capitalized M indicated mitochondria. **B-B'.** Longitudinal sections of boutons from muscle 6 of a third instar YW1118 larva. **C-C'.** Cross-section of bouton on muscle 7 (m7) in TBPH mutant third instar larva. **D-D'.** Cross-section of bouton on muscle 6 in TBPH mutant third instar larva. There are intact T-bar structures surrounded by clear vesicles containing glutamate. Scale bars are indicated on each individual micrograph.

Cacophony regulates the frequency of spontaneous release at the NMJ

An unexpected result from the analysis of synaptic transmission was the apparent *cacophony* dependence of the frequency of mEPPs (Figure 3.2E) as this parameter is not normally believed to be directly regulated by voltage-dependent calcium channels (Lee et al., 2014b). To confirm that the frequency of mEPPs was *cacophony* dependent, the small synthetic peptide plectreurys toxin (PLTX-II) was used to block *cacophony* function. PLTX-II is a specific, irreversible inhibitor of type II voltage gated calcium channels and blocks *cacophony* function (King, 2007). Both EJP amplitudes and mEPP frequencies were measured in the presence of 2 nM of PLTX-II (Figure 3.5). In the presence of PLTX-II, EJP amplitude was, as expected, reduced by over 95% in both the TBPH mutant and control animals, confirming the *cacophony* dependence of the EJPs (Figure 3.5A). The frequencies of mEPPs were similarly reduced by over 60% in both the TBPH mutant and control animals, suggesting that acute *cacophony* function is required to regulate the spontaneous vesicle release (Figure 3.5B). The amplitude of the mEPPs was, as expected, unaffected by PLTX-II (Figure 3.5C).
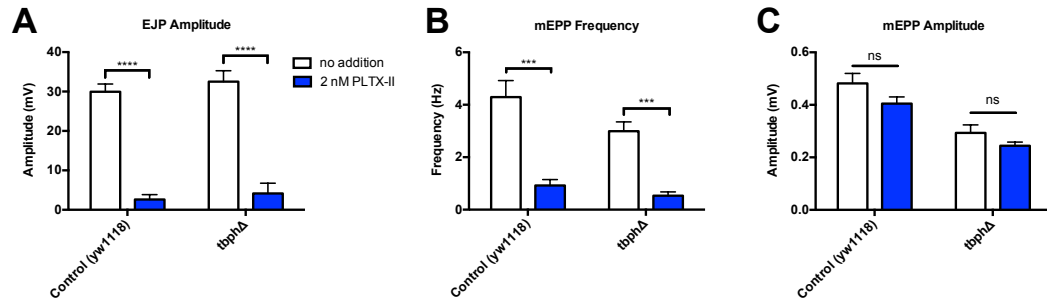
Figure 3.5. Effect of the *cacophony* irreversible antagonist PLTX-II on NMJ synaptic transmission. **A.** The EJP amplitude is blocked by over 90% in both control and TBPH mutant larvae. **B.** PLTX-II significantly reduces mEPP frequency in both control and TBPH larvae. **C.** PLTX-II has no effect on mEPP amplitudes in either control or TBPH larvae. Data were analyzed using multiple t-tests (****$p < 0.0001$).

DISCUSSION

TBPH has previously been reported to function in regulating both mEPP amplitude and frequency of spontaneous release (Diaper et al., 2013). Here, we failed to elicit a rescue in the frequency of spontaneous release, but we did observe a TBPH-dependent rescue in mEPP amplitude, confirming a function for TBPH in regulating the amplitude of mEPPs (Figure 3.2D). Spontaneous neurotransmitter release is a core element of synaptic communication in mature neurons and is thought to function in modulating activity-dependent transmission and synaptic homeostasis (Fatt and Katz, 1952; Frank et al., 2006; Lee et al., 2010). Our inability to rescue changes in mEPP

amplitude while rescuing larval crawling suggests this parameter does not directly

regulate larger, systems-dependent behavior. This conclusion is further supported by the

fact that, though driving *cacophony* with the R75C05-GAL4 driver rescued TBPH mutant

crawling, these animals showed no rescue in frequency of spontaneous release at the

NMJ (Figure 3.2E). Therefore, it appears that TBPH-dependent changes in physiology at

the neuromuscular junction are not driving the observed crawling defects.

 Cacophony is the primary voltage-gated calcium channel at the Drosophila NMJ

and is known to regulate evoked neurotransmission (Lee et al., 2014b). It localizes with

other presynaptic active zone proteins, bruchpilot and RIM, at active zones and

expression of hypomorphic versions of the channel, like *cac^s*, causes significant

reductions in EJP amplitude (Kawasaki et al., 2004; Fouquet et al., 2009; Graf et al.,

2012; Lee et al., 2014b). Blocking *cacophony* channels irreversibly with PLTX-II

similarly caused a reduction in EJP amplitude (Figure 3.5A). Although *cacophony* is

known to regulate evoked neurotransmitter release, it is not known to directly regulate

spontaneous release (Lee et al., 2014b). Therefore, not only was it initially surprising that

our TBPH mutant showed no reduction in evoked release, but equally surprising that

driving UAS-Cacophony with the OK6-GAL4 driver was sufficient to rescue the

frequency of spontaneous release (Figure 3.2E). To test directly whether *cacophony*

regulates the frequency of spontaneous release, we pharmacologically blocked

endogenous *cacophony* channels with PLTX-II. Blocking *cacophony* with PLTX-II

reduces the frequency of spontaneous release, while not reducing mEPP amplitude

(Figure 3.5B-C). Therefore, it appears that *cacophony* does, in fact, function in regulating

the basal frequency of spontaneous release at the NMJ, a function of the channel not previously reported.

Finally, though no major synaptic defects were observed in TBPH mutants, there was nonetheless a reduction in spontaneous release. While we had previously confirmed no gross change in bouton size or shape (Chang et al., 2014), we could not rule out the possibility of changes to active zone ultrastructure that could contribute to the reduction in spontaneous release. Analysis of active zone ultrastructure with electron microscopy, however, showed no obvious changes in T-bar formation or distribution at active zones in TBPH mutants (Figure 4A'-D'). Glutamate-containing vesicle clustering at the T-bars also appeared to be unchanged, suggesting the observed changes in spontaneous release of TBPH mutants are not due to changes in active zone ultrastructure (Figure 3.4).

These results demonstrate some defects in synaptic transmission due to the loss of TBPH, some of which can be reversed by expression of *cacophony* in motor neurons. However, the lack of concordance between the *cacophony*-dependence of synaptic physiology and behavior suggests that these defects are not sufficient to explain the defects in larval locomotion.

OUTSTANDING QUESTIONS

There are a few outstanding questions from the results presented in this section. The first question revolves around the nature of the *cacophony* rescue. While driving *cacophony* in all neurons and in motor neurons rescues the larval crawling defect, adult

lethality of the TBPH mutants has never been rescued. Here I will address one possible explanation for this lack of rescue. First, it has been shown that both up- and down-regulation of TBPH increases the expression of the neuronal microtubule-associated protein Map205 (Vanden Broeck et al., 2013). Up-regulation of Map205 lead to cytoplasmic accumulations of the ecdysteroid receptor and a failure to switch gene programs associated with that receptor from a pupal to adult pattern (Vanden Broeck et al., 2013). Any loss of function associated with this interaction does not appear to converge upon *cacophony*.

The second question arises from the report that *cacophony* rescues the frequency of mEPPs, but not the amplitude of mEPPs. While it was not surprising that *cacophony* did not rescue mEPP amplitude, it was surprising that it should function in regulating the frequency of their release because such a function has not been previously reported for the channel. The exact mechanisms of the rescue are startlingly unclear, primarily because little is understood about the function and mechanism of spontaneous release. In central synapses of the mammalian brain, spontaneous neurotransmission is reported as a way for the synapse to maintain tonicity, homeostasis, priming, and plays a possible function in long-term potentiation (Kavalali, 2014). At the NMJ, spontaneous release is also thought to maintain synaptic integrity and homeostasis (Frank et al., 2006; Kavalali, 2014). And there is evidence that specific active zones show higher probability of participating in spontaneous release than evoked release (Melom et al., 2013). Does *cacophony* dictate this active zone specialization? Is it a function of the channel itself or the resulting Ca^{2+} microdomains formed when it opens that causes this specialization?

In Drosophila, the rapid induction and sustained expression of synaptic homoeostasis are blocked by mutations in *cacophony*, suggesting that *cacophony* is directly involved in the presynaptic mechanisms that generate a homeostatic change in presynaptic transmitter release (Frank et al., 2006). Furthermore, this modulation appears to converge on spontaneous release, specifically mEPP amplitudes. If spontaneous release can modulate homeostasis and *cacophony* can also modulate homeostasis, is there evidence that *cacophony* could modulate homeostasis via spontaneous release? Either blocking GluR function pharmacologically with PhTx or expressing GluRIIA (previously described) elicits a reduction in mEPP amplitude, but no change in EJP amplitude, resulting in an increase in quantal content and thus intact synaptic homeostatic compensation (Frank et al., 2006; Frank, 2014). While mutations in *cacophony* do not cause reductions in mEPP amplitude, expressing *cacophony* mutants with the GluRIIA construct, or pharmacologically blocking GluR, results in a decrease in mEPP amplitude and suppressed synaptic homeostatic compensation in the GluRIIA background (Frank et al., 2006). It is unclear whether *cacophony* functions to do this via modulating either mEPP amplitude or frequency.

Finally, the third question that arises from these results is the absence of a defect in evoked neurotransmission. Though other TBPH mutant lines have also shown no changes in EJP amplitudes (Diaper et al., 2013b), the literature is rich with reports that expressing mutant forms of *cacophony,* or knocking it down with RNAi, decrease evoked neurotransmission. Here we also showed blocking endogenous *cacophony* with PLTX-II decreased EJP amplitude. Yet the TBPH mutant, that shows a decrease in *cacophony*

protein expression at the NMJ, shows normal evoked neurotransmission and intact

synaptic homeostasis. Is this a consequence of developmental compensation?

CHAPTER 4

TDP-43 loss of function mutants show defective motor program that is rescued by restoring *cacophony* in the centrally located AVM001b/2b neurons.

ABSTRACT

A variety of experimental systems have shown that neurons are sensitive to TDP-43 expression levels, yet the functional defects associated TDP-43 dysregulation in the motor program have not been well described. Using the Drosophila TDP-43 ortholog TBPH, we previously showed that TBPH null animals present severe locomotion defects in the third instar, as well as a reduction in the expression of the type II voltage-gated calcium channel *cacophony*. Locomotion in TBPH mutants is recovered by genetically restoring *cacophony* in motor neurons, suggesting the TBPH associated crawling defect is driven by loss of *cacophony*. Furthermore, we have shown that TBPH-dependent changes in physiology at the NMJ are not sufficient to drive the locomotion defect. We therefore examined the relative contribution of the motor program to the locomotion defects and identified subsets of neurons that require *cacophony* expression to restore normal locomotion. TBPH mutants displayed reduced motor neuron bursting and coordination during crawling, restoring *cacophony* selectively in two pairs of cells located in the brain, the AVM001b/2b neurons, rescued the locomotion and motor defects. These results suggest that the behavioral defects associated with loss of TBPH throughout the nervous system can be associated with defects in a small number of genes in a limited number of central neurons, rather than peripheral defects.

INTRODUCTION

TBPH mutants show severe locomotion defects (Hazelett et al., 2012; Chang et al., 2014). They crawl shorter distances, show a smaller frequency of anterior-posterior peristaltic waves, and the time in which it takes these wave to traverse the body is significantly longer (Figure 3.1). Whole third instar TBPH mutants also show reduced *cacophony* protein expression (Chang et al., 2014). Genetically restoring *cacophony* broadly in all motor neurons, using the OK6-GAL4 driver, or in the VM001b/2b cells, using the R75C05-GAL4 driver, restores locomotion (Figure 3.1). The larval crawling defect is therefore caused by the reduction in *cacophony* expression in TBPH mutants. However, though TBPH mutants show some alterations in spontaneous neurotransmitter release at the NMJ, these alterations are not sufficient to drive the crawling defect.

Crawling is the result of several coordinated processes in the larval motor circuit (Fox et al., 2006). Peristaltic waveforms are the direct result of motor neuron activation by cells upstream within the motor circuit, including the central pattern generators (Marder and Bucher, 2001; Fox et al., 2006). There is also evidence that progression of the peristaltic waveform is dependent upon motor neuron cross-talk; if motor neurons innervating abdominal segment 3 are silenced, the waveform will not continue to abdominal segment 4, 5, 6 or 7 (Inada et al., 2011). It has also been reported that mutations in proteins that affect larval crawling directly impact motor nerve burst patterns (Fox et al., 2006). We therefore hypothesized that TBPH mutant motor nerves would show a-rhythmic, un-patterned bursts. We hypothesized that genetically restoring *cacophony* in the AVM001b/2b cells, using the R75C05-GAL4 driver, would restore

patterned motor bursts and therefore establish a novel function for the AVM001b/2b cells within the motor circuit.

RESULTS

CNS Motor Output

Forward larval crawling is generated by peristaltic waves traversing the length of the larval body wall in a posterior to anterior fashion (Fox et al., 2006). The rhythmicity of these waves is likely to be generated by a central pattern generator (CPG) (Marder and Bucher, 2001; Kohsaka H1, 2012). The CPG generates rhythmic motor neuron bursts and coordinates patterns of motor bursts between neuromeres segments, generating a burst delay between adjacent segments (Inada et al., 2011; Kohsaka H1, 2012; Fushiki et al., 2016). Motor neurons in the ventral nerve cord (VNC) are not merely downstream effectors of the central pattern generator, but function to regulate the propagation of the patterned activity between adjacent segments (Inada et al., 2011). Behavioral analysis has shown that TBPH mutants have far fewer anterior-posterior peristaltic waves (Figure 3.1B), a higher occurrence of incomplete waves (Figure 3.1D), and longer times-to-completion of their peristaltic waves (Figure 3.1E) than control animals. These components of the crawling behavior are restored by expressing *cacophony* in motor neurons and neurons in the brain. To determine whether restoring expression of *cacophony* in these populations of neurons had the same effect on the output from the central pattern generator, I monitored the motor output from the CNS in semi-intact larvae.

Focal extracellular recordings were made *en passant* from intact peripheral nerves projecting on muscle 6/7 in abdominal segment 2 (A2) and abdominal segment 7 (A7; Figure 4.1). When the preparation was bathed only in saline solution with calcium, spontaneous bursting in control animals that became more reliable with the addition of pilocarpine was observed. Subsequent experiments used pilocarpine (30 µM) to activate the motor program and has been shown previously to stimulate fictive crawling (Johnston and Levine, 1996; Baudoux et al., 1998). In TBPH mutants, consistent bursting was not observed, even with the addition of pilocarpine, although non-patterned activity was clearly visible (Figure 4.2).

In order to quantify the motor patterns from the nerves innervating A7 and A2, the traces were first rectified and grouped each data point into bins of 50ms (Figure 4.1B). Each rectified trace was then run through an autocorrelation function (Figure 4.1C). Autocorrelation is a mathematical tool for finding non-random patterns within a time-dependent data set and can be used to measure the similarity between observations as a function of the time lag between them (Ryan, 2006). From the lag time of the first peak, the frequency of bursts for the nerves innervating A7 and A2 was calculated (Figure 4.1C). To calculate the lag time between corresponding A7 and A2 bursts, the A7 and A2 recordings were cross-correlated. Cross-correlation is a mathematical tool in which the similarity of two series is measured as a function of the displacement of one relative to the other (Ryan, 2006). The lag time between A7 and A2 bursts was calculated from the cross-correlation coefficient (Figure 4.1D).
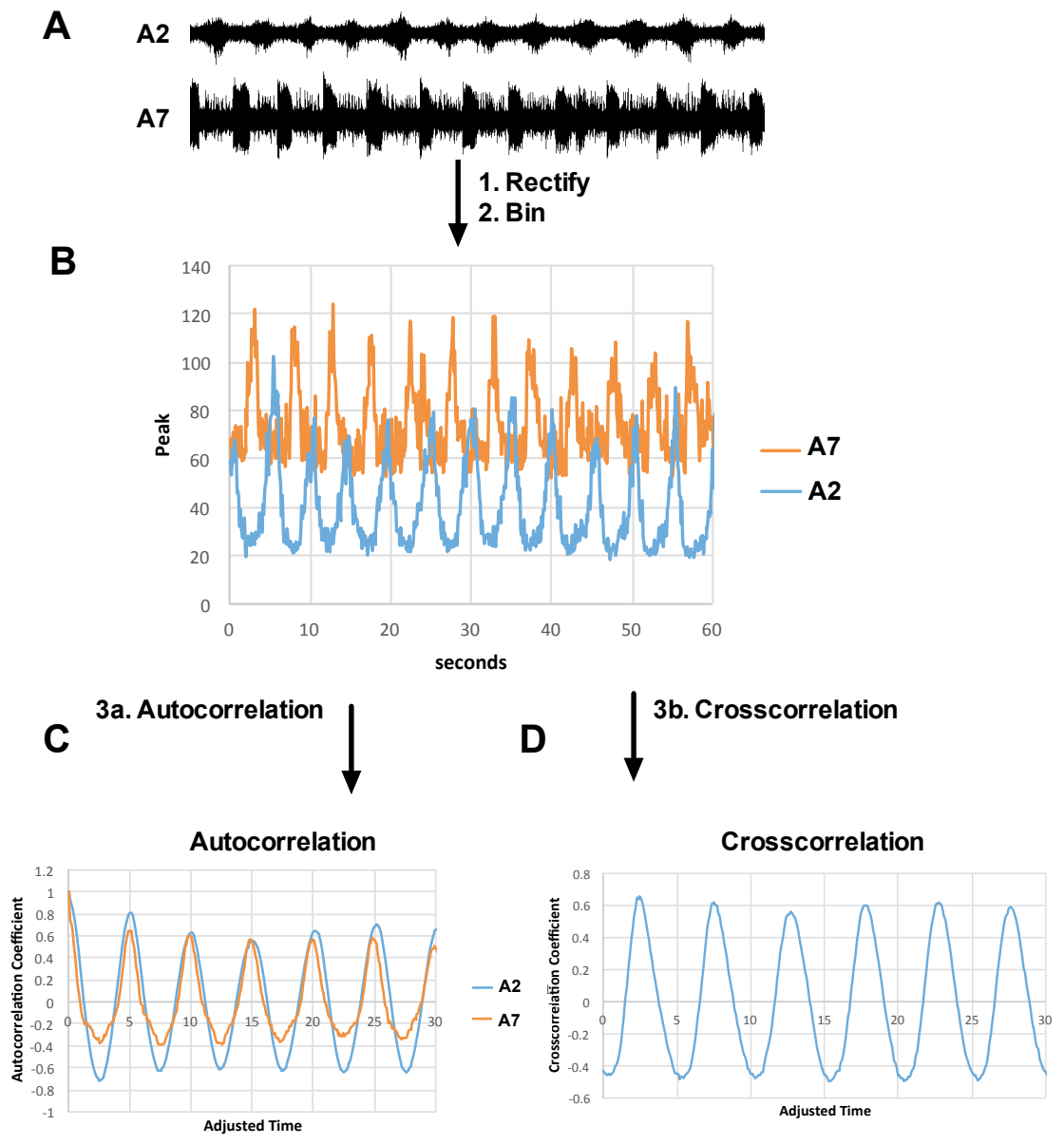
Figure 4.1. Extracellular recordings of motor bursts from intact nerves in control animals were analyzed via auto-correlation and cross-correlation. **A.** Extracellular recordings were made of intact nerves innervating abdominal segment 2 (A2) and abdominal segment 7 (A7). The example trace was taken over 60 seconds of a control

animal. **B.** To smooth and decrease the size of the data file, each trace was rectified and

data averaged into 1200 bins of 50 msec. **C.** In order to calculate the frequency of motor

bursts in each recording, an autocorrelation was performed and the auto-correlation

coefficient taken from the peak of the first lag (lag 1). Note that the peak at t=0 is 1.0

because the undelayed data correlates perfectly with itself. Also note that adjusted time is

in seconds. **D.** In order to calculate the time between A7 and A2 bursts, a cross-

correlation was performed on each set of recordings. The time between bursts was

extrapolated from the first peak of the cross-correlation.
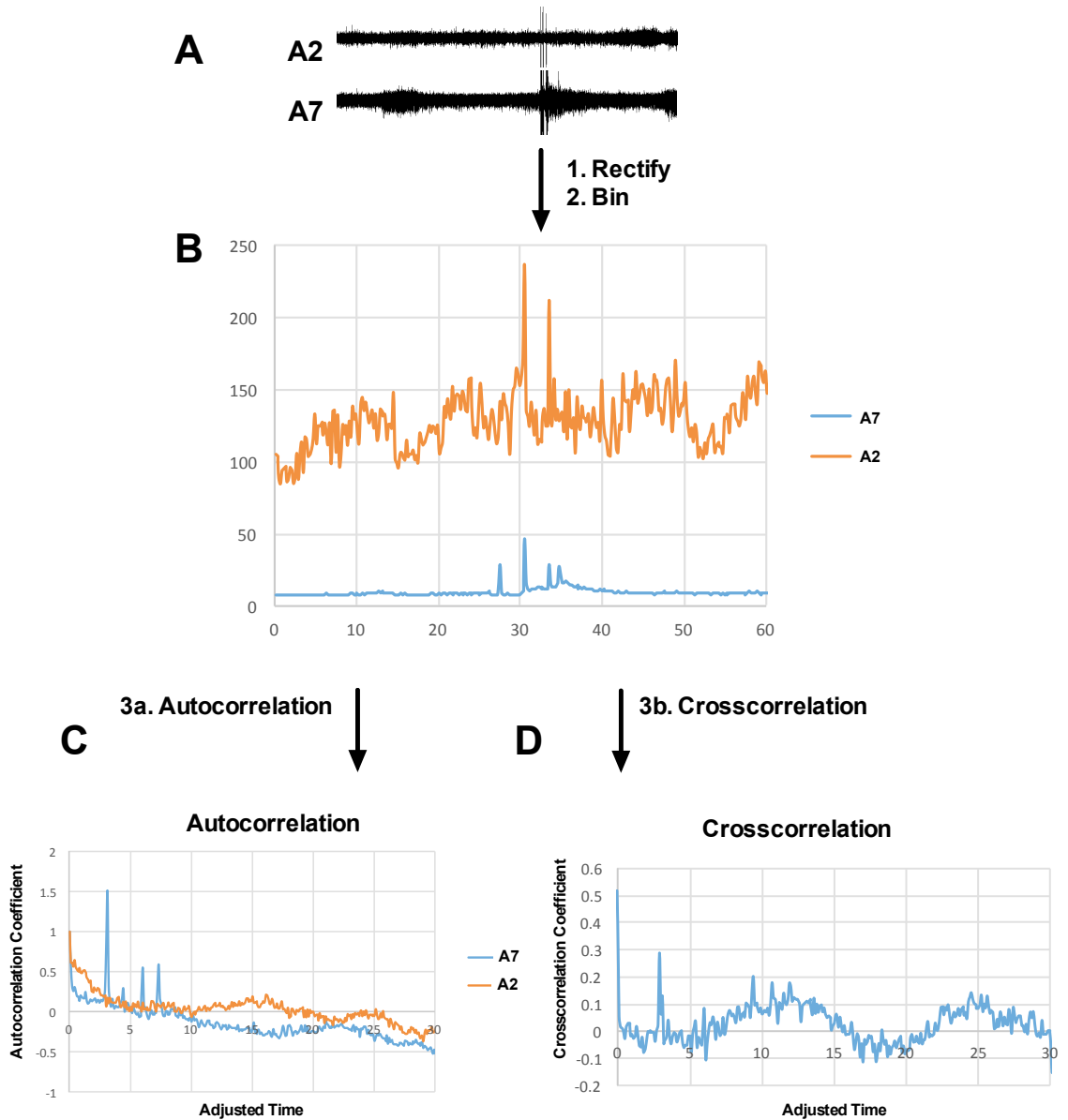
Figure 4.2. Extracellular recordings of motor bursts from intact nerves of TBPH mutants. **A.** Extracellular recordings were made of intact nerves innervating abdominal segment 2 (A2) and abdominal segment 7 (A7). The example trace was taken over 60 seconds of a TBPH mutant. **B.** To smooth and decrease the size of the data file, each trace was rectified and data averaged into 1200 bins of 50 msec. **C.** In order to calculate the frequency of motor bursts in each recording, an autocorrelation was performed. If the

algorithm detected non-randomness in the data set, there would be peaks corresponding to time lags. This is an example of a trace without lag peaks. A time of lag 1 could not be extrapolated because there is not a lag 1, indicating a loss of non-randomness in the recording. **D.** In order to calculate the time between A7 and A2 bursts, a cross-correlation was performed on each set of recordings. A time between bursts could not be calculated because there are no peaks in the trace.

Of the recordings made on the TBPH null mutant, only 30% of recordings elicited an autocorrelation peak. These animals showed an average frequency of 5 bursts per minute, a 50% reduction from the 10 burst per minute of the control (Figure 4.3C). Restoring TBPH with the TBPH-GAL4 driver reversed this effect. Restoring *cacophony* with either the OK6- or R75C05-GAL4 driver also reversed this effect. It should be noted that, because these recordings are made *en passant*, there is likely intact sensory neuron feedback acting on the motor program.

Of the 30% of TBPH null mutant recordings eliciting a cross correlation peak, the average delay between segments 7 and 2 was 8 seconds (Figure 4.3D). This delay is twice as long as the 4 seconds delay measured in controls. Restoring TBPH with the TBPH-GAL4 driver reversed this effect. Restoring *cacophony* with the OK6 or R75C05 driver also reversed this effect. In fact, restoring *cacophony* with the R75C05 driver produced the most robust reversal of this effect.
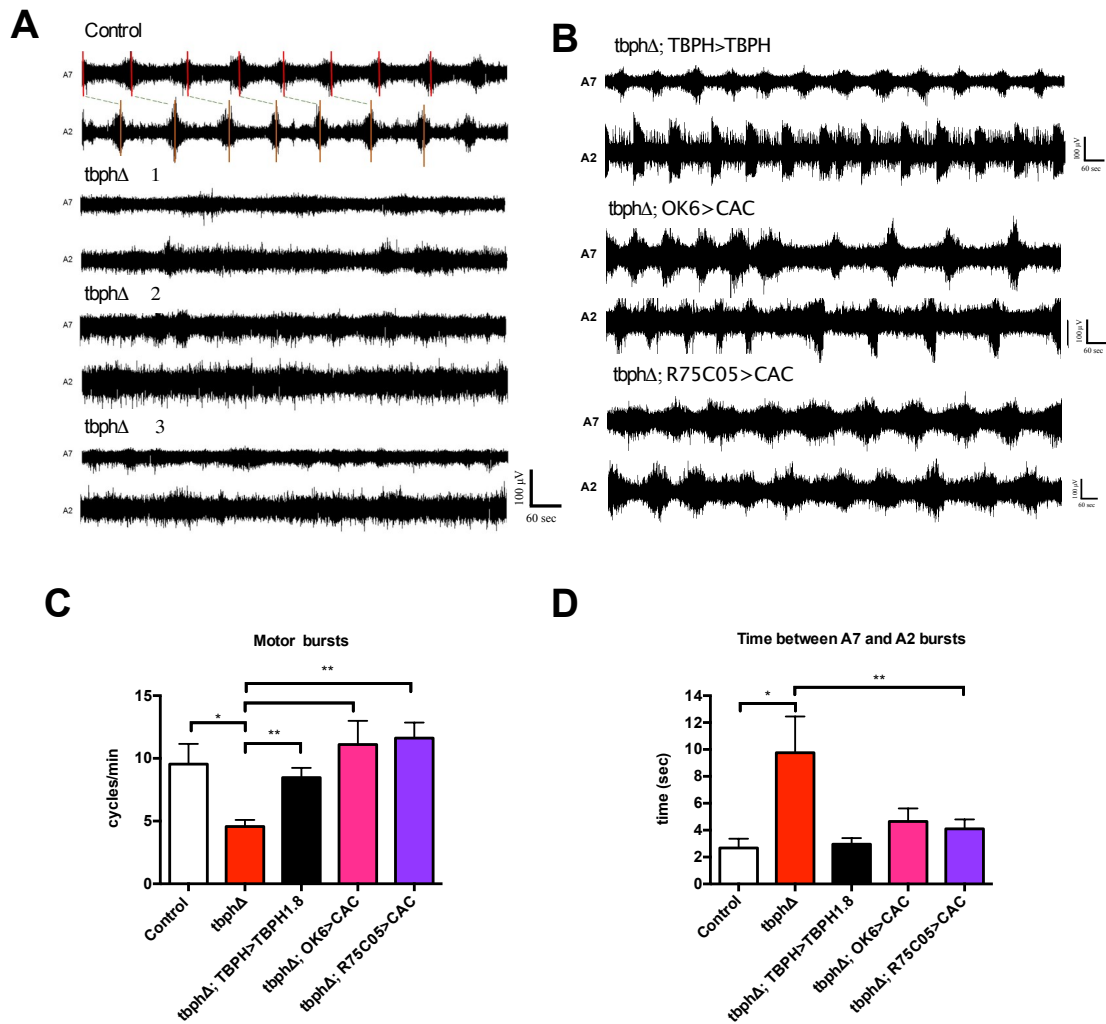
Figure 4.3. The motor output from the CNS of TBPH null mutants is un-patterned and uncoordinated. **A.** Representative examples of the motor output shows that control larvae exhibit regular, patterned motor bursts that progress from abdominal segment 7 (A7) and abdominal segment 2 (A2). By contrast, recordings from TBPH mutant larvae show infrequent, poorly defined, uncoordinated bursts (recordings from 3 different TBPH mutant larvae are shown). **B.** Representative examples of recordings from TBPH mutant larvae expressing TBPH and *cacophony* in motor neurons (OK6>CAC), and *cacophony*

in AV001b/2b cells (R75C05>CAC) showing that the patterned output is restored. **C-E.** Quantification of patterned bursting parameters using autocorrelation and cross correlation of rectified recordings. **C.** Frequency of non-random bursting patterns. An autocorrelation analysis was performed on each recording (see text for details) to test whether the bursting showed non-randomness. Less than 50% of the recordings from TBPH mutant larvae showed non-random bursting. The number of recordings that showed non-random bursting was rescued by expression of either TBPH or *cacophony* in the TBPH mutant larvae. **D.** Frequency of motor bursts. For the TBPH mutant larvae that showed nonrandom bursting, the frequency of bursts was reduced by approximately 50% compared to control larvae. This reduction was restored by expression of either TBPH or *cacophony* in both motor neurons and the AVM001b/2b cells (R75C05>CAC; D). **E.** Bursting delay between A7 and A2. The offset between bursts in A7 and A2 was calculated from cross correlations (see text for details) between A7 and A2 traces in each animal. The non-random pattern recordings from TBPH mutant larvae exhibited an offset between A7 and A2 motor neurons of approximately twice that of the control animals. This increased delay was restored by expression of both TBPH and *cacophony*. All recordings were done in HL3.1 saline solution containing 1.8 mM calcium and 30 μM pilocarpine. Recordings were taken from A2 and A7 motor nerves of at least 10 animals of each genotype. Data shown represent the mean and SEM and analyzed using ordinary one-way ANOVA with a Sidak's multiple comparisons test (** $p < 0.01$, * $p < 0.05$).

The AVM001b/2b cells are not an integral component of the motor circuit

Activation of AV001b/2b cells has been reported to drive escape behavior in crawling larvae (Vogelstein et al., 2014). I have shown genetically driving *cacophony* in these cells, in the TBPH mutant restores larval crawling behavior and rhythmic motor bursts. Therefore, I asked whether this rescue could be reproduced by acute activation of the AVM001b/2b cells in the TBPH mutant background. To answer this question, the temperature-activated channel, TrpA1, was driven under UAS-GAL4 control with the R75C05-GAL4 driver in the TBPH mutant background. TrpA1 (transient receptor potential A1) is one of three thermosensation channels in Drosophila that detect subtle changes in ambient temperature and opens in temperatures about 25°C (Neely et al., 2011; Luo et al., 2016).

Larval crawling was measured at 25°C, when TrpA1 is inactive, and 30°C, a temperature that activates TrpA1, over 5 minutes (Figure 4.4A). To confirm that the UAS-TrpA1 was being activated on the apparatus, I expressed it using the OK6-GAL4 driver and observed that at 30°C, the animals were, as expected, completely paralyzed (Figure 4.4A). At room temperature they crawled the same distance as controls (Figure 4.4B). Driving UAS-TrpA1 with the R75C05-GAL4 driver in the TBPH mutant background had no effect on crawling distance at 30°C (Figure 4.4A), crawling no further than either parental control. In order to rule out the possibility of a sensory defects in the TBPH mutants that could be causing them to simply not sense elevated temperature, I repeated the experiments in which UAS-cacophony was driven with the R75C05-GAL4 driver was repeated. These animals show an increase in distance crawled over time at 30°C, a similar increase to that observed in the control animals (Figure 4.4A). These

results suggest that the *cacophony* rescue is not solely due to the activation of the

AVM001b and AVM002B cells, but rather is likely dependent upon the chronic

restoration of *cacophony* in the TBPH mutants throughout development.
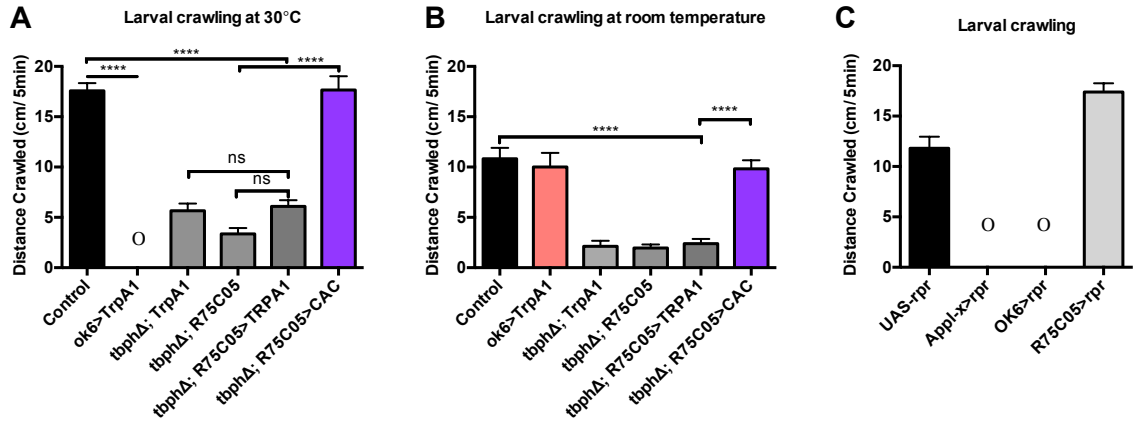
Figure 4.4. TrpA1 activation of AVM001b and AVM002b cells does not rescue

crawling in TBPH mutants. **A.** Larval crawling was measured at 30°C over 5 minutes and

total distance crawled recorded. TBPH mutants show no increase in larval crawling at

30°C. Driving UAS-TrpA1 with the R75C05-GAL4 driver in the TBPH mutant

background showed no increase in larval crawling at 30°C compared to the parental

controls. Driving *cacophony* with the R75C05-GAL4 driver, however, showed a

significant increase in distance crawled at 30°C compared to the parental controls and

restoring the total distance crawled to the same level as the wild type controls. Driving

UAS-TrpA1 expression with the OK6-GAL4 driver in a wild type background produced

immediate paralysis. **B.** Larval crawling at room temperature over 5 minutes prior to

being placed at 30°C. TBPH mutants show reduced crawling. Driving UAS-TrpA1 with

the R75C05-GAL4 driver in the TBPH mutant background had no effect on larval

crawling compared to the parental controls, whereas driving *cacophony* expression with the R75C05-GAL4 driver restored crawling at room temperature. **C.** Elimination of AVM001b/2b neurons has no effect on larval crawling. Embryos in which UAS-rpr was driven with either ApplX-GAL4 or OK6-GAL4 failed to hatch into the first instar (denoted by O). By contrast, third instar animals in which UAS-rpr was driven by R75C05-GAL4 showed no defects in crawling behavior. All data shown represent the mean and SEM of at least 10 animals and were analyzed using ordinary one-way ANOVA with a Sidak's multiple comparisons test (****$p<0.0001$, ns indicates a non-significant difference).

Killing AVM001n/2b cells does not impact larval development or locomotion

As the AVM001b and AVM002b cells act on the motor circuit, I tested whether eliminating these cells would inhibit larval crawling behavior (Figure 4.4C). In order to kill these cells, I made use of the gene *reaper* (rpr), the protein that activates programmed cell death in Drosophila (Chen et al., 1996; Mohseni et al., 2009). I drove UAS-rpr in a wild type background under the pan-neuronal driver Appl-GAL4, in addition to the OK6-GAL4 and R75C05-GAL4 drivers. Embryos in which UAS-rpr was driven with ApplX-GAL4 or OK6-GAL4 failed to hatch into the first instar, which was expected according to previous reports (Mohseni et al., 2009). Driving UAS-rpr with R75C05-GAL4, however, produced third instar larvae that crawled normally (Figure 4.4C). It therefore appears that killing these cells is not sufficient to inhibit larval crawling.

DISCUSSION

We have shown that genetically restoring the Type II voltage gated calcium channel *cacophony* in the AVM001b and AVM002b cells in our TBPH mutant is sufficient to restore larval crawling and rhythmic motor bursts. TBPH mutants show significant defects in larval crawling (Figure 3.1) and significant loss of rhythmic motor bursts (Figure 4.3A). Surprisingly, driving *cacophony* in the AVM001b and AVM002b cells, in the TBPH mutant background, was sufficient to rescue both larval crawling and rhythmic motor pattern. It was not, however, sufficient to rescue the changes in synaptic physiology.

Activation of AVM001b and AVM002b cells with channel rhodopsin caused a slightly higher probability of larvae to present escape behavior during crawling (International Glossina Genome Initiative et al., 2014). The function of these cells in third instar larvae or adults has not been characterized beyond that report. Therefore, it was quite surprising that restoring *cacophony* in these cells, in the TBPH mutant, was sufficient to rescue both the crawling and rhythmic motor bursts. This result suggests these cells are either part of, or act on, the motor program in such a way as to regulate the rhythmic pattern of motor neuron bursts. How they do this remains unclear. Is this rescue intrinsic to *cacophony* or does it result from a general activation of these cells?

To answer that question, we tested whether activation of the AVM001b/2b cells with TrpA1 in the TBPH mutant could elicit the same rescue in crawling behavior as restoring *cacophony* does. We observed no rescue of the crawling defect, suggesting that it was dependent upon the restoration of *cacophony* specifically, not just an acute

activation of these cells (Figure 4.4A). The possibility of a thermosensory defect in TBPH mutants was also ruled out, as animals expressing *cacophony* under the R75C05-GAL4 driver completely rescued the increase in distance crawled at 30°C. We also showed that eliminating these cells had no effect on crawling (Figure 4.4C). Therefore, it seems that the rescue of crawling behavior is specific to the chronic restoration of *cacophony* in the AVM001b/2b cells through development.

Finally, we sought to better characterize the function of the AVM001b/2b cells within the motor circuit. To do this, we eliminated the cells by expressing *rpr*. When we drove UAS-rpr in the AVM001b/2b cells, the embryos were able to hatch and develop into third instar larvae. These larvae showed no defects in locomotion, confounding whatever action AVM001b/2b cells may hold within or around the motor circuit.

In conclusion, our data show that TBPH-dependent defects at the NMJ are insufficient to explain the TBPH-dependent locomotion observed in Drosophila larvae. Furthermore, restoring the TBPH-dependent loss of *cacophony* in either motor neurons or a discrete set of central neurons is sufficient to restore the locomotion defects. If these effects are mirrored in human TDP-43 proteinopathies, our observations could open new avenues to investigate alternative therapeutic targets for these neurodegenerative diseases.

OUTSTADNING QUESTIONS

The most confounding question from the results presented here surrounds the normal function of the AVM001b/2b cells within the motor circuit and the nature of the *cacophony* rescue. Eliminating the AVM001b/2b cells is not sufficient to cause locomotion defects. Activating the AVM001b/2b cells is also not sufficient to drive over-active locomotion defects. Because it is unknown where these cells lie within brain circuitry, i.e. which cells activate them and which cells they subsequently activate, and what type of neurotransmitters and receptors these cells express, their endogenous function remains elusive.

It is clear, however, that driving *cacophony* expression in AVM001b/2b in the TBPH mutant background is sufficient to restore rhythmic, patterned motor bursts. The mechanism behind this rescue remains obscure, but is clearly dependent upon the specific restoration of *cacophony,* not merely the activation of the cells. Do AVM001b/2b cells endogenously express *cacophony* in a wild type genetic background? *Cacophony* is broadly expressed at synapses within the CNS (Ryglewski et al., 2012b), but there is no direct evidence showing AVM001b/2b cells normally express *cacophony*. Further, it is unclear whether the mechanism of *cacophony* rescue in the AVM001b/2b cells and motor neurons is the same. We do not know whether the OK6-GAL4 driver expresses in the AVM001b/2b cells and therefore we do not know if the mechanism of the OK6-GAL4 rescue is dependent upon restoring *cacophony* in the AVM001b/2b cells.

CHAPTER 5

Selective expression of *Cacophony* isoforms lacking exon 7 shows changes in *Cacophony* protein expression, larval locomotion, and motor neuron physiology in third instar larvae.

Effort statements:

Crawling assays, locomotion assays, electrophysiology at the NMJ,

immunohistochemistry at larval boutons, extracellular recordings, and adult courtship

assays were done by Kayly Lembke.

Fly line generation was done by Alex Law, with Dr. Jer-Cherng Chang.

Crawling assays, Western analysis, PCR analysis, and adult motor behavior were done by

Alex Law.

Adult survival and adult activity were done by Dr. David Morton.

ABSTRACT

TDP-43 is an RNA binding protein with characterized functions in transcription, translation, and spliceosome function. We have shown previously that dysregulation of the Drosophila ortholog, TBPH, causes severe locomotion defects in larvae driven by a reduction in the expression of the type II voltage gated calcium channel *cacophony*. Further, we have shown that TDP-43 appears to regulate the inclusion of alternatively spliced exons of *cacophony*; TBPH mutants show enrichment of *cacophony* isoforms lacking exon 7. Deletion of the exon 7 coding region causes a reduction in *cacophony* protein expression and locomotion defects in third instar larvae. This defect is rescued with expression of *cacophony* transcripts containing exon 7. Exon 7 deletion larvae also show a reduction in the frequency of spontaneous release at the neuromuscular junction, as well as non-normal motor neuron burst patterns. These data suggest that deletion of exon 7 is sufficient to cause locomotion defects.

INTRODUCTION

TDP-43 is an RNA binding protein that regulates the expression and splicing of thousands of gene transcripts (Sephton et al., 2011; Hazelett et al., 2012). We have shown previously that loss of the Drosophila TDP-43 ortholog, TBPH, causes a decrease in the expression of the type II voltage gated channel *cacophony* (Chang et al., 2014). TBPH mutants also show severe defects in larval locomotion (Hazelett et al., 2012; Chang et al., 2014) and motor neuron physiology that are rescued by genetically restoring *cacophony* (Chang et al., 2014).

Though TBPH mutants show a 50% reduction in *Cacophony* protein expression, there is no decrease in total *cacophony* transcript levels (Chang et al., 2014). Of the *cacophony* transcripts expressed, there is a significant enrichment for transcripts lacking exon 7 (Chang et al., 2014), suggesting that TBPH functions to regulate the inclusion of specific *cacophony* exons. Of the 14 reported *cacophony* isoforms, only one lacks exon 7, suggesting this exon is of functional importance to the channel (http://flybase.org/).

There is evidence that functional specificity of channels can be conferred by the differential expression of discreet channel isoforms (Lipscombe et al., 2013b). Throughout the mouse brain, a variety of populations of voltage gated calcium channel isoforms are differentially expressed in discreet brain regions (Bell et al., 2004; Gray et al., 2007). These isoform populations are specific to cell-type, tissue, and developmental stage. Thus, each isoform is thought to contribute to the functional specificity of each tissue region (Bell et al., 2004; Gray et al., 2007). TBPH mutants show a variety of

cacophony dependent locomotion defects. Therefore we tested whether deletion of exon 7, using CRISPR-CAS, would be sufficient to drive locomotion defects.

Targeted deletion of exon 7 reduced *cacophony* protein expression (Law and Morton, unpublished observation; see Appendix B) and locomotion defects in third instar larvae, similar to those reported in TBPH mutants (Hazelett et al., 2012; Chang et al., 2014). These phenotypes are rescued by driving exon 7 containing *cacophony* transcripts. Because *cacophony* is the primary voltage gated calcium channel at the neuromuscular junction (NMJ), and necessary for full evoked neurotransmission (Kawasaki et al., 2002, 2004), we tested whether evoked or spontaneous release at the neuromuscular junction was defective in deletion animals. Defective larval locomotion has been shown to coincide with non-normal motor nerve burst patterns (Fox et al., 2006). As deletion of exon 7 causes defects in larval locomotion, we hypothesized they would also show un-patterned, a-rhythmic motor bursts similar to those of TBPH mutants. Finally, because mutations in *cacophony* were first identified to alter courtship song in adult flies, we tested whether exon 7 deletion adult flies would show abnormal courtship song.

RESULTS

Deletion of exon 7 causes locomotion defects in third instar larvae

Larval crawling is a highly stereotyped behavior dependent upon the synchronous contraction of muscles driven by motor neuron activation (Fox et al., 2006; Inada et al., 2011). TBPH mutants show defective larval locomotion that is rescued by driving exon 7 containing *cacophony* in motor neurons (Chang et al., 2014). We therefore tested whether

deleting exon 7 in all cell types would produce similar defects in larval locomotion. Total distance crawled was measured in two exon 7 deletion lines: $cac^{exon7\Delta(6)}$ and $cac^{exon7\Delta(8)}$. Both lines showed decreased crawling distance in males (Figure 5.1A) that was rescued by driving exon 7 containing *cacophony* in motor neurons using D42-GAL4. In addition to restoring *cacophony* using the GAL4-UAS system, we separately restored *cacophony* using an X-duplication line in which the entire *cacophony* gene is duplicated onto chromosome 3. Duplicating *cacophony* on chromosome 3 also rescued the crawling distance of both deletion lines (Figure 5.1A).

To determine a more detailed understanding of the apparent locomotion defect of the deletion lines, I measured the frequency of peristaltic waves and the time it took each wave to traverse the larval body in a posterior to anterior fashion. Both deletion lines show a reduction in the frequency of peristaltic waves (Figure 5.1B). This reduction was *cacophony* dependent, as expressing a duplication of *cacophony* on chromosome 3 restored frequency levels. This decrease was also rescued by restoring *cacophony* with the D42-GAL4 driver (Figure 5.1B).

The time-to-completion of each posterior to anterior peristaltic wave was also quantified (Figure 5.1C). Each peristaltic wave in the deletion lines took approximately 1.5 milliseconds to traverse the larval body wall, whereas each wave took approximately 0.8 milliseconds in control animals (Figure 5.1C). Restoring *cacophony* in the $cac^{exon7\Delta(8)}$ deletion line with D42-GAL4 rescued this defect. Rescue with the X-duplication lines has not been tested yet. Nonetheless, these data suggest that deletion of exon 7 is sufficient to drive locomotion defects in third instar larvae that affect not only distance crawled, but more specifically the generation and progression of the peristaltic waveform.
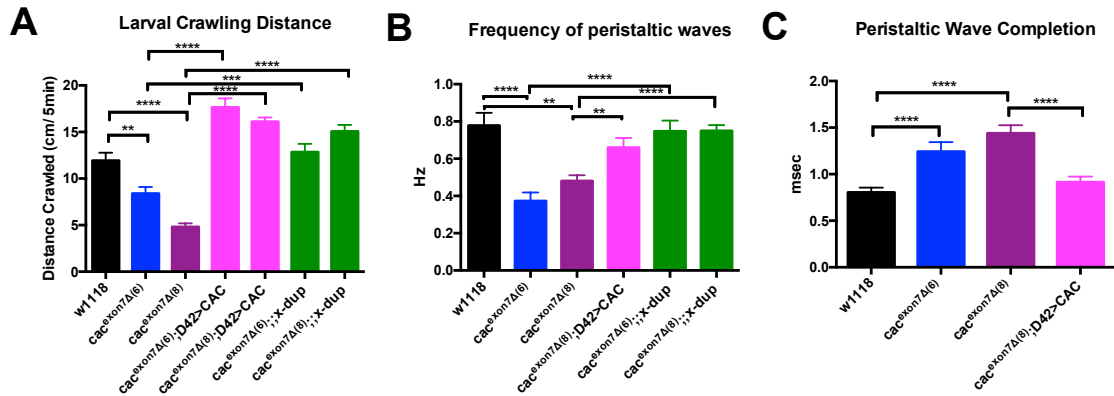
Figure 5.1. Exon 7 deletion animals show defective motor behavior, which can be rescued by *Cacophony* expression. **A.** Exon 7 deletion animals, *cac*$^{exon7\Delta(6)}$ (blueberry) and *cac*$^{exon7\Delta(8)}$ (plum), crawl shorter distances than control larvae, w1118 (black), which is partially rescued with the expression of UAS-cacophony with the D42-GAL4 driver (magenta), or a duplication of *Cacophony* on the third chromosome (clover). **B.** Frequency of peristaltic waves. Exon 7 deletion animals show a 50-40% reduction in the number of complete waves that progress along the larval body, which is rescued by expressing *Cacophony* with either UAS-cacophony under the D42-GAL4 driver (magenta), or by expressing a duplication of *Cacophony* on the 3rd chromosome (clover). **C.** Duration of peristaltic wave. The time taken for a complete peristaltic wave to traverse the larva was significantly increased in exon 7 deletion animals. This was rescued by driving UAS-cacophony with the D42-GAL4 driver (magenta). Data shown represent the mean and SEM of at least 10 animals and were analyzed using ordinary one-way ANOVA with a Sidak's multiple comparisons test (**** $p<0.0001$, *** $p< 0.001$, ** $p <0.01$).

Cacophony staining at boutons of the NMJ

PCR analysis has show that total levels of *cacophony* transcripts are unchanged in *cac*$^{exon7\Delta(6)}$ and *cac*$^{exon7\Delta(8)}$ (Law and Morton, unpublished observations), similar to results reported in the TBPH mutant (Chang et al., 2014). Western analysis has shown that *cacophony* protein levels are decreased in both whole third instar larvae and larval central nervous systems (Law and Morton, unpublished results; see Appendix B). I therefore tested whether this reduction in *cacophony* protein expression was sustained at the boutons of the NMJ. To measure the presence of *cacophony* only at the boutons, I used immunohistochemistry.

Both *cac*$^{exon7\Delta(6)}$ and *cac*$^{exon7\Delta(8)}$, as well as the control line w1118, were treated with antibodies against *cacophony* (Chang et al., 2014) and bruchpilot. Bruchpilot was used as a marker for boutons. Total fluorescence of the secondary antibody against *cacophony* was measured (Figure 5.2). Using an anti-CAC concentration of 1:1000, no difference in total fluorescence was detected between the two deletion lines and control animals (Figure 5.2A). To test whether I was using a supersaturated concentration of *cacophony* antibody, anti-CAC, I repeated these experiments using smaller concentrations, 1:2000 and 1:4000. Using an anti-CAC concentration of 1:2000, *cac*$^{exon7\Delta(8)}$ showed no decrease in total fluorescence compared to control. *Cac*$^{exon7\Delta(6)}$, however, showed a significant reduction in total fluorescence (Figure 5.2B). Using anti-CAC at 1:4000, the results were similar in that *cac*$^{exon7\Delta(8)}$ boutons show no reduction in total fluorescence, but *cac*$^{exon7\Delta(6)}$ boutons show a significant reduction in total fluorescence (Figure 5.2C).

This apparent difference in *cacophony* expression at the boutons is the first difference observed between $cac^{exon7\Delta(6)}$ and $cac^{exon7\Delta(8)}$. Though Western analysis shows a reduction in *cacophony* expression in whole-larva, it appears this decrease is only sustained at boutons in $cac^{exon7\Delta(6)}$.
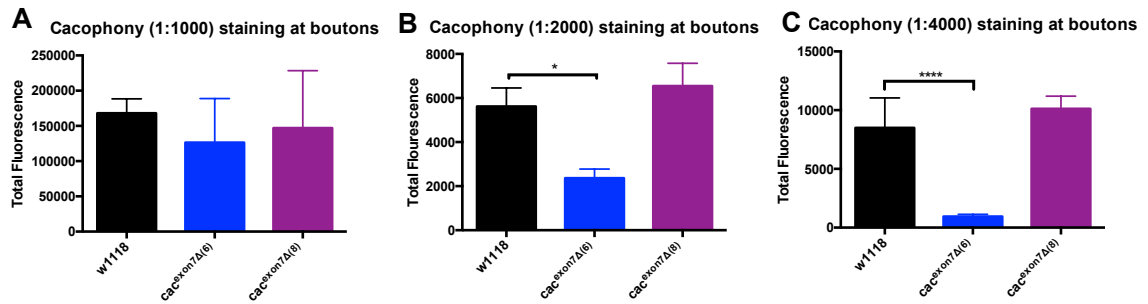
Figure 5.2. *Cacophony* fluorescence is decreased in boutons of $cac^{exon7\Delta(6)}$ animals, but not $cac^{exon7\Delta(8)}$ animals. **A.** *Cacophony* fluorescence, using a 1:1000 concentration of anti-cac. **B.** *Cacophony* fluorescence, using a 1:2000 concentration of anti-cac, showed a reduction in boutons of the $cac^{exon7\Delta(6)}$ line (blueberry), but not $cac^{exon7\Delta(8)}$ (plum), compared to control animals. **C.** *Cacophony* fluorescence, using a 1:4000 concentration of anti-cac, showed a reduction in boutons of the $cac^{exon7\Delta(6)}$ line (blueberry), but not $cac^{exon7\Delta(8)}$ (plum), compared to control animals. Data shown represent the mean and SEM of at least 4 male larvae and were analyzed using ordinary one-way ANOVA with a Sidak's multiple comparisons test (**** $p<0.0001$, * $p <0.05$).

Synaptic Neurotransmission at the NMJ

   Cacophony is necessary for evoked neurotransmission at the NMJ (Kawasaki et al., 2004; Lee et al., 2014a). As Western analysis shows a reduction in *cacophony* protein expression (Law and Morton, unpublished data), and immunohistochemistry showed a reduction in *cacophony* fluorescence at boutons of $cac^{exon7\Delta(6)}$, I hypothesized I would see some effect on evoked and spontaneous neurotransmission at the NMJ.

   Surprisingly, when I measured EJP amplitudes of $cac^{exon7\Delta(6)}$ and $cac^{exon7\Delta(8)}$, I found that there was a decrease in amplitudes of $cac^{exon7\Delta(8)}$, but not $cac^{exon7\Delta(6)}$, and is thus the second phenotypic difference between the two deletion lines (Figure 5.3B). This result was unexpected because of the two lines, only $cac^{exon7\Delta(6)}$ showed any type of change in *cacophony* levels at boutons. To test whether the reduction in EJP amplitudes of $cac^{exon7\Delta(8)}$ was *cacophony* dependent, *cacophony* was restored using either the X-duplication or driving UAS-cacophony with D42-GAL4 (Figure 5.3B). Both rescue constructs significantly rescued the reduction in EJP amplitude, suggesting the reduction was, in fact, *Cacophony* dependent (Figure 5.3B).

   The amplitude and frequency of spontaneous release of $cac^{exon7\Delta(6)}$ and $cac^{exon7\Delta(8)}$ were also measured (Figure 5.3C). Unlike the TBPH mutant, neither deletion line showed a reduction in mEPP amplitude (Figure 5.3D). However, like the TBPH mutant, both lines show a reduction in mEPP frequency (Figure 5.3E). This reduction appears to be *cacophony* dependent only when *cacophony* is restored by driving UAS-cacophony with D42-GAL4; restoring *cacophony* with the X-duplication does not appear to rescue the reduction in mEPP frequency (Figure 5.3E). This difference could potentially be due to protein expression level or transcript differences between the GAL4-UAS system and the

X-duplication. I have shown previously that the frequency of spontaneous release is sensitive to *cacophony* expression levels (Figure 3.5B). Therefore, the inability of the X-duplication to restore the mEPP frequency could be due to inadequate *cacophony* expression levels.
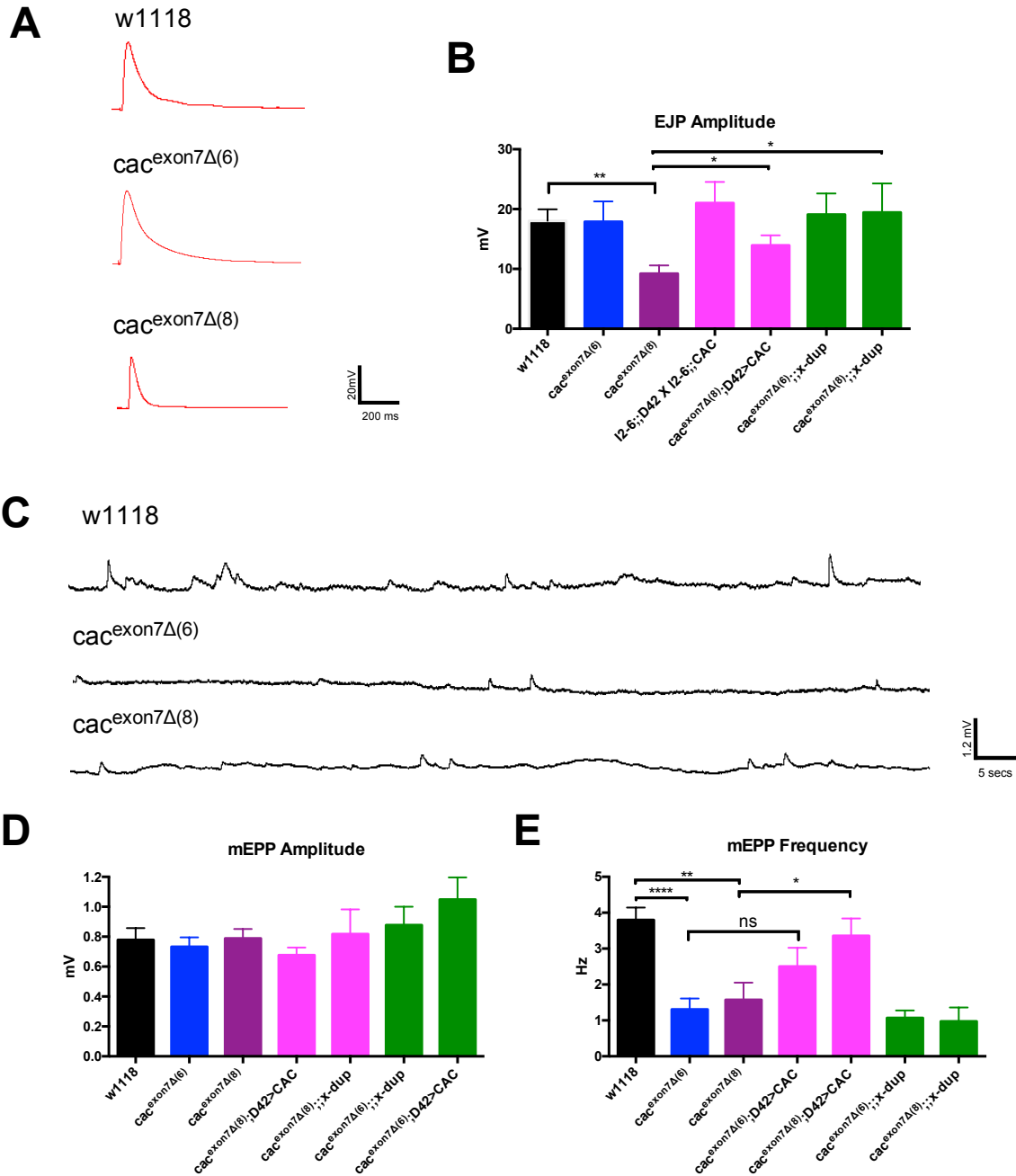
Figure 5.3. Synaptic physiology at the larval NMJ is defective in exon 7 deletion animals. **A.** Representative examples of excitatory junctional potentials (EJPs) from control and exon 7 deletion larvae. **B.** EJP amplitude is unchanged in $cac^{exon7\Delta(6)}$ animals (blueberry), but reduced in $cac^{exon7\Delta(8)}$ animals (plum), which is rescued by either restoring *Cacophony* with UAS-cacophony driven by D42-GAL4, or duplication of *Cacophony* on the third chromosome. **C.** Representative example of miniature end plate potentials (mEPPs) control and exon 7 deletion larvae. **D.** The mEPP amplitude is unchanged in both exon 7 deletion lines. **E.** The mEPP frequency is reduced in both deletion lines and restoring *Cacophony* with UAS-cacophony driven by D42-GAL4 restores frequencies in the $cac^{exon7\Delta(8)}$ line, but not the $cac^{exon7\Delta(6)}$ line. Expressing *Cacophony* by duplication on the third chromosome also does not restore the decrease in mEPP frequency in either deletion line. All experiments were carried out in 1 mM calcium using male larvae. Data represent the mean and SEM of at least 10 animals and were analyzed using ordinary one-way ANOVA with a Sidak's multiple comparisons test (**** $p<0.0001$, ** $p< 0.01$, * $p <0.05$, ns = not significant).

Motor Pattern Output

Exon 7 deletion animals show a reduction in the frequency of peristaltic waves and an increase in the time-to-completion of each peristaltic wave that traverses the body wall. These phenotypes suggest defective motor nerve bursts (Fox et al., 2006), and I therefore monitored the motor output from the CNS in semi-intact larvae.

Focal extracellular recordings were made *en passant* from intact peripheral nerves projecting on muscle 6/7 in abdominal segment 2 (A2) and abdominal segment 7 (A7; Figure 5.4) as previously described in Chapter 4. It should be noted that, while TBPH mutants did not show consistent bursting, even with the addition of pilocarpine, exon 7 deletion animals would occasionally show patterned output (Figure 5.4A). Extracellular recordings were analyzed as previously described Chapter 4.

In the presence of pilocarpine, both deletion lines show motor bursts with patterns un-like those of control animals (Figure 5.4A). Both deletion lines show a range of cycles per minute, sometimes very high, peaking at 126 in $cac^{exon7\Delta(6)}$ animals, and sometimes very low, at less than 1in $cac^{exon7\Delta(8)}$ animals (Figure 5.4B). Though the average cycles per minute in $cac^{exon7\Delta(8)}$ animals was not significantly different from those of control animals, the distribution of cycles was reduced when *cacophony* was restored by driving UAS-cacophony with D42-GAL4 (Figure 5.4C).
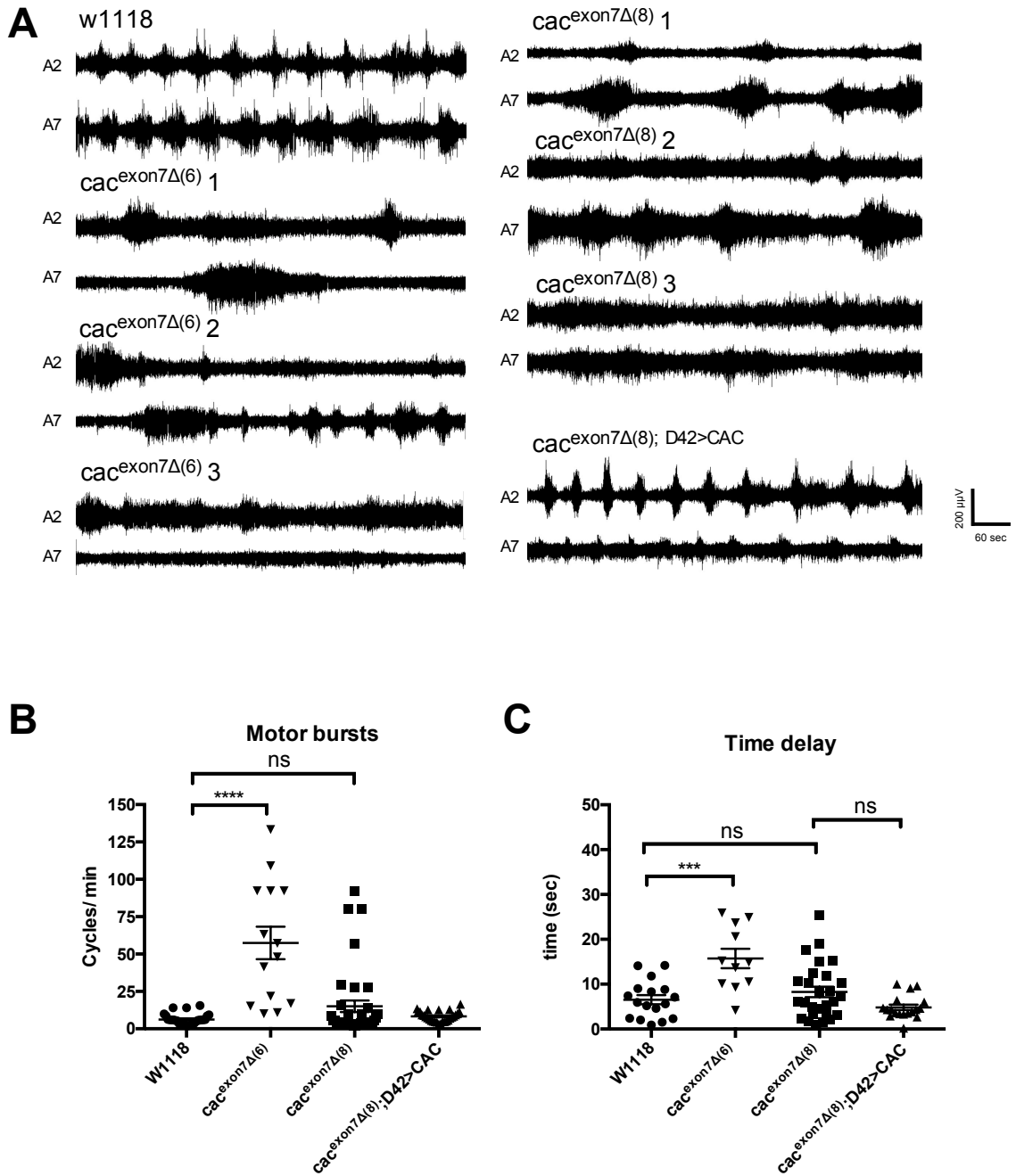
Figure 5.4. The motor output from the CNS of exon 7 deletion animals is variable and frequently un-patterned and uncoordinated. **A.** Representative examples of the motor output shows that control larvae exhibit regular, patterned motor bursts that progress from abdominal segment 7 (A7) and abdominal segment 2 (A2). By contrast, recordings

from exon 7 deletion larvae frequently show well defined bursts that are uncoordinated between A2 and A7 (recordings from 3 different $cac^{exon7\Delta(6)}$ and $cac^{exon7\Delta(8)}$ larvae are shown). Driving UAS-cacophony with D42-GAL4 restores coordinated bursts in $cac^{exon7\Delta(8)}$ larvae. **B.** Frequency of non-random bursting patterns. An autocorrelation analysis was performed on each recording (see Ch. 3 and Ch. 5 for details) to test whether the bursting showed non-randomness. Both deletion lines show a broad range of cycles per minute, compared to control animals. Driving UAS-cacophony with D42-GAL4 decreases the range of observed motor bursts in $cac^{exon7\Delta(8)}$ larvae. **E.** Bursting delay between A7 and A2. The offset between bursts in A7 and A2 was calculated from cross correlations (see Ch. 3 and Ch.5 for details) between A7 and A2 traces in each animal. The un-coordinated pattern recordings from exon 7 deletion animals show a wide range of offsets. All recordings were done in HL3.1 saline solution containing 1.8 mM calcium and 30 μM pilocarpine. Recordings were taken from A2 and A7 motor nerves of at least 10 animals of each genotype. Data shown represent the mean and SEM and analyzed using ordinary one-way ANOVA with a Sidak's multiple comparisons test (**** $p <$ 0.0001, *** $p < 0.001$, ns = not significant).

Adult Courtship Behavior

The gene *cacophony* was first identified in a screen of courtship-song mutants (von Schilcher, 1977). Mutations in *cacophony* cause defective patterning of courtship lovesong in adult male flies, which leads to delayed copulation (von Schilcher, 1977;

Smith et al., 1998). I therefore tested whether adult exon 7 deletion flies would also show delayed time to copulation.

Five day old virgin males and virgin females were placed in courtship chambers and video recorded. Courtship is a highly stereotyped, innate behavior that involves the coordination of multiple sensory and motor mechanic cues (Billeter et al., 2006). The general scheme runs as follows: orientation, tapping, wing extension and courtship lovesong, licking, attempted copulation, and finally copulation with sperm transfer (Billeter et al., 2006).

Any variations in behavior during the scheme can alter the total time to copulation and, therefore, that was the first parameter I measured (Figure 5.5A). Of the deletion lines, only $cac^{exon7\Delta(8)}$ showed a significantly longer time to copulation as compared to control animals (Figure 5.5B). The time to copulation of $cac^{exon7\Delta(6)}$ adults was unchanged. Because only male flies produce lovesong, I also quantified the total ratio of males succeeding in copulation. There was no difference between $cac^{exon7\Delta(8)}$, $cac^{exon7\Delta(6)}$, and control animals.
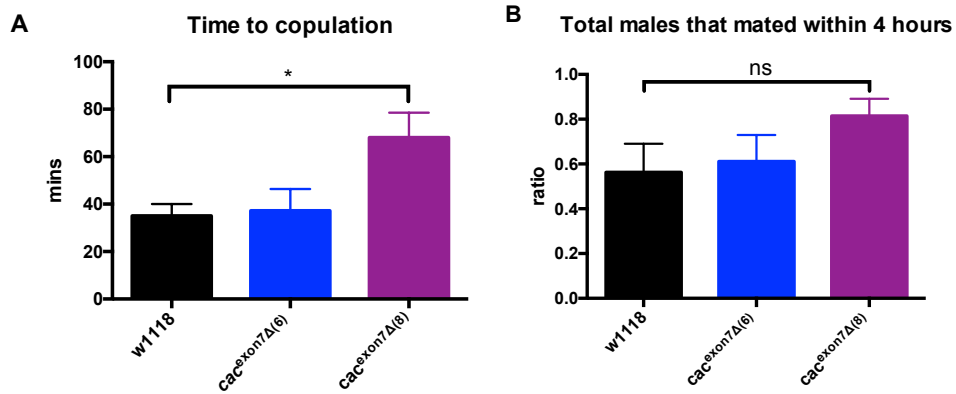
Figure 5.5. The time to courtship is delayed in $cac^{\text{exon}7\Delta(8)}$ animals, but not $cac^{\text{exon}7\Delta(6)}$ animals. **A.** $Cac^{\text{exon}7\Delta(8)}$ pairs take approximately twice the amount of time to mate, compared to control animals. **B.** There is no difference in the ratio of virgin males that complete courtship and copulation between control and exon 7 deletion animals. Data was collected from at least 8 pairs of 5-day old virgin females and virgin males per genotypes. Data shown represent the mean and SEM and analyzed using ordinary one-way ANOVA with a Sidak's multiple comparisons test (* $p < 0.05$ ns = not significant).

DISCUSSION

Regulation of voltage gated calcium channel isoform expression is a key way cells can regulate functional specificity of channels (Bell et al., 2004; Gray et al., 2007; Lipscombe et al., 2013b). We have shown that TBPH mutants show a reduction in *cacophony* protein expression and *cacophony* dependent locomotion and motor defects (Chang et al., 2014). We have also shown that, in addition to the decrease in *cacophony* protein expression, TBPH mutants show an enrichment of *cacophony* transcripts that lack

exon 7 (Chang et al., 2014). We therefore tested whether deletion of exon 7 would be sufficient to recapitulate locomotion and motor defects.

Deletion of exon 7 causes a reduction in *cacophony* protein expression (Law and Morton, unpublished observations; see Appendix B), similar to that of TBPH mutants. Third instar deletion larvae likewise show a decrease in larval crawling, fewer peristaltic waveforms, and elongated times-to-completions of these waveforms (Figure 5.1), also similar to those defects observed in TBPH mutants (Figure 3.1). We confirmed these defects in both deletion lines were *cacophony* dependent two genetic ways: first, by driving exon 7 containing UAS-cacophony in motor neurons with the D42-GAL4 driver and, second, by duplicating the *cacophony* genomic region onto chromosome 3 in all cells. Both rescue constructs rescued the locomotion defects of the exon 7 deletion lines, confirming the defects to be *cacophony* dependent.

However, from there similarities between the two exon 7 deletions lines, $cac^{exon7\Delta(6)}$ and $cac^{exon7\Delta(8)}$, and their recapitulation of TBPH mutant phenotypes, began to diverge. Both lines show a reduction in *cacophony* protein expression in whole third instar larvae (Law and Morton, unpublished observations; see Appendix B), and in TBPH mutants this reduction is also observed at NMJ boutons (Chang et al., 2014). However, in the exon 7 deletion lines, reduction in *cacophony* expression at the larval boutons was only detected in $cac^{exon7\Delta(6)}$, but not $cac^{exon7\Delta(8)}$, animals (Figure 5.2). As both deletion lines share the same genetic background, it is unclear what is driving this apparent difference in *cacophony* expression at the boutons.

As *cacophony* is necessary for full evoked neurotransmission at the NMJ

(Kawasaki et al., 2000, 2004), we measured both evoked and spontaneous release at third

instar larval NMJs. Despite showing a reduction in *cacophony* at boutons (Chang et al.,

2014), TBPH mutants show normal EJP amplitudes, but reduced frequencies and

amplitudes of mEPPs (Figure 5.3). It should be remembered that while the reduction in

mEPP frequency was *cacophony*-dependent, the reduction in mEPP amplitude was not

cacophony-dependent (Figure 5.3D&E). Neither deletion lines showed a reduction in

mEPP amplitude, further confirming that *cacophony* does not function in regulating

mEPP amplitude (Figure 5.3D). Exon 7 deletion animals both show a similar reduction in

mEPP frequency that is rescued in $cac^{exon7\Delta(8)}$ by driving UAS-cacophony with D42-

GAL4 (Figure 5.3E). Duplicating the *cacophony* gene on the third chromosome,

however, was not sufficient to rescue the reduction in mEPP frequency. This dichotomy

could reflect differences in *cacophony* protein levels or transcript expression between the

two rescue constructs in that the UAS-GAL4 system is an overexpression system,

whereas the *cacophony* duplication on the X chromosome is under the endogenous

promoter (Law and Morton, unpublished observation; see Appendix B). Finally, despite

showing no reduction in *cacophony* at boutons, only $cac^{exon7\Delta(8)}$ animals show a reduction

in EJP amplitude, and this reduction is apparently *cacophony* dependent (Figure 5.3B).

Like TBPH mutants, $cac^{exon7\Delta(6)}$ show no decrease in EJP amplitudes, despite showing a

reduction in *cacophony* at boutons (Figure 5.2).

I have shown previously that changes in neurotransmitter release at the NMJ are

not sufficient to drive defects in generation and progression of the peristaltic waveform in

larvae (Ch. 2 & 3). Therefore, we performed extracellular recordings on intact motor

nerves of third instar larvae to see whether motor nerve bursts were patterned and coordinated. TBPH mutants showed un-patterned, uncoordinated burst patterns (Figure 4.3), and thus we expected exon 7 deletion larvae to show the same phenotype. Both $cac^{exon7\Delta(6)}$ and $cac^{exon7\Delta(8)}$ show motor bursts similar to control animals (Figure 5.4A). However, their frequency of bursts is much more variable than those of control animals (Figure 5.4B). Also, there is loss of coordinated bursting between motor units in A2 and A7, resulting in uncoordinated bursting between the two segments (Figure 5.4C), similar to that reported from TBPH mutants (Figure 4.4D).

Finally, a major phenotypic difference between TBPH mutants and the exon 7 deletion animals is that, where TBPH mutants do not eclose into adult flies, exon 7 deletion animals will eclose into adulthood and mate. *Cacophony* was first identified to function in the generation and patterning of courtship lovesong performed by male flies. We therefore tested whether deletion of exon 7 resulted in defective courtship song (Figure 5.5). Of the two deletion lines, only $cac^{exon7\Delta(8)}$ showed a longer time to copulation compared to control animals (Figure 5.5A) and there was no difference in the number of successful male flies between the deletion lines and control animals (Figure 5.5B).

Like TBPH mutants, deletion of exon 7 of *cacophony* causes and reduction in *cacophony* protein expression and locomotion defects in third instar larvae. Also similar to TBPH mutants, defects in synaptic physiology at the NMJ in exon 7 deletion animals are not sufficient to drive locomotion defects. Exon 7 deletion animals show un-patterned motor bursts that are uncoordinated between segments, like TBPH mutants. Therefore, it appears that deletion of exon 7 is sufficient to drive larger, motor defects.

LIMITATIONS & OUTSTANDING QUESTIONS

There are several limitations, and thus outstanding questions, of the data presented in this chapter that must be addressed. The greatest limitation I must first address is the nature of the two modes of *cacophony* rescue. First, though Western analysis suggests there is not difference in expression levels of *cacophony* between the UAS-GAL4 system and x-duplication in adult heads (see Appendix B), *cacophony* expression levels of the modes of rescue in third instar larva have not yet been quantified. Regardless of the level of protein expression, we can also say nothing about the transcript isoforms being expressed in these two systems. It is possible that differences in rescues between these methods (for example, the UAS-GAL4 system rescues the reduction in mEPP frequency, but the X-duplication does not) is not only due to differences in protein expression, but also specifically in the isoforms expressed. Regardless of the method of rescue, however, none of the *cacophony*-dependent phenotypes of the exon 7 deletion animals can be attributed to the specific deletion of exon 7.

There are two outstanding questions. The first concerns the similarities and differences between the two deletion lines: $cac^{exon7\Delta(6)}$ and $cac^{exon7\Delta(8)}$. The two lines are derived from the same injection of CRISPR-CAS plasmid, and thus theoretically share the same genetic background. Both lines show a reduction in the expression of *cacophony* protein in whole larvae, but no change in transcript expression. Both lines eclose into adulthood, and both lines show locomotion defects in third instar larvae. However, both lines show significant differences in protein expression and physiology at boutons. What the mechanism behind these differences is remains unclear. $Cac^{exon7\Delta(6)}$ shows similar physiology at the NMJ to TBPH mutants: no change in EJP amplitude and a reduction in

mEPP frequency (Figure 3.3). However, $cac^{exon7\Delta(6)}$ boutons show no change in

cacophony protein expression levels. $Cac^{exon7\Delta(8)}$, like TBPH mutants, shows a

cacophony–dependent reduction in mEPP frequency, in contrast to TBPH mutants, shows

a *cacophony*-dependent reduction in EJP amplitude. This difference between TBPH

mutants and $cac^{exon7\Delta(8)}$ asserts that while both show decreases in EJP amplitudes, the

decrease is due to different mechanisms.

The second outstanding question from the data presented here is whether any of

the described phenotypes of the deletion lines are due to the specific deletion of exon 7.

Due to the limitations on the nature of the rescue constructs, described earlier, we cannot

definitively state that any of the phenotypes described in the deletion lines are due

specifically to the deletion of exon 7.

CHAPTER 6

Discussion & Future Directions

TDP-43 is a nuclear RNA and DNA binding protein associated with 96% of ALS patient pathology. Tissue samples taken post-mortem from patients show a loss of nuclear localization and the presence of TDP-43 in cytoplasmic inclusions in the cell body. Whether the pathogenesis of the disease is driven by loss of nuclear function, gain of cytotoxicity with the formation of the cytoplasmic inclusions, or some other yet unidentified cause is not known. The goal of the research presented here was to understand the downstream effects of loss of nuclear TDP-43 function on motor behavior and physiology, using *Drosophila melanogaster* as a model.

Loss of TBPH, the Drosophila ortholog of TBDP-43, causes severe locomotion defects in third instar larvae. It also causes a 50% reduction in protein expression of the gene *cacophony*, as well as enrichment in *cacophony* transcripts lacking exon 7. *Cacophony* is the type-II voltage gated calcium channel at the neuromuscular junction and is necessary for evoked neurotransmission. We found that genetically restoring *cacophony* rescued the locomotion defects on TBPH mutant larvae. I therefore asked the following questions, which guided the work presented here: First, is the larval locomotion defect driven by the loss of *cacophony* in all motor neurons or in a subset of neurons in the motor circuit? Second, what physiology of the larval neuromuscular junction is changed in at TBPH dependent- and *cacophony* dependent- manner? Third, does the enrichment of *cacophony* exon 7 deleted transcripts recapitulate defects in larval locomotion observed in TBPH mutants?

CHAPTER 3 CONCLUSIONS

TBPH mutants show defective larval locomotion that is rescued by driving *cacophony* in all motor neurons. The first question I asked was whether this rescue was dependent upon the restoration of *cacophony* in all motor neurons or in a subset of neurons that act to modulate locomotion behavior. I asked this question in response to Vogelstein et al 2014, in which activation of discreet subsets of neurons in the brain and ventral nerve cord were determined to be sufficient to drive sub-behaviors of larval crawling. From the screen I performed, I found genetically restoring *cacophony* in the AVM001b/2b neurons in the brain was sufficient to rescue the locomotion defect in TBPH mutant animals. Thus, it appears that the TBPH dependent loss of *cacophony* in a subset of cells is sufficient to drive defective locomotion in an entire larva.

I then asked whether TBPH mutants showed *cacophony* –dependent changes in evoked or spontaneous neurotransmission at the neuromuscular junction. TBPH mutants show no changes in evoked neurotransmitter release, but significant reduction in both the amplitude and frequency of spontaneous release. The reduction in the amplitude of spontaneous release was TBPH dependent, but not *cacophony* dependent. This observation is novel, as other TDP-43 models have not reported changes in mEPP amplitude. The reduction in the frequency of spontaneous release, however, was not TBPH dependent, but was *cacophony* dependent. This observation was unusual and novel, as it is the first time a suggestion that *cacophony* functions in regulating spontaneous release has been made. It was therefore essential to further test the function

of *cacophony* in regulating spontaneous release by pharmacologically blocking the channel with PLTX-II. These experiments showed, quite beautifully, that *cacophony* functions to regulate the frequency of spontaneous release, while not affecting the amplitude of mEPPs.

Though genetically restoring *cacophony* in motor neurons rescued the reduction in frequency of spontaneous release in TBPH mutants, driving *cacophony* in just the AVM001b/2b cells was not sufficient to rescue the defect. From these experiments, I concluded that changes in physiology at the neuromuscular junction in TBPH mutants are not sufficient to drive the defective larval locomotion. This is of especial significance because, in ALS and TDP-43 literature, much emphasis is placed on physiological experiments at the neuromuscular junction.

CHAPTER 4 CONCLUSIONS

Having determined that changes in physiology at the neuromuscular junction were not sufficient to drive locomotion defects in TBPH mutants, I decided to measure motor burst patterns from intact motor nerves. Forward larval crawling is achieved by peristaltic waves that originate in the posterior abdominal wall segments and traverse the body toward the anterior segments. Peristaltic waves are generated by central pattern generators of the motor circuit, which activate motor neurons and stimulate muscle contraction. Having observed abnormal peristaltic waves in TBPH mutants, I recorded motor bursts from intact motor nerves. TBPH mutants showed un-patterned, uncoordinated motor bursts within segments and between segments. This lack of

coordination directly impacts the ability of the larva to crawl and move, and is completely TBPH dependent. These results show that the motor circuit is defective with loss of TBPH.

The most astonishing observation from these experiments, and yet the least surprising based on the locomotion data, was that driving *cacophony* in the AVM001b/2b cells in the brain was sufficient to restore patterned, coordinated motor bursts in TBPH mutants. The AVM001b/2b cells are situated in the protocerebrum of the larval brain. They are virtually absent in the literature, apart from Vogelstein et al 2014. There is absolutely no visual evidence that they project out of the ventral nerve cord, and the cells with which they might be synapsing is unknown. Nevertheless, the specific restoration of *cacophony* in these cells was sufficient to restore motor burst pattern and coordination in the ventral nerve cord. This observation further supports the earlier assertion I made that greater emphasis must be placed on central motor circuit physiology in ALS models.

Because the AVM001b/2b cells are virtually absent from the literature, I therefore sought to characterize their function in the motor circuit. Unfortunately, killing them genetically with *reaper* produced no effect on larval locomotion or viability. Activating them with TrpA1 also did not affect locomotion or viability. While these acute experiments did nothing to hint at the functions of AVM001b/2b in the motor circuit, they reaffirmed the importance of the *cacophony* specific nature of the rescue. These results further asserted the importance of the specific interaction between TDP-43 and voltage gated calcium channels in the etiology of locomotion defects.

CHAPTER 5 CONCLUSIONS

In addition to a 50% reduction in *cacophony* protein expression, TBPH mutants

show a significant enrichment of *cacophony* transcripts lacking exon 7. Because TBPH

mutants show several *cacophony*-dependent locomotion defects, we decided to test

whether deleting the coding region of exon 7 in all cells could recapitulate some of these

defects. It is important to remember, however, due to limitation in the mechanisms of

rescue, that none of the phenotypes described can be attributed specifically to the deletion

of exon 7. Rather, because exon 7 deletion animals show a reduction in the expression

level of *cacophony* protein, and the rescue constructs include exon 7, we can only

identify phenotypes that are *cacophony* dependent.

Before proceeding in my discussion of the data presented in Chapter 4, I want to

write a few words about the rescue constructs used. We chose to genetically restore

cacophony in the deletion lines two independent ways. The first mode of rescue uses the

UAS-GAL4 system to drive UAS-cacophony in motor neurons using the D42-GAL4

driver. We initially chose D42-GAL4 because it shows broad expression in the ventral

nerve cord and the brain, and gives a robust locomotion rescue in TBPH mutants. It is

important to remember, however, that the UAS-GAL4 system is inherently an

overexpression system, and will therefore surpass what would be endogenous expression

levels. The second mode of rescue was to utilize an x-duplication line in which the

cacophony gene and endogenous promoter has been copied onto chromosome 3. Because

this is under the endogenous promoter, it does not necessarily express *cacophony* to the

same levels as the GAL-UAS system. Finally, while both the UAS-Cacophony and the x-

duplication include exon 7 coding region, they also include alternative exons and we do

not know the full populations of transcript isoforms expressed with each rescue construct. It is important to keep these nuances between modes of rescue in mind in the following discussion of the data presented.

Both exon 7 deletion lines show *cacophony*-dependent locomotion defects in third instar larvae. While these defects are not as severe as those of TBPH mutants, they show defective peristaltic waves and decreased crawling distance. Because *cacophony* is so necessary to neurotransmission at the neuromuscular junction, I measured both mEPPs and EJPs in deletion larvae. Both lines show normal mEPP amplitudes, which agrees with previous reports that *cacophony* does not function to regulate mEPP amplitude. Both lines also show a reduction in mEPP frequency, similar to TBPH mutants. Unlike the TBPH mutants, however, the dependence of this decrease on *cacophony* is more obscure, due to inconsistencies in the rescue constructs. While driving UAS-Cacophony with the D42-GAL4 driver rescues mEPP frequency in $cac^{exon7\Delta(6)}$, it does not in $cac^{exon7\Delta(8)}$. This difference could potentially be due to differences in expression level of *cacophony* at the bouton between the deletion lines, or due to differences in isoform expression. Also, the x-duplication rescues the reduction in neither of the deletion lines, which could reflect differences in expression level with the GAL4-UAS system.

EJP amplitudes were also measured between the two deletion lines and, while $cac^{exon7\Delta(6)}$ showed normal amplitudes, $cac^{exon7\Delta(8)}$ showed a reduction in amplitudes. This reduction appears to be *cacophony* dependent in that both modes of rescue restored the amplitude. Why one deletion line would show a decrease and not the other is unclear, especially in light of *cacophony* fluorescence at boutons. Immunohistochemistry showed a decrease in *cacophony* protein at $cac^{exon7\Delta(6)}$ boutons, but not at $cac^{exon7\Delta(8)}$ boutons. EJP

amplitude is sensitive to *cacophony* expression, and yet the deletion line showing no change at boutons is the one with a decrease in EJP amplitude. These results seem contradictory and further obscure the differences between the two deletion lines.

Regardless of changes in physiology at the neuromuscular junction, both exon 7 deletion lines show uncoordinated motor burst patterns. While the motor neurons are clearly bursting, and while they are doing so in a quasi-patterned way, compared to the lack of pattern in TBPH mutants, there appears to be a lack of coordination between the segments. While TBPH mutant larvae motor neurons are clearly firing, they are doing so without a refined, rhythmic bursting pattern. Exon 7 deletion animals, however, show bursting patterns, but they are a-rhythmic and uncoordinated between segments. This lack of coordination would contribute to the increase in time-to-completion of each peristaltic wave that is present in exon 7 deletion animals. Whether this lack of coordination is due to deletion of exon 7 cannot be determined, however driving UAS-Cacophony with D42-GAL4 restores both the rhythmicity and coordination of motor bursting. Thus, these defects are clearly *cacophony* dependent.

FUTURE DIRECTIONS

There are several outstanding questions from the data presented in this dissertation that I have touched on in Chapters 3, 4, and 5. Here I will touch on the larger outstanding questions that could give credence to future experiments.

First, the *cacophony* rescue in AVM001b/2b cells is one of the most exciting

aspects of the data presented here. Not only unexpected, it added unknown functional

attributes to the AVM001b/2b cells. The mechanism of this rescue is still unclear. I have

shown the rescue is specific to *cacophony*; mere acute activation of the cells is not

sufficient to rescue locomotion defects. However, I never tested whether chronic

activation of the cells from egg laying through instar development could recapitulate a

rescue. To test whether chronic activation of the AVM001b/2b cells through development

could rescue locomotion defects, flies containing the UAS-TrpA1 construct, in the TBPH

mutant background, could be mated with flies containing the R75C05-GAL4 driver, also

in the TBPH mutant background. This cross could be made at 30°C and progeny kept at

30°C throughout development, and their locomotion assessed at third instar stage.

The second outstanding question from the data presented here pertains to the

endogenous function of the AVM001b/2b cells in the motor circuit. Acute activation of

these cells with channel rhodopsin indicated that they function to drive mild escape

behavior in third instar larvae. Killing these cells genetically with *reaper* had no effect on

larval crawling or vitality. Activating these cells in a wild type background with TrpA1

also had no significant effect on larval locomotion. What are these cells? What are they

synapsing to? What neurotransmitter might they be releasing? These are all questions

whose answers would give clues to the endogenous function of these cells in the motor

circuit.

The final outstanding question pertains to the function of exon 7 in *cacophony*-

dependent physiology. As I have belabored the limitations set by our rescue constructs in

attributing phenotypes of the exon 7 deletion animals to loss of *cacophony,* and I will not

do it here. Rather, I will merely contend that a negative control for deletion of exon 7 will act to clear the murkiness surrounding *cacophony*-dependent interpretations of the data. A negative control, in which a UAS-Cacophony lacking exon 7 will be driven by a GAL4 driver, would at least provide a way to identify which *cacophony*-dependent changes in physiology could be due to loss of exon 7.

CONCLUSIONS

In conclusion, I wish to address a question that gets posed to me occasionally at the end of seminars: is the TBPH mutant a real model of ALS? The quick answer is no, it is not. It does not recapitulate late stage TDP-43 inclusions observed in patients. Rather, this model is a complete removal of the protein, which is not a phenotype observed in patient tissue. But this model was never intended to recapitulate end stage ALS pathology. I have always contended that this model was meant to identify downstream effects of the loss of TDP-43 nuclear function, which we know causes a locomotion defect, a hallmark of the disease in patients. By identifying downstream effects, such as changes to the motor circuit, we could begin to understand disease pathogenesis and identify possible points of intervention or therapeutic targets. The data I have collected using this model shows that TDP-43 dependent changes in centrally located neurons drive systemic locomotion defects, not changes to the neuromuscular junction. These changes to motor neurons are voltage gated calcium channel dependent and, thus, it is defective TDP-43 – voltage gated calcium channel dynamics that drives the locomotion defects. What initiates the defective relationship between TDP-43 and voltage gated

calcium channels is not known. Regardless, this is a relationship that is regulating

systemic locomotion behavior.

APPENDIX A

Validation of GluRIIA and TBPH Mutant Recombinant Fly Line

RATIONALE

As *cacophony* levels are reduced in TBPH mutants and they nevertheless exhibit synaptic homeostasis, it is possible that no further homeostasis was possible. To test this, I imposed a post synaptic challenge by genetically expressing a loss of function allele of the alpha-2 subunit of the glutamate receptor (GluRIIA[sp16]; Petersen et al., 1997) in the TBPH mutant. Genetically, TBPH is on the Drosophila chromosome 2. GluRIIA[sp16] is also on chromosome 2. Thus, in order to make a fly that expressed two copies of both allele, the two alleles had to be recombined.

In order to verify that the recombination was made successfully, two phenotypes were tracked. First, TBPH mutants show a crawling defect in third instar larvae. Second, GluRIIA[sp16] homozygotes show a significant reduction in mEPP amplitude but no defect in larval crawling. Thus, these two phenotypes were tracked to verify that the GluRIIA, tbphΔ indeed had two copies of each allele.

RESULTS

Crawling distance was measured of homozygote {GluRIIA, tbphΔ} and heterozygote {GluRIIA, tbphΔ/+} third instar larvae (Figure A1.A). Homozygote {GluRIIA, tbphΔ} animals showed a significant reduction in distance crawled similar to that of the TBPH mutants (Figure A1.A). The heterozygote did not show a reduction in locomotion, thus confirming the presence of two TBPH mutant alleles in the {GluRIIA, tbphΔ} animal.

The amplitude of mEPPs was measured in the homozygote {GluRIIA, tbphΔ} and parental controls, tbphΔ and GluRIIA (Figure A1.B). The homozygote showed a significant reduction in mEPP amplitudes, similar to the GluRIIA parental control (Figure A1.B).
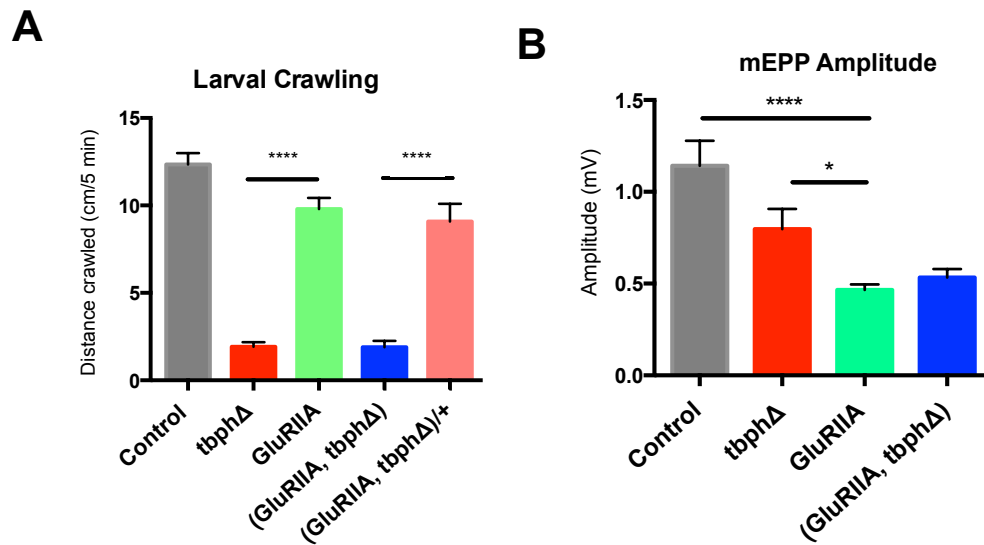
Figure A1. {GluRIIA, tbphΔ} larvae show reduced crawling distance and reduced mEPP amplitudes. **A**. {GluRIIA, tbphΔ} larvae crawl shorter distances compared to heterozygote {GluRIIA, tbphΔ/+}, validating the presence of two tbphΔ alleles. **B**. {GluRIIA, tbphΔ} animals show a reduction in mEPP amplitude to the same extent as the parental GluRIIA line. Data shown represent the mean and SEM of at least 10 animals and were analyzed using ordinary one-way ANOVA with a Sidak's multiple comparisons test (**** p<0.0001, * p <0.05).

APPENDIX B

Quantification of *cacophony* protein expression in exon 7deletion fly lines.

Alex Law collected the data presented here. This appendix was added to supplement data

I report in Chapter 5.

SUMMARY

TBPH mutants show an enrichment in *cacophony* transcripts lacking exon 7 (Chang et al., 2014). Of the fourteen described *cacophony* isoforms, only one lacks exon 7, suggesting it is of functional significance (Figure A2). We therefore tested whether deletion of exon 7 would be sufficient to recapitulate any of the *cacophony*-dependent locomotion defects observed in TBPH mutants. Deletion of exon 7 from the *cacophony* coding region was achieved using CRISPR-CAS (described in Chapter 5 Materials & Methods; Figure A3) shows a schematic of how the exon 7 deletion lines were generated.

Following generation of the two *cacophony* exon 7 deletion lines, $cac^{exon7\Delta(6)}$ and $cac^{exon7\Delta(8)}$, Western analysis was used to quantify *cacophony* protein expression in the larval CNS and adult heads (Figure A4). TBPH mutants show a 50% reduction in *cacophony* protein expression (Chang et al., 2014), and thus we expected there to also be a reduction in the exon 7 deletion lines. *Cacophony* protein expression was also quantified in adult heads of the two approaches to *cacophony* rescue: UAS-Cacophony drive by D42-GAL4, and the x-duplication line where the *cacophony* allele has been duplicated with its endogenous promoter onto chromosome 3.

Both deletion lines show a greater than 50% reduction in *cacophony* protein expression in both the larval CNS and adult heads (Figure A4). Western analysis thus far has only been performed on adult heads of the rescue constructs. Both modes of rescue show an increase in *cacophony* expression, compared to the parental deletion lines (Figure A4). However, the expression level is not significantly different between the two

modes of rescue. Expression levels of *cacophony* in larvae of the rescue constructs have

not yet been measured.

Figure A2. Of the fourteen reported *cacophony* isoforms, only one lacks exon 7.

Image taken from http://flybase.org.
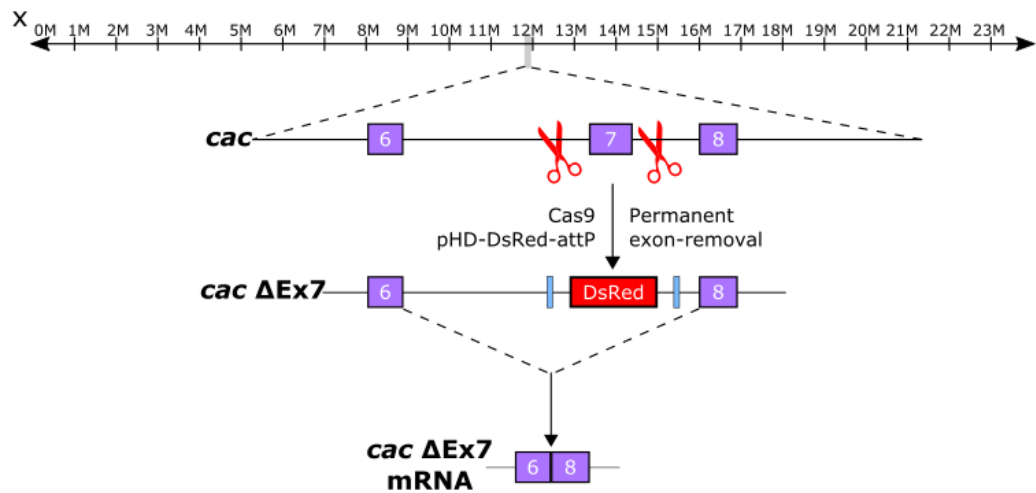
Figure A3. Schematic representation of the removal of exon 7 from the coding region of *cacophony* using CRISPR-CAS. This method was used to generate the two deletion lines: $cac^{\text{exon}7\Delta(6)}$ and $cac^{\text{exon}7\Delta(8)}$. Figure used courtesy of Alex Law.
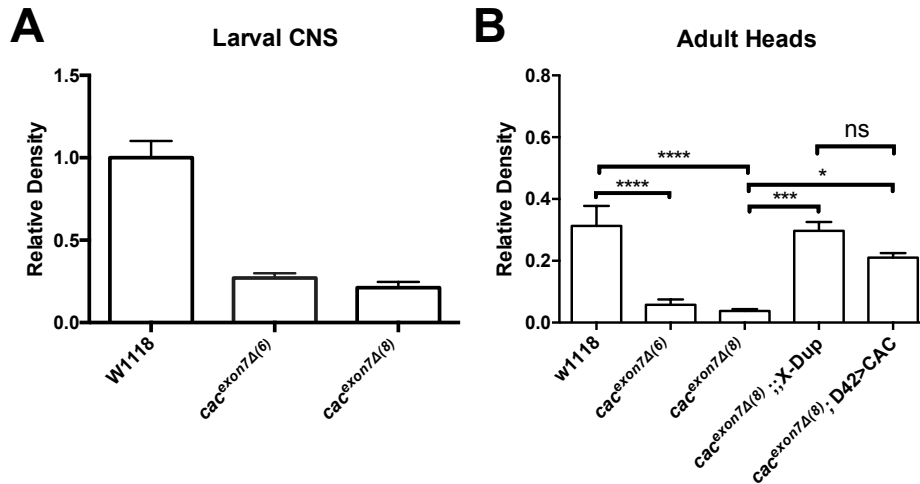
Figure A4. *Cacophony* exon 7 deletion lines show a decrease in *cacophony* protein expression using Western analysis. All tissues analyzed came from male flies. Data presented represents the average and SEM of four replicates and was analyzed using ordinary one-way ANOVA with a Sidak's multiple comparisons test (**** $p<0.0001$, ***$p<0.001$, * $p <0.05$, ns = not significant). Figure used courtesy of Alex Law.

APPENDIX C

Feeding Assays with Calcium Channel Agonists and Octopamine

BACKGROUND & RATIONALE

TBPH mutants show a decrease in the expression of *cacophony*, the Type II voltage gated calcium channel, as well as *cacophony* – dependent locomotion defects and reduction in the frequency of spontaneous release at the NMJ. In 2013, Armstrong et al showed that zebra fish embryos expressing human TDP-43 with an ALS associated mutation, G348C, presented shorter swimming durations, distances, and velocities (Armstrong and Drapeau, 2013). These animals also showed significantly reduced mEPC frequencies and amplitudes (Armstrong and Drapeau, 2013). Application of either Bay K or FPL64176, both voltage gated calcium channel agonists, rescued both the impaired locomotion and the reduction in mEPC frequency and amplitudes (Armstrong and Drapeau, 2013), suggesting an interaction between TDP-43 and voltage gated calcium channels.

All of these phenotypes were reminiscent of the phenotypes characterized in TBPH mutants (Figures 3.1 & 3.3). We therefore tested whether feeding TBPH mutant larvae   (-)Bay K8644 or nefiracetam could rescue the larval crawling defect. (-)Bay K8644 is an L type voltage gated calcium channel agonist (Endo et al., 2000; Ji et al., 2014). Nefiracetam is an N/L type voltage gated calcium channel agonist (Yamada et al., 1994). Reduction in octopamine has also been reported to cause severe locomotion defects in Drosophila larvae (Saraswati et al., 2004). Though we did not know whether TBPH mutants showed a reduction in octopamine levels, I also tested whether feeding larvae octopamine could also restore larval crawling.

MATERIALS & METHODS

In order to test whether feeding Drosophila larvae Bay K, nefiracetam, or octopamine could rescue the crawling defects of TBPH mutants, I fed TBPH mutants food containing different concentrations of the drug. Drosophila food was prepared with 9.6% yellow dye, as a mechanism to verify the larvae were, in fact, eating the food. A 96 well plate was loaded with 0.5 mL of food + dye and Bay K, nefiracetam, or octopamine added at varying concentrations. At least 10 third instar larvae were placed in each well and larvae left on the food for 5 hours. Larvae were then taken out of the food and crawling assays performed as previously described.

RESULTS

Third instar TBPH mutants (tbphΔ) and heterozygote TBPH mutants (tbphΔ/+) were placed on food containing increasing concentrations of (-)Bay K8466. After 5 hours, the total larval crawling distance was measured over 5 minutes. There was no significant increase in distance crawled by TBPH mutants at any concentration, though there was an increase in distance of larvae fed on concentrations from 10-50 μM (Figure A5A).

TBPH mutants placed on increasing concentrations of nefiracetam showed the greatest increase in crawling distance on 10 μM (Figure A5B). On food containing no drug, TBPH mutants crawled 3 cm (Figure A5B). On 10 μM nefiracetam, TBPH mutants

on 10 μM nefiracetam crawled 10 cm (Figure A5B). A complete rescue was never achieved, however.

Finally, TBPH mutants placed on food containing octopamine showed a significant increase in crawling distance when placed on 20 mM octopamine (Figure A5C). Animals did not crawl, and many did not survive, when fed on food containing 50 mM octopamine (Figure A5C). However, these results proved difficult to replicate and thus no further studies were pursued.

DISCUSSION

Within the context of the data presented in Chapters 3 & 4, the experiments described here were carried out prior to the more detailed characterization of the locomotion defects of TBPH mutants, the screen which lead to the identification of the AVM001b/2b cells, and the analysis of motor bursts in TBPH mutants. These experiments were also carried out with limitations: there was no easy way to quantify the amount of drug that entered each individual larva and the results from octopamine feeding proved difficult to replicate. Had a full rescue of the TBPH mutant crawling defect been achieved, further experiments would have been performed. It is possible that the increase in crawling distance of TBPH mutants on 10 μM nefiracetam could have been achieved by modulation of motor bursts. Whether a chronic exposure of the animal to this concentration of nefiracetam could have sustained the rescue is not known, but would be a potential future direction.

A Larval feeding assays in food containing BayK

B Larval feeding assays in food containing nefiracetam

C Larval feeding assay in food containing octopamine
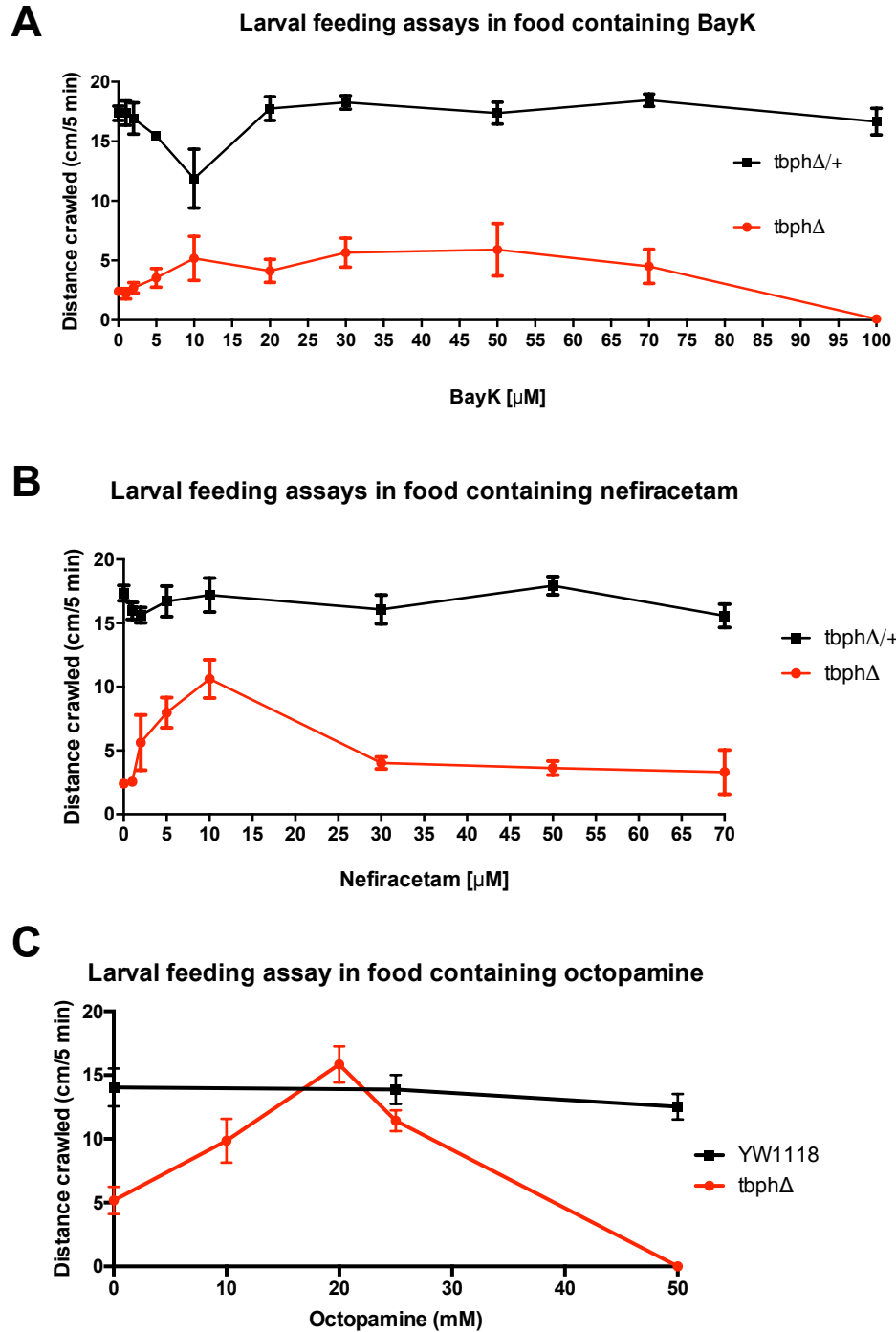
Figure A5. TBPH mutant larvae show defective motor behavior when fed on voltage gated calcium channel agonists or octopamine. **A.** TBPH null mutants do not show improved crawling when placed for 5 hours on food containing (-)Bay K8644, compared

to the heterozygote control animals. **B.** TBPH mutants show moderate increase in crawling distance when placed for 5 hours on food containing 10 μM nefiracetam. **C.** TBPH mutants show increased crawling distance when placed for 5 hours on food containing 20 mM octopamine. The majority of larvae did not survive being placed on food containing 50 mM octopamine. Data shown represent the mean and SEM of at least 10 animals.

APPENDIX D

Deletion of PKA-C3 Produces Decreased Amplitudes and Frequencies of Spontaneous
Release at the NMJ.

Data presented here was collected in collaboration with Elizabeth Sunderhaus, an OHSU

PhD candidate in MMG in the lab of Doris Kretzschmar.

RATIONALE

PKA-C3 is the C3 catalytic subunit of Protein Kinase A and is regulated by Drosophila Swiss Cheese (SWS) protein (Bettencourt da Cruz et al., 2008). SWS is the Drosophila ortholog of Neuropathy Target Esterase (NTE), which plays a functional role in organophosphate induced delayed neuropathy (Bettencourt da Cruz et al., 2008). Key characterizations of this delayed neuropathy are degeneration of long axons in the central and peripheral nervous systems (Bettencourt da Cruz et al., 2008). Mutations in the human homolog of PKA-C3, called PRKX, were also sufficient to drive hereditary spastic paraplegia.

Little is known about the endogenous function of PKA-C3 and its orthologs. The Kretzschmar lab generated a PKA-C3 deletion fly line (BRL6). Deletion of PKA-C3 caused crawling defects in third instar larvae (Kretzschmar lab, unpublished observations). We therefore tested whether this crawling defect was concomitant with changes in evoked and spontaneous neurotransmitter release at the NMJ.

RESULTS

Evoked and spontaneous neurotransmitter release was measured at the NMJs of BRL6 and control (w1118) third instar larvae. To test whether knocking down PKA-C3, using RNAi, would have an affect on synaptic physiology, I also measured EJPs and mEPPs from animals expressing UAS-PKAC3RNAi under the control of three different GAL4 drivers: ElaV (a pan-neuronal driver), NT (natalisin expressing interneurons that endogenously express PKA-C3), and OK371 (a motor neuron driver).

Deletion of PKA-C3 showed no affect on EJP amplitude, compared to control animals (Figure A6A). Knockdown of PKA-C3 in all neurons, using ElaV-GAL4, also had no affect on EJP amplitudes (Figure A6A). Knockdown of PKA-C3 in natalisin interneurons, using NT-GAL4, non-significantly increased EJP amplitudes (Figure A6A). Finally, knockdown of PKA-C3 in motor neurons, using OK371-GAL4, significantly increased EJP amplitudes (Figure A6A).

Amplitudes and frequencies of mEPPs were then measured in all fly lines as previously described. mEPP amplitudes were significantly reduced in animals with deleted PKA-C3 (Figure A6B). Knockdown of PKA-C3 had no affect on mEPP amplitudes (Figure A6B). It is interesting to note that knockdown of PKA-C3 in motor neurons caused an increase in EJP amplitude, but no change in mEPP amplitude, indicating an increase in quantal content. Increased quantal content indicates an activation of synaptic homeostatic processes at the NMJ.

Frequencies of spontaneous release were significantly reduced in PKA-C3 deletion animals, as well as those in which PKA-C3 was knocked-down in all neurons (Figure A6C). Knockdown of PKA-C3 in natalisin neurons and motor neurons had no affect on mEPP frequency.

SUMMARY

Interpretation of these results is limited by the absence of rescue constructs, especially a rescue of PKA-C3 in the BRL6 deletion lines. Therefore, none of the reported results can be solely attributed to the loss of PKA-C3. However, these results

show evidence that deletion of PKA-C3 causes significant defects on the amplitude and frequency of spontaneous release at the NMJ.

Knockdown of PKA-C3 in a variety of cell types also caused modest effects on EJP amplitude and mEPP frequency. Animals with knocked down PKA-C3 in motor neurons showed an increase in EJP amplitudes and unchanged mEPP amplitudes, indicating an increase in quantal content at the NMJ (Figure A6). Increased quantal content is an indicator of activated synaptic homeostasis processes, in response to synaptic challenges, at the NMJ. This was the only construct to show such a response.

While knockdown of PKA-C3 in motor neurons or natalisin interneurons, using OK371-GAL4 or NT-GAL4 respectively, was not sufficient to decrease mEPP frequency, knockdown in all neurons with ElaV-GAL4 did produce a decrease in mEPP frequency. It is unclear why knockdown in all neuron is sufficient, but only in motor neurons is not sufficient, to cause a decrease in mEPP frequency.

Finally, natalisin interneurons endogenously express PKA-C3. While knockdown of PKA-C3 in natalisin neurons increased EJP amplitudes, this increase was not significant. Amplitudes and frequencies of mEPPs were also not changed in these animals, suggesting that these interneurons do not function to directly regulate motor neuron physiology at the NMJ.
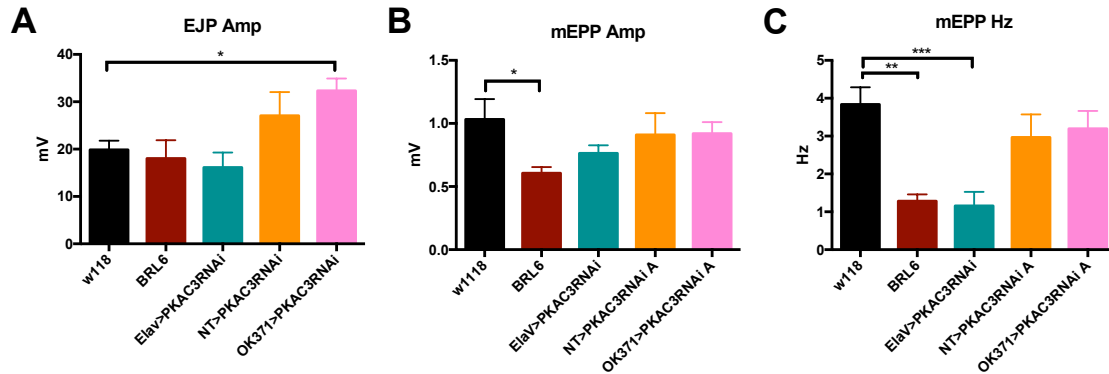
Figure A6. Synaptic physiology at the larval NMJ is defective in PKA-C3 deletion and knock down animals. **A.** EJP amplitude is unchanged in the PKA-C3 deletion line and most of the knock down lines. It is significantly increased in OK371>PKAC3RNAi knock down animals (carnation). **B.** The mEPP amplitude is reduced in PKA-C3 deletion animals (cayenne). It is unchanged in all knock down animals. **C.** The mEPP frequency is reduced in PKA-C3 deletion animals (cayenne) and ElaV>PKAC3RNAi knock down animals. All experiments were carried out in 1 mM calcium. Data represent the mean and SEM of at least 8 animals and were analyzed using ordinary one-way ANOVA with a Sidak's multiple comparisons test (*** p<0.01, ** p< 0.05, * p <0.1).

REFERENCES

Arai T, Hasegawa M, Akiyama H, Ikeda K, Nonaka T, Mori H, Mann D, Tsuchiya K,

    Yoshida M, Hashizume Y, Oda T (2006) TDP-43 is a component of ubiquitin-

    positive tau-negative inclusions in frontotemporal lobar degeneration and

    amyotrophic lateral sclerosis. Biochem Biophys Res Commun 351:602–611.

Armstrong G a B, Drapeau P (2013) Calcium channel agonists protect against

    neuromuscular dysfunction in a genetic model of TDP-43 mutation in ALS. J

    Neurosci 33:1741–1752.

Ask-Upmark E, Meurling S (1955) On the Presence of a Deficinecy Factor in the

    Pathogenesis of Amyotrophic Lateral Sclerosis. Acta Med Scand 152:217–222.

Avendaño-Vázquez SE, Dhir A, Bembich S, Buratti E, Proudfoot N, Baralle FE (2012)

    Autoregulation of TDP-43 mRNA levels involves interplay between transcription,

    splicing, and alternative polyA site selection. Genes Dev 26:1679–1684.

Ayala YM, Pantano S, D'Ambrogio A, Buratti E, Brindisi A, Marchetti C, Romano M,

    Baralle FE (2005) Human, Drosophila, and C.elegans TDP43: nucleic acid binding

    properties and splicing regulatory function. J Mol Biol 348:575–588.

Ayala YM, Zago P, D'Ambrogio A, Xu Y-F, Petrucelli L, Buratti E, Baralle FE (2008)

    Structural determinants of the cellular localization and shuttling of TDP-43. J Cell

    Sci 121:3778–3785.

Baudoux S, Duch C, Morris OT (1998) Coupling of efferent neuromodulatory neurons to

rhythmical leg motor activity in the locust. J Neurophysiol 79:361–370.

Bell TJ, Thaler C, Castiglioni AJ, Helton TD, Lipscombe D (2004) Cell-specific
alternative splicing increases calcium channel current density in the pain pathway.
Neuron 41:127–138.

Bellen HJ, Tong C, Tsuda H (2010) 100 years of Drosophila research and its impact on
vertebrate neuroscience: a history lesson for the future. Nat Rev Neurosci 11:514–
522.

Bettencourt da Cruz A, Wentzell J, Kretzschmar D (2008) Swiss Cheese, a Protein
Involved in Progressive Neurodegeneration, Acts as a Noncanonical Regulatory
Subunit for PKA-C3. J Neurosci 28.

Billeter J-C, Rideout EJ, Dornan AJ, Goodwin SF (2006) Control of Male Sexual
Behavior in Drosophila by the Sex Determination Pathway. Curr Biol 16:R766–
R776.

Bogousslavsky J, Moulin T (2010) Birth of modern psychiatry and the death of alienism:
The legacy of jean-martin charcot. In: Following Charcot: A Forgotten History of
Neurology and Psychiatry, vol. 29. (Bogousslavsky J, ed), pp 1–8.

Bradley WG (1977) Axonal Transport and its Possible Role in Motor Neurone Disease.
In: Motor Neurone Disease (Rose FC, ed). Bath: Grune & Stratton.

Brand AH, Perrimon N (1993) Targeted gene expression as a means of altering cell fates
and generating dominant phenotypes. Development 118:401–415.

Broadie K, Bate M (1993) Innervation directs receptor synthesis and localization in

   Drosophila embryo synaptogenesis. Nature 361:350–353.

Brosenitsch TA, Katz DM (2001) Physiological patterns of electrical stimulation can

   induce neuronal gene expression by activating N-type calcium channels. J Neurosci

   21:2571–2579.

Buratti E, Baralle FE (2011) TDP-43: new aspects of autoregulation mechanisms in RNA

   binding proteins and their connection with human disease. FEBS J 278:3530–3538.

Casci I, Pandey UB (2015a) A fruitful endeavor: modeling ALS in the fruit fly. Brain Res

   1607:47–74.

Casci I, Pandey UB (2015b) A fruitful endeavor: Modeling ALS in the fruit fly. Brain

   Res 1607:47–74.

Chang JC, Hazelett DJ, Stewart JA, Morton DB (2014) Motor neuron expression of the

   voltage-gated calcium channel cacophony restores locomotion defects in a

   Drosophila, TDP-43 loss of function model of ALS. Brain Res 1584:39–51.

Chen K, Featherstone DE (2005) Discs-large (DLG) is clustered by presynaptic

   innervation and regulates postsynaptic glutamate receptor subunit composition in

   Drosophila. BMC Biol 3:1.

Chen P, Lee P, Otto L, Abrams J (1996) Apoptotic activity of REAPER is distinct from

   signaling by the tumor necrosis factor receptor 1 death domain. J Biol Chem

   271:25735–25737.

Cozzolino M, Pesaresi MG, Gerbino V, Grosskreutz J, Carrì MT (2012) Amyotrophic

lateral sclerosis: new insights into underlying molecular mechanisms and

opportunities for therapeutic intervention. Antioxid Redox Signal 17:1277–1330.

Davison C (1943) Effect of Vitamin E Therapy on the Central Nervous System in

Amyotrophic Lateral Sclerosis. Am J Pathol 19:883–899.

Dewey CM, Cenik B, Sephton CF, Johnson BA, Herz J, Yu G (2012) TDP-43

aggregation in neurodegeneration: Are stress granules the key? Brain Res 1462:16–

25.

Diaper DC, Adachi Y, Lazarou L, Greenstein M, Simoes FA, Di Domenico A, Solomon

DA, Lowe S, Alsubaie R, Cheng D, Buckley S, Humphrey DM, Shaw CE, Hirth F

(2013a) Drosophila TDP-43 dysfunction in glia and muscle cells cause cytological

and behavioural phenotypes that characterize ALS and FTLD. Hum Mol Genet

22:3883–3893.

Diaper DC, Adachi Y, Sutcliffe B, Humphrey DM, Elliott CJH, Stepto A, Ludlow ZN,

Broeck L Vanden, Callaerts P, Dermaut B, Al-Chalabi A, Shaw CE, Robinson IM,

Hirth F (2013b) Loss and gain of Drosophila TDP-43 impair synaptic efficacy and

motor control leading to age-related neurodegeneration by loss-of-function

phenotypes. Hum Mol Genet 22:1539–1557.

Dolphin AC (2009) Calcium channel diversity: multiple roles of calcium channel

subunits. Curr Opin Neurobiol 19:237–244.

Endo M, Kurachi Y, Mishina M (2000) Pharmacology of Ionic Channel Function:

Activators and Inhibitors. Springer Berlin Heidelberg.

Engel AG (2008) Synaptic Electrophysiology of the Drosophila Neuromuscular Junction Bing Z, Freeman MR, Waddell S, eds. Handb Clin Neurol / Ed by PJ Vinken GW Bruyn 91:103–120.

Fatt P, Katz B (1952) SPONTANEOUS SUBTHRESHOLD ACTIVITY AT MOTOR NERVE ENDINGS. J Physiol 117:109–128.

Feiguin F, Godena VK, Romano G, D'Ambrogio A, Klima R, Baralle FE (2009) Depletion of TDP-43 affects Drosophila motoneurons terminal synapsis and locomotive behavior. FEBS Lett 583:1586–1592.

Fouquet W, Owald D, Wichmann C, Mertel S, Depner H, Dyba M, Hallermann S, Kittel RJ, Eimer S, Sigrist SJ (2009) Maturation of active zone assembly by Drosophila Bruchpilot. J Cell Biol 186:129–145.

Fox LE, Soll DR, Wu C-F (2006) Coordination and modulation of locomotion pattern generators in Drosophila larvae: effects of altered biogenic amine levels by the tyramine beta hydroxlyase mutation. J Neurosci 26:1486–1498.

Frank CA (2014) How voltage-gated calcium channels gate forms of homeostatic synaptic plasticity. Front Cell Neurosci 8:40.

Frank CA, Kennedy MJ, Goold CPP, Marek KW, Davis GWW (2006) Mechanisms Underlying the Rapid Induction and Sustained Expression of Synaptic Homeostasis. Neuron 52:663–677.

Fushiki A, Zwart MF, Kohsaka H, Fetter RD, Cardona A, Nose A (2016) A circuit
mechanism for the propagation of waves of muscle contraction in Drosophila. Elife
5.

Gan G, Lv H, Xie W (2014) Morphological identification and development of neurite in
Drosophila ventral nerve cord neuropil. PLoS One 9:e105497.

Gjorgjieva J, Berni J, Evers JF, Eglen SJ (2013) Neural circuits for peristaltic wave
propagation in crawling Drosophila larvae: analysis and modeling. Front Comput
Neurosci 7:24.

Goetz CG (2011) The history of Parkinson's disease: Early clinical descriptions and
neurological therapies. Cold Spring Harb Perspect Med 1.

Gorczyca D, Ashley J, Speese S, Gherbesi N, Thomas U, Gundelfinger E, Gramates LS,
Budnik V (2007) Postsynaptic membrane addition depends on the Discs-Large-
interacting t-SNARE Gtaxin. J Neurosci 27:1033–1044.

Gorczyca M, Augart C, Budnik V (1993) Insulin-like receptor and insulin-like peptide
are localized at neuromuscular junctions in Drosophila. J Neurosci 13.

Gowers WR (1902) A Lecture on Abiotrophy. Lancet:1003-.

Graf ER, Valakh V, Wright CM, Wu C, Liu Z, Zhang YQ, DiAntonio A (2012) RIM
promotes calcium channel accumulation at active zones of the Drosophila
neuromuscular junction. J Neurosci 32:16586–16596.

Gramates LS, Budnik V (1999) Assembly and maturation of the Drosophila larval

neuromuscular junction. Int Rev Neurobiol 43:93–117.

Gray AC, Raingo J, Lipscombe D (2007) Neuronal calcium channels: splicing for optimal performance. Cell Calcium 42:409–417.

Greenspan RJ (1997) Fly pushing: The theory and practice of Drosophila genetics. Cold Spring Harb Lab Press:418.

Gu H, Jiang SA, Campusano JM, Iniguez J, Su H, Hoang AA, Lavian M, Sun X, O'Dowd DK (2009) Cav2-type calcium channels encoded by cac regulate AP-independent neurotransmitter release at cholinergic synapses in adult Drosophila brain. J Neurophysiol 101:42–53.

Guerrero EN, Wang H, Mitra J, Hegde PM, Stowell SE, Liachko NF, Kraemer BC, Garruto RM, Rao KS, Hegde ML (2016) TDP-43/FUS in motor neuron disease: Complexity and challenges. Prog Neurobiol 145–146:78–97.

Guillain G, Bailey P trans (1959) J.-M. Charcot, 1825-1893; his life, his work. New York Hoeber.

Hanson KA, Kim SH, Wassarman DA, Tibbetts RS (2010) Ubiquilin modifies TDP-43 toxicity in a Drosophila model of amyotrophic lateral sclerosis (ALS). J Biol Chem 285:11068–11072.

Harris KP, Littleton JT (2015) Transmission, development, and plasticity of synapses. Genetics 201:345–375.

Hasegawa M, Arai T, Nonaka T, Kametani F, Yoshida M, Hashizume Y, Beach TG,

Buratti E, Baralle F, Morita M, Nakano I, Oda T, Tsuchiya K, Akiyama H (2008) Phosphorylated TDP-43 in frontotemporal lobar degeneration and amyotrophic lateral sclerosis. Ann Neurol 64:60–70.

Hazelett DJ, Chang J-C, Lakeland DL, Morton DB (2012) Comparison of parallel high-throughput RNA sequencing between knockout of TDP-43 and its overexpression reveals primarily nonreciprocal and nonoverlapping gene expression changes in the central nervous system of Drosophila. G3 (Bethesda) 2:789–802.

Henneman E, Mendell LM, Henneman E, Mendell LM (2011) Functional Organization of Motoneuron Pool and its Inputs. In: Comprehensive Physiology. Hoboken, NJ, USA: John Wiley & Sons, Inc.

Hirano A, Iwata M (1978) Pathology of Motor Neurons with Special Reference to Amyotrophic Lateral Sclerosis and Related Diseases. In: Amyotrophic lateral sclerosis: proceedings of the International Symposium on Amyotrophic Lateral Sclerosis help February 2 and 3, 1978 (Tsubaki T, Toyokura Y, eds). Baltimore: University Park Press.

Hoang B, Chiba A (2001) Single-cell analysis of Drosophila larval neuromuscular synapses. Dev Biol 229:55–70.

Hou J, Tamura T, Kidokoro Y (2008) Delayed Synaptic Transmission in Drosophila cacophonynull Embryos. J Neurophysiol 100:2833–2842.

Iguchi Y, Katsuno M, Niwa JI, Takagi S, Ishigaki S, Ikenaka K, Kawai K, Watanabe H, Yamanaka K, Takahashi R, Misawa H, Sasaki S, Tanaka F, Sobue G (2013) Loss of

TDP-43 causes age-dependent progressive motor neuron degeneration. Brain 136:1371–1382.

Inada K, Kohsaka H, Takasu E, Matsunaga T, Nose A (2011) Optical dissection of neural circuits responsible for drosophila larval locomotion with Halorhodopsin Brembs B, ed. PLoS One 6:e29019.

International Glossina Genome Initiative IGG et al. (2014) Genome sequence of the tsetse fly (Glossina morsitans): vector of African trypanosomiasis. Science 344:380–386.

Jackson CE, Bryan WW (1998) Amyotrophic Lateral Sclerosis. Semin Neurol 18:27–39.

Jan LY, Jan YN (1976) Properties of the larval neuromuscular junction in Drosophila melanogaster. J Physiol 262:189–214.

Jenett A et al. (2012) A GAL4-Driver Line Resource for Drosophila Neurobiology. Cell Rep 2:991–1001.

Ji J, Kang J, Rampe D (2014) L-type Ca2+ channel responses to bay k 8644 in stem cell-derived cardiomyocytes are unusually dependent on holding potential and charge carrier. Assay Drug Dev Technol 12:352–360.

Jia XX, Gorczyca M, Budnik V (1993) Ultrastructure of neuromuscular junctions in Drosophila: comparison of wild type and mutants with increased excitability. J Neurobiol 24:1025–1044.

Johnston RM, Levine RB (1996) Crawling motor patterns induced by pilocarpine in

isolated larval nerve cords of Manduca sexta. J Neurophysiol 76:3178–3195.

Kavalali ET (2014) The mechanisms and functions of spontaneous neurotransmitter release. Nat Rev Neurosci 16:5–16.

Kawasaki F, Collins SC, Ordway RW (2002) Synaptic calcium-channel function in Drosophila: analysis and transformation rescue of temperature-sensitive paralytic and lethal mutations of cacophony. J Neurosci 22:5856–5864.

Kawasaki F, Felling R, Ordway RW (2000) A temperature-sensitive paralytic mutant defines a primary synaptic calcium channel in Drosophila. J Neurosci 20:4885–4889.

Kawasaki F, Zou B, Xu X, Ordway RW (2004) Active zone localization of presynaptic calcium channels encoded by the cacophony locus of Drosophila. J Neurosci 24:282–285.

Kim MD, Wen Y, Jan Y-N (2009) Patterning and organization of motor neuron dendrites in the Drosophila larva. Dev Biol 336:213–221.

King GF (2007) Modulation of insect Ca(v) channels by peptidic spider toxins. Toxicon Off J Int Soc Toxinology 49:513–530.

Kittel RJ, Wichmann C, Rasse TM, Fouquet W, Schmidt M, Schmid A, Wagh DA, Pawlu C, Kellner RR, Willig KI, Hell SW, Buchner E, Heckmann M, Sigrist SJ (2006) Bruchpilot promotes active zone assembly, Ca2+ channel clustering, and vesicle release. Science (80-) 312:1051–1054.

Kohsaka H1 OSIYFANA (2012) Development of larval motor circuits in Drosophila. Dev Growth Differ 54:408–419.

Kraemer BC, Schuck T, Wheeler JM, Robinson LC, Trojanowski JQ, Lee VMY, Schellenberg GD (2010) Loss of murine TDP-43 disrupts motor function and plays an essential role in embryogenesis. Acta Neuropathol 119:409–419.

Kuromi H, Honda A, Kidokoro Y (2004) Ca2+ influx through distinct routes controls exocytosis and endocytosis at drosophila presynaptic terminals. Neuron 41:101–111.

Landgraf M, Bossing T, Technau GM, Bate M (1997) The origin, location, and projections of the embryonic abdominal motorneurons of Drosophila. J Neurosci 17:9642–9655.

Landgraf M, Sánchez-Soriano N, Technau GM, Urban J, Prokop A (2003) Charting the Drosophila neuropile: a strategy for the standardised characterisation of genetically amenable neurites. Dev Biol 260:207–225.

Lawyer Jr T, Netsky MG (1953) Amyotrophic Lateral Sclerosis: A Clinicoanatomical Study of Fifty-Three cASES. AMA Arch Neurol Psychiatry 69:171–192.

Lee J, Ueda A, Wu C-F (2014a) Distinct roles of *Drosophila cacophony* and *Dmca1D* Ca $^{2+}$ channels in synaptic homeostasis: Genetic interactions with *slowpoke* Ca $^{2+}$ - activated BK channels in presynaptic excitability and postsynaptic response. Dev Neurobiol 74:1–15.

Lee J, Ueda A, Wu C-FF (2014b) Distinct roles of Drosophila cacophony and Dmca1D

Ca2+ channels in synaptic homeostasis: Genetic interactions with slowpoke Ca2+-activated BK channels in presynaptic excitability and postsynaptic response. Dev Neurobiol 74:1–15.

Lee MC, Yasuda R, Ehlers MD (2010) Metaplasticity at Single Glutamatergic Synapses. Neuron 66:859–870.

Lejeune F, Maquat LE (2005) Mechanistic links between nonsense-mediated mRNA decay and pre-mRNA splicing in mammalian cells. Curr Opin Cell Biol 17:309–315.

Lipscombe D, Allen SE, Toro CP (2013a) Control of neuronal voltage-gated calcium ion channels from RNA to protein. Trends Neurosci 36:598–609.

Lipscombe D, Andrade A, Allen SE (2013b) Alternative splicing: Functional diversity among voltage-gated calcium channels and behavioral consequences. Biochim Biophys Acta - Biomembr 1828:1522–1529.

Liu Z, Chen Y, Wang D, Wang S, Zhang YQ (2010) Distinct presynaptic and postsynaptic dismantling processes of Drosophila neuromuscular junctions during metamorphosis. J Neurosci 30:11624–11634.

Luo J, Shen WL, Montell C (2016) TRPA1 mediates sensation of the rate of temperature change in Drosophila larvae. Nat Neurosci 20:34–41.

Marder E, Bucher D (2001) Central pattern generators and the control of rhythmic movements. Curr Biol 11.

McGurk L, Berson A, Bonini NM (2015) Drosophila as an in vivo model for human neurodegenerative disease. Genetics 201:377–402.

McGurk L, Lee VM, Trojanowksi JQ, Van Deerlin VM, Lee EB, Bonini NM (2014) Poly-A binding protein-1 localization to a subset of TDP-43 inclusions in amyotrophic lateral sclerosis occurs more frequently in patients harboring an expansion in C9orf72. J Neuropathol Exp Neurol 73:837–845.

Melom JE, Akbergenova Y, Gavornik JP, Littleton JT (2013) Spontaneous and evoked release are independently regulated at individual active zones. J Neurosci 33:17253–17263.

Menon KP, Carrillo RA, Zinn K (2013) Development and plasticity of the Drosophila larval neuromuscular junction. Wiley Interdiscip Rev Dev Biol 2:647–670.

Mohseni N, McMillan SC, Chaudhary R, Mok J, Reed BH (2009) Autophagy promotes caspase-dependent cell death during Drosophila development. Autophagy 5:329–338.

Monastirioti M, Gorczyca M, Rapus J, Eckert M, White K, Budnik V (1995) Octopamine immunoreactivity in the fruit flyDrosophila melanogaster. J Comp Neurol 356:275–287.

Morton DB, Clemens-Grisham R, Hazelett DJ, Vermehren-Schmaedick A (2010) Infertility and male mating behavior deficits associated with Pde1c in Drosophila melanogaster. Genetics 186:159–165.

Müller M, Davis GW (2012) Transsynaptic Control of Presynaptic Ca2+ Influx Achieves
Homeostatic Potentiation of Neurotransmitter Release. Curr Biol 22:1–7.

Neely GG, Keene AC, Duchek P, Chang EC, Wang QP, Aksoy YA, Rosenzweig M,
Costigan M, Woolf CJ, Garrity PA, Penninger JM (2011) TrpA1 regulates thermal
nociception in Drosophila Zars T, ed. PLoS One 6:e24343.

Neumann M, Sampathu DM, Kwong LK, Truax AC, Micsenyi MC, Chou TT, Bruce J,
Schuck T, Grossman M, Clark CM, McCluskey LF, Miller BL, Masliah E,
Mackenzie IR, Feldman H, Feiden W, Kretzschmar HA, Trojanowski JQ, Lee VM-
Y (2006) Ubiquitinated TDP-43 in Frontotemporal Lobar Degeneration and
Amyotrophic Lateral Sclerosis. Science (80-) 314:130–133.

Ohyama T, Jovanic T, Denisov G, Dang TC, Hoffmann D, Kerr RA, Zlatic M (2013)
High-throughput analysis of stimulus-evoked behaviors in Drosophila larva reveals
multiple modality-specific escape strategies. PLoS One 8:e71706.

Ou SH, Wu F, Harrich D, García-Martínez LF, Gaynor RB (1995) Cloning and
characterization of a novel cellular protein, TDP-43, that binds to human
immunodeficiency virus type 1 TAR DNA sequence motifs. J Virol 69:3584–3596.

Peng I-F, Wu C-F (2007) Drosophila cacophony channels: a major mediator of neuronal
Ca2+ currents and a trigger for K+ channel homeostatic regulation. J Neurosci
27:1072–1081.

Peron S, Zordan MA, Magnabosco A, Reggiani C, Megighian A (2009) From action
potential to contraction: Neural control and excitation–contraction coupling in larval

muscles of Drosophila. Comp Biochem Physiol Part A Mol Integr Physiol 154:173–183.

Pesiridis GS, Lee VM-YY, Trojanowski JQ (2009) Mutations in TDP-43 link glycine-rich domain functions to amyotrophic lateral sclerosis. Hum Mol Genet 18:R156-62.

Petersen SA, Fetter RD, Noordermeer JN, Goodman CS, DiAntonio A (1997) Genetic analysis of glutamate receptors in drosophila reveals a retrograde signal regulating presynaptic transmitter release. Neuron 19:1237–1248.

Rieckhof GE, Yoshihara M, Guan Z, Littleton JT (2003a) Presynaptic N-type Calcium Channels Regulate Synaptic Growth. J Biol Chem 278:41099–41108.

Rieckhof GE, Yoshihara M, Guan Z, Littleton JT (2003b) Presynaptic N-type calcium channels regulate synaptic growth. J Biol Chem 278:41099–41108.

Robinson J (2001) Mechanisms of Synaptic Transmission: Bridging the Gaps (1890-1990). Oxford University Press.

Rosen D (1993) Erratum: Mutations in Cu/Zn superoxide dismutase gene are associated with familial amyotrophic lateral sclerosis. Nature 364:362–362.

Rubin GM et al. (2000) Comparative genomics of the eukaryotes. Science 287:2204–2215.

Ryan TP (2006) Modern Engineering Statistics. John Wiley & Sons, Inc.

Ryglewski S, Lance K, Levine RB, Duch C (2012a) Ca(v)2 channels mediate low and high voltage-activated calcium currents in Drosophila motoneurons. J Physiol

590:809–825.

Ryglewski S, Lance K, Levine RB, Duch C (2012b) Ca $_v$ 2 channels mediate low and high voltage-activated calcium currents in *Drosophila* motoneurons. J Physiol 590:809–825.

Sanyal S (2009) Genomic mapping and expression patterns of C380, OK6 and D42 enhancer trap lines in the larval nervous system of Drosophila. Gene Expr Patterns 9:371–380.

Saraswati S, Fox LE, Soll DR, Wu C-F (2004) Tyramine and octopamine have opposite effects on the locomotion ofDrosophila larvae. J Neurobiol 58:425–441.

Savolainen H, Palo J (1973) Amyotrophic lateral sclerosis: Proteins of neuronal cell membranes, axons and myelin of the precentral gyrus and other cortical areas. Brain 96:537–546.

Schaefer JE, Worrell JW, Levine RB (2010) Role of intrinsic properties in Drosophila motoneuron recruitment during fictive crawling. J Neurophysiol 104:1257–1266.

Schmid A, Chiba A, Doe CQ (1999) Clonal analysis of Drosophila embryonic neuroblasts: neural cell types, axon projections and muscle targets. Development 126:4653–4689.

Schuster CM, Davis GW, Fetter RD, Goodman CS (1996) Genetic dissection of structural and functional components of synaptic plasticity. II. Fasciclin II controls presynaptic structural plasticity. Neuron 17:655–667.

Sephton CF, Cenik C, Kucukural A, Dammer EB, Cenik B, Han Y, Dewey CM, Roth FP, Herz J, Peng J, Moore MJ, Yu G (2011) Identification of neuronal RNA targets of TDP-43-containing ribonucleoprotein complexes. J Biol Chem 286:1204–1215.

Sephton CF, Good SK, Atkin S, Dewey CM, Mayer P, Herz J, Yu G (2010) TDP-43 is a developmentally regulated protein essential for early embryonic development. J Biol Chem 285:6826–6834.

Shan X, Chiang P-M, Price DL, Wong PC (2010) Altered distributions of Gemini of coiled bodies and mitochondria in motor neurons of TDP-43 transgenic mice. Proc Natl Acad Sci U S A 107:16325–16330.

Smith LA, Peixoto AA, Kramer EM, Villella A, Hall JC (1998) Courtship and visual defects of cacophony mutants reveal functional complexity of a calcium-channel alpha1 subunit in Drosophila. Genetics 149:1407–1426.

Spiller KJ, Cheung CJ, Restrepo CR, Kwong LK, Stieber AM, Trojanowski JQ, Lee VM-Y (2016) Selective Motor Neuron Resistance and Recovery in a New Inducible Mouse Model of TDP-43 Proteinopathy. J Neurosci 36:7707–7717.

St Johnston D (2002) The art and design of genetic screens: Drosophila melanogaster. Nat Rev Genet 3:176–188.

Swank RL, Putnam T (1943) Amyotrophic Lateral Sclerosis and Related Conditions. Arch Neurol Psychiatry 49:151.

Tan RH, Ke YD, Ittner LM, Halliday GM (2017) ALS/FTLD: experimental models and

reality. Acta Neuropathol 133:177–196.

Turrigiano G (2007) Homeostatic signaling: the positive side of negative feedback. Curr Opin Neurobiol 17:318–324.

Vanden Broeck L, Naval-Sánchez M, Adachi Y, Diaper D, Dourlen P, Chapuis J, Kleinberger G, Gistelinck M, Van Broeckhoven C, Lambert JC, Hirth F, Aerts S, Callaerts P, Dermaut B (2013) TDP-43 Loss-of-Function Causes Neuronal Loss Due to Defective Steroid Receptor-Mediated Gene Program Switching In Drosophila. Cell Rep 3:160–172.

Veit H (1947) Dynamic view of amyotrophic lateral sclerosis. J Nerv Ment Dis 106:129–136.

Vogelstein JT, Park Y, Ohyama T, Kerr RA, Truman JW, Priebe CE, Zlatic M (2014) Discovery of brainwide neural-behavioral maps via multiscale unsupervised structure learning. Science 344:386–392.

von Schilcher F (1977) A mutation which changes courtship song in Drosophila melanogaster. Behav Genet 7:251–259.

Wagh DA, Rasse TM, Asan E, Hofbauer A, Schwenkert I, Dürrbeck H, Buchner S, Dabauvalle M-C, Schmidt M, Qin G, Wichmann C, Kittel R, Sigrist SJ, Buchner E (2006) Bruchpilot, a protein with homology to ELKS/CAST, is required for structural integrity and function of synaptic active zones in Drosophila. Neuron 49:833–844.

Wang H-Y, Wang I-F, Bose J, Shen C-KJ (2004) Structural diversity and functional implications of the eukaryotic TDP gene family. Genomics 83:130–139.

Wang IF, Tsai KJ, Shen CKJ (2013) Autophagy activation ameliorates neuronal pathogenesis of FTLD-U mice A new light for treatment of TARDBP/TDP-43 proteinopathies. Autophagy 9:239–240.

Wechsler IS, Sapirstein MR, Stein A (1944) Primary and Symptomatic Amyotrophic Lateral Sclerosis. Am J M Sc 208.

Wiemerslage L, Lee D (2015) Role of Drosophila calcium channel cacophony in dopaminergic neurodegeneration and neuroprotection.

Worrell JW, Levine RB (2008) Characterization of Voltage-Dependent Ca2+ Currents in Identified Drosophila Motoneurons In Situ. J Neurophysiol 100:868–878.

Wu L-S, Cheng W-C, Hou S-C, Yan Y-T, Jiang S-T, Shen C-KJ (2010) TDP-43, a neuro-pathosignature factor, is essential for early mouse embryogenesis. Genesis 48:56–62.

Xing B, Ashleigh Long A, Harrison DA, Cooper RL (2005) Developmental consequences of neuromuscular junctions with reduced presynaptic calcium channel function. Synap New York Ny 57:132–147.

Yamada K, Nakayama S, Shiotani T, Hasegawa T, Nabeshima T (1994) Possible involvement of the activation of voltage-sensitive calcium channels in the ameliorating effects of nefiracetam on scopolamine-induced impairment of

performance in a passive avoidance task. J Pharmacol Exp Ther 270:881–892.

Ziegler L (1930) Psychotic and emotional phenomena, associate with amyotrophic lateral sclerosis. For Sci 24:930–936.